TALLINN UNIVERSITY OF TECHNOLOGY
DOCTORAL THESIS
5/2020

Photo- and Electropolymerization Approaches for Molecular Imprinting of a Neurotrophic Factor Protein

ANNA KIDAKOVA

TAL TECH PRESS

TALLINN UNIVERSITY OF TECHNOLOGY
School of Engineering
Department of Materials and Environmental Technology

This dissertation was accepted for the defence of the degree of Doctor of Philosophy in Natural and Exact Sciences on 03/02/2020

Supervisor: Dr. Vitali Syritski
School of Engineering
Tallinn University of Technology
Tallinn, Estonia

Co-supervisor: Prof. Andres Öpik
School of Engineering
Tallinn University of Technology
Tallinn, Estonia

Opponents: Dr. Peter Lieberzeit, Full professor
Department of Physical Chemistry
University of Vienna
Vienna, Austria

Dr. Evgenia Korzhikova-Vlakh, Associate professor
Institute of Macromolecular Compounds
of Russian Academy of Sciences
Saint Petersburg, Russia

Defence of the thesis: 06/03/2020, Tallinn, TalTech, Ehitajate tee 5, lecture hall U06A-229

Declaration:
Hereby I declare that this doctoral thesis, my original investigation and achievement, submitted for the doctoral degree at Tallinn University of Technology has not been submitted for doctoral or equivalent academic degree.

Anna Kidakova

---
signature

European Union
European Regional
Development Fund

Investing
in your future

ISSN 2585-6898 (publication)
ISBN 978-9949-83-531-7 (publication)
ISSN 2585-6901 (PDF)
ISBN 978-9949-83-532-4 (PDF)

TALLINNA TEHNIKAÜLIKOOL
DOKTORITÖÖ
5/2020

Foto- ja elektropolümerisatsiooni meetodid neurotroofsete tegurite molekulaarseks jäljendamiseks

ANNA KIDAKOVA

TAL TECH
KIRJASTUS

Contents

List of Publications

The thesis is based on the following publications, which are referred to in the text by the Roman numerals I- III:

I A. Kidakova, R. Borozнjak, J. Reut, A. Öpik, M. Saarma and V. Syritski, Molecularly imprinted polymer-based SAW sensor for label-free detection of cerebral dopamine neurotrophic factor protein, Sensors and Actuators B: Chemical, 308, (2020), 127708.

II A. Kidakova, J. Reut, J. Rappich, A. Öpik, V. Syritski, Preparation of a surface-grafted protein-selective polymer film by combined use of controlled/living radical photopolymerization and microcontact imprinting, React. Funct. Polym. 125 (2018) 47–56.

III A. Kidakova, J. Reut, R. Borozнjak, A. Öpik, V. Syritski, Advanced sensing materials based on molecularly imprinted polymers towards developing point-of-care diagnostics devices, Proc. Est. Acad. Sci. 68 (2019) 158–167.

Copies of these papers are included in Appendix.

Author's Contribution to the Publications

The contribution by the author to the papers included in the thesis is as follows:

I Planning a part of the experimental work, data analysis, writing a manuscript with the help of co-authors.

II Planning and performing of all experimental work, data analysis, with the exception of conducting SEM studies also measurements and analysis of XPS, writing a manuscript with the help of co-authors.

III Planning all experimental work and performing a major part of all experiments, writing a manuscript with the help of co-authors.

Introduction

Since the development of the first blood serum test to detect colon cancer by Dr. Joseph Gold in 1965 [1] the discovery and application of proteins as diagnostic biomarkers for diseases have been gradually increased. Today, more than 100 different proteins are analyzed in serum and plasma for diagnostics purposes, and their number continues to grow [2,3]. Moreover, in clinical practice the discovery and application of new, more relevant biomarkers is ongoing. One example of such biomarkers are proteins from neurotrophic factors (NF) family [4]. This is a group of small proteins secreted by neurons and neuron-supporting cells and supporting the survival of neurons. The correlation between the level of these proteins in serum and a number of neurological and mental diseases has been established [5,6]. For example, it was shown that serum level of the brain-derived neurotrophic factor (BDNF) is associated with disorders of brain function caused by neurodegenerative diseases (such as Alzheimer's and Parkinson's) and depression [7–9]. Simultaneously, it was noted that cerebral dopamine neurotrophic factor (CDNF) is a therapeutic protein and is able to cause a positive effect in the treatment of traumatic spinal cord injury [10,11].

The greatest analytical challenge is the determination of low protein concentrations usually occurring at the early stages of the disease, whilst the early and reliable diagnosis of the disease helps prevent fatal changes in the body. Nowadays, the concentration of proteins in body fluids is determined in various ways, including chemical, biochemical and immunological methods. However, in many methods, biological molecules are used as receptors, that are not stable under environmental changes and are subject to rapid aging. From the point of view of a clinical chemist, the optimal analytical device for the quantitative determination of protein should be simple, require a small number of operations and be resistant to environmental fluctuations. Sensors based on synthetic receptors can meet these requirements.

Molecular imprinting technology is widely recognized as a promising strategy for the development of robust synthetic receptors with high selectivity to the analyte [12]. Molecularly imprinted polymers (MIP) have been shown to be a promising alternative to natural biological receptors in biosensors providing more stable and low-cost recognition elements [13]. Currently, this approach is widely used as a simple and universal technique for the synthesis of artificial receptors for small organic compounds and large biological macromolecules [14]. Concept of the molecular imprinting consists in polymerization of a mixture of functional monomers in the presence of a target molecule that acts as a template. The binding sites that are generated during the imprinting process often have affinities and selectivities approaching those of antibody-antigen systems, and molecularly imprinted materials have therefore been dubbed "antibody mimics" [15]. MIPs demonstrate some obvious advantages over biological receptors for sensor technology: due to their artificial polymer nature, they are intrinsically stable and robust, facilitating their application in extreme environments, such as in the presence of acids or bases, in organic solvents, or at high temperatures and pressures [16]. Additionally, due to the high number of different monomers that are commercially available (more than 4000 polymerizable compounds), their properties can be tuned to detect a specific analyte [17].

The application of MIP-based sensors for detection of different proteins has been widely studied. Thus, it was reported about the successful detection of cancer biomarkers (such as breast cancer tumour marker (CA15-3) [18], or prostate specific

antigen [19], cardiovascular disease biomarkers (myoglobin [20] and cardiac troponin T [21]), clinically-relevant protein such as IgG antibody [22,23], by MIP-modified sensors. Nevertheless, despite the increase in the number of publications dedicated to the use of MIPs for the detection of proteins, the molecular imprinting of NFs has not yet been reported.

When designing a MIP for a chemosensor it is very important to ensure the reliable interface between the recognition element and a sensor transducer. The surface-initiated polymerization method is apparently a suitable in situ synthesis of MIP films, and assists in the creation of reliable adhesion of the polymer film on the surface [24]. Electropolymerization is a simple and widely used method for realization of this idea because the reaction product is a film already localized on the electrode surface having a good electrical conductivity. Moreover, this type of polymerization has a high stoichiometry of the process that allows obtaining sufficiently pure polymers. However, the unstable operation of electrolytes, the limited number of monomers from which high-quality polymer layers can be obtained [25], and the complex synthesis of highly cross-linked polymers [26] limit the use of electropolymerization for synthesis of MIPs. Meanwhile, the use of surface-initiated photopolymerization allows the synthesis of a cross-linked polymer with high adhesion to the surface. Photopolymerization provides the possibility of a good control of both film thickness and internal morphology, as well as the ability of the reaction to be carried out at room temperature [27]. The method of controlled/living radical polymerization (C/LRP) can be used to obtain MIP films with controlled thickness and composition [28]. The reversible addition-fragmentation chain transfer (RAFT) polymerization is the most versatile process among C/LRP techniques. There are few studies on the RAFT approach for imprinting of protein MIPs [29] and the preparation of MIPs for some small molecules [30,31].

The integration of MIP-based recognition elements into various label-free sensor platforms has been intensively studied [32,33]. Sensors based on electrochemical transduction mechanisms such as screen-printed electrodes (SPE) meet the diagnostic objectives since they include, ease of manufacture, compactness, simplicity in handling, quantitative determination of analyte in microvolumes of samples and good sensitivity at a low cost [34,35]. In addition, sensors based on surface acoustic wave (SAW) transmission as well as surface plasmon resonance (SPR) allow observing the process of protein binding to the surface in real-time and without using a label. The aforementioned platforms are compatible with large-scale manufacturing and multiplexing technologies and represent an ideal starting point for the implementation of inexpensive and portable sensing platforms suitable for point-of-care devices [36].

Thus, the aim of the research is at developing synthesis methods employing electro- and photopolymerization techniques for preparation of polymer films molecularly imprinted with a NF-protein. The synthesis methods should allow the reliable integration of MIP films into various label-free sensor platforms. Two clinically relevant NF-proteins: CDNF and BDNF, were used as target molecules for molecular imprinting to generate CDNF-MIP and BDNF-MIP, respectively. Capability of the films to bind selectively the respective target protein was assessed by the label-free techniques such as SAW, SPR, SPE.

List of abbreviations and acronyms

4-ATP	4-aminothiophenol
3.5-DClPDT	3.5-dichlorophenyl diazonium tetrafluoroborate
3.5-DClP	3.5-dichlorophenyl
3-GPS	(3-Glycidyloxypropyl)trimethoxysilane
Ag/AgCl/Sat. KCl	Silver/Silver Chloride Electrode
ATRP	Atom-Transfer Radical Polymerization
a.u.	arbitrary unit
BAA	N,N'-Methylenebis(acrylamide)
BDNF	Brain-Derived Neurotrophic Factor
BDNF-MIP/SPE	SPE modified by MIP film with molecular imprints of BDNF
BSA	Bovine Serum Albumin
BSA-MIP/SPR	SPR modified by MIP film with molecular imprints of BSA
CA	Contact Angle
CDNF	Cerebral dopamine neurotrophic factor
CDNF-MIP/SAW	SAW modified by MIP film with molecular imprints of CDNF
C/LRP	Controlled/Living Radical Polymerization
CV	Cyclic voltammetry
DEAEM	Diethylaminoethyl Methacrylate
DEDTC	sodium Diethyldithiocarbamate
DLS	Dynamic Light Scattering
DPV	Differential Pulse Voltammetry
DTSSP	3,3-dithiobis (sulfosuccinimidyl propionate)
EIS	Electrochemical Impedance Spectroscopy
FRP	Free Radical Polymerization
HSA	Human Serum Albumin
IF	Imprinting Factor
LOD	Limit of Detection
LOQ	Limit of Quantitation
MANF	Mesencephalic Astrocyte-derived Neurotrophic Factor
mCD48	mouse recombinant Cluster of Differentiation 48
MIP	Molecularly Imprinted Polymer
NIP	Non-imprinted Polymer
m-PD	m-phenylenediamine
NF	Neurotrophic Factor
PBS	Phosphate Buffered Saline
p-MP	p-maleimidophenyl
p-MPDT	p-maleimidophenyl diazonium tetrafluoroborate
RAFT	Reversible Addition–Fragmentation chain Transfer
RIU	Refractive Index Unit
SAW	Surface Acoustic Wave

SI-C/LR	Surface-initiated Controlled/Living Radical
SD	Standard deviation
SDS	Sodium Dodecyl Sulfate
SPE	Screen-Printed Electrode
SPR	Surface Plasmon Resonance
XPS	X-ray Photoelectron Spectroscopy

1. Theory and literature review

1.1 The general principle of molecularly imprinting

The term “molecular imprinting” refers to the technology for producing synthetic molecular systems – molecularly imprinted polymers (MIPs) – capable of mimic natural biological receptors. Such synthetic receptors are capable to recognize and bind the target molecule with high affinity and specificity [37]. Molecular imprinting is the process of producing synthetic polymers in which functional and cross-linking monomers are copolymerized around a target molecule to form a tightly cross-linked polymer lattice, which acts as a molecular template. The functional monomers initially form a complex with the imprint molecule, and following polymerization, their functional groups maintain their spatial position due to the highly cross-linked polymer structure [38]. After removal of the target molecule in the polymer matrix stay specific binding sites. Thus, the molecular memory is introduced into the polymer, and now it is able to bind analyte with a high specificity [37]. Depending on the further application MIPs may be obtained in different physical forms: particles, films or membranes [39]. There are two distinct approaches to molecular imprinting: covalent and non-covalent interaction (Fig. 1.1).

The covalent approach

Covalent imprinting is distinguished by the use of templates which are covalently bound to one or more functional groups of the monomer. After polymerization, the template is cleaved, and the functionality left in the binding site is capable of binding the target molecule by re-establishment of the covalent bond. The advantage of this approach is that the functional groups are only associated with the template site; however, only a limited number of compounds (alcohols (diols), aldehydes, ketones, amines and carboxylic acids) can be imprinted with this approach [40]. The covalent coupling process can achieve stable coupling, but it needs derivation steps, which are complicated and costly, and limited sites for attachment lead to shorter lifetime [41].

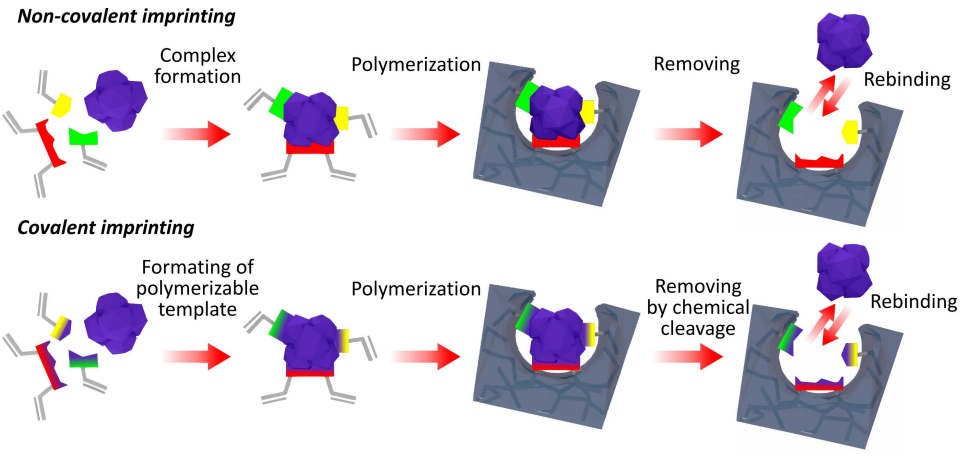

Figure 1.1. Schematic representation of the non-covalent and covalent molecular imprinting procedures.

Non-covalent approach

The great attraction of the non-covalent method is its simplicity. As the formation of the template monomer complex is accomplished via non-covalent forces such as H-bonding, ion-pairing and dipole-dipole interactions. In non-covalent imprinting the interactions between functional monomer and template during polymerization are the same as those between polymer and template in the rebinding step. Due to its simplicity, this method is the most widely used to create imprinted polymers [40]. However, the drawback is an unavoidable inhomogeneity of the binding sites obtained. This owes to the formation of a multitude of complexes between the functional monomers and template during the initial stages of polymerization [38].

1.2 Polymerization processes for synthesis of molecularly imprinted polymers

The synthesis of MIPs can be carried out by thermal polymerization, electropolymerization or photopolymerization. The chain reaction of polymerization begins with the activation of monomer molecules, which subsequently become active centers of the reaction. The radical formation in a polymerization mixture is usually carried out by the presence of a specific initiator molecule or by the action of free electrons. As initiators for the thermal and photopolymerization substances are used, which can decompose under the action of heat or light to form an active radical. After activation, the growth of the polymer chain occurs until the chain is broken, or the external effect no longer disappears.

1.2.1 Thermal polymerization

The best known initiator of FRP is N,N-azobisisobutyronitrile (AIBN), which is fragmented when heated to isobutyronitrile radicals (Scheme 1.1).

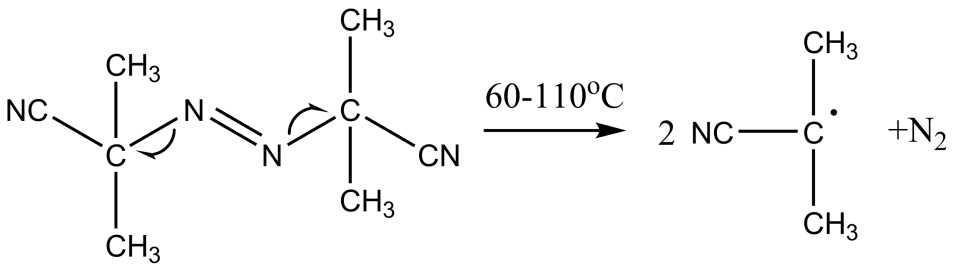

Scheme 1.1. The thermal decomposition of AIBN. Eliminating a molecule of nitrogen gas to form two 2-cyanoprop-2-yl radicals.

Some of the new radicals bind and deactivate each other or become disproportionate to $(CH_3)_2CH(CN) + CH_2 = C(CN)CH_3$. Thus, only a portion of the initially formed isobutyronitrile residues can initiate polymerization of the monomers [42]. Thermal initiators are quite expensive, although trace quantities of initiators have been reported by Chiefari et al to be sufficient to initiate the polymerization [43]. The use of thermal polymerization is fraught with difficulties because of impurity traces that can accelerate or retard polymerization leading to non-reproducible results. However, the careful removal of oxygen that inhibits polymerization and the use of purified fresh monomer that has not been exposed to oxygen result in reproducible polymerization [44]. A major

shortcoming of thermal polymerization for the synthesis of MIPs, especially protein-MIPs, is an elevated temperature (85–160 °C) required to initiate the reaction [45] since proteins or other biomolecule used as target/template molecules, can be easily destroyed at increased temperature. Another disadvantage is that the known thermal polymerization initiators are insoluble in water [42] that limits their use for protein MIPs synthesis, where the aqueous solutions are preferable in order to keep the native conformation of protein molecule.

1.2.2 Electropolymerization

Electrochemical polymerization has several advantages over the thermal process. First, the reaction product is a polymer film deposited directly on the surface of the electrode or sensor transducer. Another advantage of the process is a high stoichiometry of the process, which makes it possible to obtain sufficiently pure polymers [46]. Finally, the properties of the polymer coating such as porosity and morphology can be conveniently controlled by appropriate selection of the experimental conditions such as amount of electric charge transferred, solution pH, electrolyte nature. The disadvantages are as follows: an unstable operation of the electrolytes, a limited number of monomers from which high-quality polymer layers can be obtained, as well as a complicated synthesis of highly cross-linked polymers [26]. Electropolymerization is only suitable for MIP film formation on electrically conductive surfaces such as gold, silver or graphite. Nevertheless, electropolymerization has become one of the popular methods for the synthesis of MIP films especially for sensing application, because a polymer can be deposited directly on the sensor transducer and the thickness of the polymer layer can be easily controlled by the amount of electrical charge passed through the electrode. Moreover, after electropolymerization the polymer films do not require any additional treatment except the template removal and can be applied directly for analyte determination [47]. Using electropolymerization, proteins such as troponin T [21], myoglobin [20], immunoglobulin G [23], breast cancer biomarker (CA 15-3) [48], and others have been recently imprinted.

1.2.3 Photopolymerization

In photopolymerization the initiations of radicals proceeds under UV or visible light radiation. Such radical formation does not require thermal activation energies, and polymerization proceeds at room temperature or even at very low temperatures [42]. In photopolymerization, the probability of chain transfer is usually high, resulting in a significant number of branched macromolecules [49]. For a successful photopolymerization process, it is necessary to provide an oxygen-free medium because molecular oxygen can physically quench the activated state of the photoinitiator as well as reduce the number of free radicals or active radical sites by forming non-reactive peroxide radicals. This problem can be solved with special photoinitiators such as thioxanthone anthracene, a polyaromatic photoinitiator, which initiates the polymerization of monomers in an air atmosphere. This initiator requires oxygen to form endoperoxide and to decompose and generate initiating radicals [50]. The observed insensitivity of thiol-based systems to oxygen inhibition is due to the ability of the oxygen-bond-forming peroxy radicals to abstract one hydrogen atom from thiols, thereby forming a new initiating phenyl radical [51,52]. Thin MIP films prepared using photopolymerization have found application in the development of sensors for both small molecules such as diclofenac [53] or vanillylmandelic acid [54]) and high molecular weight molecules such as lysozyme [55], bovine serum albumin [56], immunoglobulin G [57].

1.3 The polymerization mechanisms

The radical mechanism of polymerization is widely used for the synthesis of MIPs, mainly due to its multipurpose. The radical mechanism does not require rigorous conditions and applies to most monomers. However, using free radical polymerization (FRP), it is difficult to control chain growth, which leads to high polydispersity and irregularity of the cross-linked polymer matrix. Whereas, the controlled radical polymerization mechanism provides a linear increase in the molecular weight of the polymer over time, resulting in uniform growth of the polymer.

1.3.1 Free radical polymerization

FRP is initiated by radicals and propagated by macroradicals. These radicals exhibit an unpaired electron. Initiating radicals are rarely formed by monomers themselves but rather thermal or photochemical decomposition of initiators or are initiated electrochemically. FRP process includes the following steps (Scheme 1.2):

1. *Initiation.* Firstly, under the influence of thermal or UV radiation, the initiator decomposes with the formation of active radicals. In the case of electro-initiated, the formation of active radicals occurs due to the redox process on the cathode or anode. The radicals thus generated are capable of chain initiation, resulting in a fairly significant proportion of unsaturated end groups. Radical Ri starts polymerization.
2. *Propagation and transfer.* During polymerization, a polymer spends most of its time increasing or increasing its chain length. In the propagation reaction, more monomer molecules are added and macroradicals are formed. The propagating chain length macroradical deprives the transfer agent of a weakly bound atom (e.g., hydrogen or halogen). As a result, a polymer chain with a saturated end group is generated as well as a new free-radical, which in turn can react with monomer units. The transfer agent may be the monomer itself, the initiator, the solvent or any other intentionally added transfer agent [58].
3. *Termination*. There are two models for the chain termination process. First, direct coupling (combination) of two free macroradicals to give a dead polymer chain of chain length i + j. The second model, so-called disproportionation, where a hydrogen atom is abstracted from one of the radical chain ends, yielding two stabilized polymer chains, one of which carries a double bond.

Various types of initiators can be used for FRP: azobis-compounds; aromatic ketones and alcohols, esters or t-amines; benzoin derivatives etc. The FRP mechanism is implemented in a variety of polymerization types (photo-, thermo-, electropolymerization). However, the main advantage of the use of photoinitiator is the possibility to define exact start- and endpoints of the polymerization process via the duration of the irradiation period. In addition, the rate of decomposition of the photoinitiator depends on the intensity of the light and is practically independent of the temperature of the reaction medium [58].

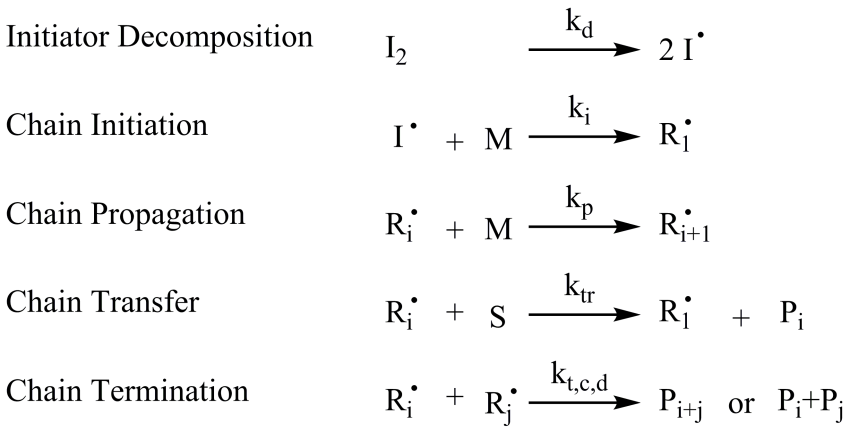

Scheme 1.2. Schematic illustration of the free radical mechanism [58], where I_2 is the initiator, M is the monomer, R_i is a radical of chain length i, S is a transfer agent.

1.3.2 Controlled/"Living" Radical Polymerization (C/LRP)

The C/LRP mechanism (Scheme 1.3) consists of replacing an irreversible bimolecular chain termination by a reversible reaction with propagating radical initiator fragments or special additives introduced into the polymer in a "catalytic" quantities [59]. Initiators for C/LRP can be either prepared in advance or formed *in situ*. Generally, the structure of the initiator should resemble the dormant macromolecular species. In C/LRP, radicals are formed reversibly at both the initiation and propagation stages. The concentration of radicals is essentially established by balancing rates of activation and deactivation [58]. Radicals may either be reversibly trapped in a deactivation/activation process according to Scheme 1.3, or they can be involved in a "reversible transfer", degenerative exchange process (Scheme 1.4) [59].

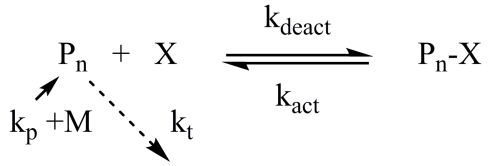

Scheme 1.3. Schematic diagrams of C/LRP by reversible termination.

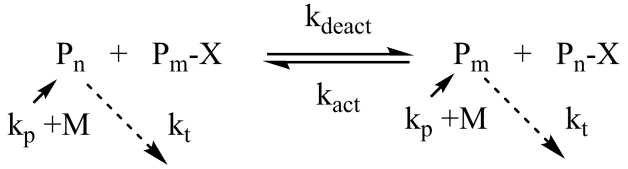

Scheme 1.4. Schematic diagrams of C/LRP by degenerative exchange process.

C/LRP and FRP follow the same radical mechanism, show the same chemical and stereoselective effect, and can polymerize a similar range of monomers. However, in C/LRP, the lifetime of growing chains is significantly increased due to the participation of

alternating reversible activation. The activation/deactivation process in C/LRP reduces the amount of dead chains by less than 10% [59]. When applying C/LRP to MIP synthesis, Salian and co-workers [30] demonstrated the improvement in network homogeneity and imprinting efficiency in weakly crosslinked polymer networks made via C/LRP compared to FRP. C/LRP extended the reaction-controlled regime of the polymerization reaction and formed more homogeneous polymer chains and networks with smaller mesh sizes. In addition, C/LRP reduces the effect of the template on polymer chain growth, resulting in polymers with a more consistent polydispersity index that was independent of the template concentration in the prepolymerization solution.

Reversible Addition Fragmentation Chain Transfer (RAFT) Polymerization

RAFT polymerization is a reversible deactivation radical polymerization and one of the more versatile methods for providing living characteristics to radical polymerization. Effective chain transfer agents for RAFT are different dithioesters, dithiocarbamates, trithiocarbonate and xanthates [58,59]. RAFT polymerization consists of the simple introduction of a small amount of dithioester in a conventional free-radical system (monomer + initiator). The transfer of the chain-transfer agent between growing radical chains, present at a very low concentration, and dormant polymeric chains, present at a higher concentration, regulates the growth of polymer chain and limit the termination reactions (Scheme 1.5) [60].

In an ideal RAFT process, the RAFT agent should behave as a transfer agent [61]. The product of chain transfer is also a chain transfer agent with similar activity to the precursor transfer agent [62]. The extent to which the side reactions of retardation and termination occur in RAFT depends in part upon the selection of transfer agent/monomer combinations and of the reaction conditions [59]. The RAFT agent must be selected in such a way that its chain transfer activity is appropriate to the monomer(s) to be polymerized. RAFT polymerization has also been applied for MIPs preparation because of its versatility and simplicity. For example, MIP nanoparticles were synthesized via RAFT polymerization with a yield of 14%, that is a significant increase compared with similar methods using high monomer concentration and UV initiation [31].

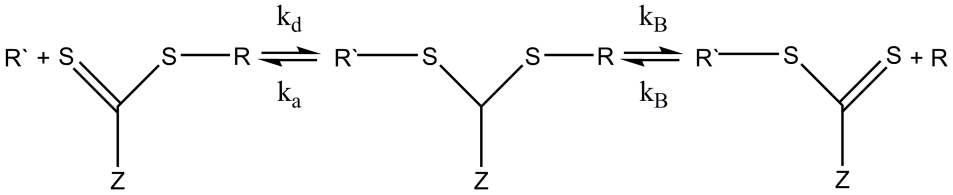

Scheme 1.5. The mechanism of chain activation/deactivation in RAFT with thiocarbonylthio agents.

1.4 Synthesis strategies for protein-MIP film formation

The synthesis of thin polymer films has become a popular method for imprinting of proteins. Various synthesis strategies of protein-imprinted polymer (protein-MIP) films have been developed to prevent the restriction of diffusion of macromolecules in highly crosslinked polymer matrices. One of the first strategies proposed was the use of a slightly cross-linked hydrogel [63]. A hydrogel is a crosslinked hydrophilic polymer chain

that swells under the influence of water but does not dissolve in it. In order to improve diffusion in macroporous polymer matrices significantly reduce the number of cross-links, which leads to a decrease of density of polymers and, as a result, to the loss of specific recognition and the rebinding efficiency after several regeneration cycles. It is also difficult to imprint large proteins, such as immunoglobulins, since with increasing physical parameters of the template it becomes more difficult to maintain selectivity [64]. Another approach for the synthesis of protein-MIP films was proposed by Rachkov with colleagues. They used a short peptide sequence, which frequently occurs on the protein surface, to create specific binding sites. As a result, the imprinted matrix is able to recognize the whole protein by a small amino acid sequence-epitope [65,66]. The so-called "epitope imprinting" allows the synthesis of protein-MIP films from non-aqueous solvents. However, the binding of a large protein can be difficult due to the deficiency of 3D binding sites. Therefore, it is recommended to use epitopes with a 3D structure, with a sequence of more than 200 amino acids [67].

1.4.1 Surface imprinting

The surface imprinting approach leading to the formation of polymer with imprinted sites located on or close to the polymer surface, enabling easy access to the target macromolecules, was shown to be a promising way for protein-MIP preparation [68]. Various techniques have been developed to create the protein-selective binding sites on the polymer surface. H. Shi with co-workers were first proposed to immobilize the protein on the mica surface before the polymerization [69]. Thus, the growth of the polymer matrix was limited to the surface of the protein stamp, and the resulting specific cavities were located very close to the polymer surface. Electropolymerization has increasingly been used to realize the principle of surface imprinting, since this method allows precise control of the film thickness by controlling the charge consumed [70–73].

1.4.2 Microcontact imprinting of proteins

One of the prospective approaches to producing protein-MIP films with surface-confined binding sites is microcontact imprinting [74]. The microcontact imprinting technique consists in the polymerization of monomers in a sandwich structure between a substrate and a protein stamp. This method includes three main steps: formation of a protein stamp, assembling a sandwich structure and polymerization, separating the protein stamp and the formed polymer (Fig. 1.2). In most cases, physical adsorption of the template protein on the surface is used to form a protein stamp by incubation in a protein solution followed by drying of nitrogen gas [68,75,76]. However, physical adsorption, in spite of its simplicity and particularly suitable for the deposition of proteins on various surfaces, does not ensure the homogeneity of the layer and the molecules are loosely attached to the surface [77]. Alternatively, it is possible to form a protein stamp by covalently attaching the protein to a glass pre-modified with reactive groups [78,79]. This approach allows to obtain a very homogeneous monolayer of proteins on the surface [80]. An important advantage of microcontact imprinting is that after the removal of the protein stamp, there is very little or no template left in the polymer matrix, which leads to the production of a MIP film with more homogeneous binding sites [79]. Also, a small amount of protein is usually needed for the formation of a protein stamp in microcontact imprinting [74]. The method of microcontact imprinting was used to prepare MIP films with lysozyme and RNase A [75], myoglobin [79], prostate specific antigen [81], C-reactive protein [74] on glass substrates.

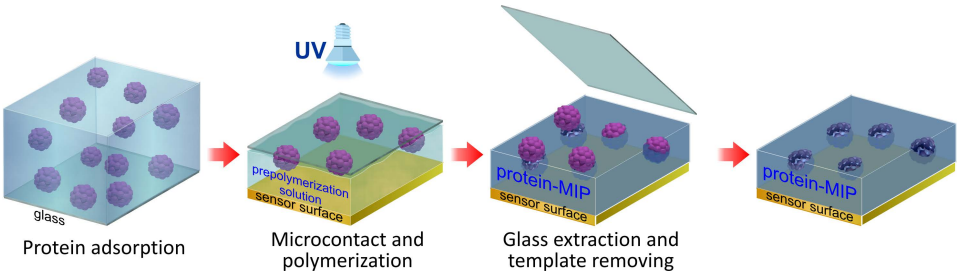

Figure 1.2. Schematic diagram of microcontact imprinting procedure for protein-MIP preparation.

1.5 MIP-sensors for protein detection

1.5.1 Interfacing a MIP film with a sensor transducer

To create chemical sensors MIP films can be integrated with the transducer surface with various types of transduction such surface plasmon resonance (SPR), surface acoustic wave (SAW), voltammetry, impedance spectrometry, piezoelectric microgravimetry, fluorescence and chemiluminescence spectroscopy. When designing a MIP for a chemosensor it is very important to ensure the perfect interaction between MIP film as a recognition element and a sensor transducer. MIP films on planar surfaces can be prepared by spin coating, surface-initiated polymerization or direct electrodeposition. However, the latter method is only suitable for electrically conductive surfaces such as gold, silver or graphite. The surface-initiated polymerization method is apparently a suitable in situ synthesis of MIP films, and assists in the creation of reliable adhesion of the polymer film to the sensor surface [24].

Surface-initiated polymerization

The fixing of polymer films on the substrate surface by the most popular methods, such as dip-coating, spin-coating and plasma deposition leads to the formation of a polymer film physically (hydrophobic or van der Waals interactions) adsorbed on the surface. This gives relatively weak adhesion, making these films not resistant to external factors (solvents, high temperature, mechanical stress) and limits the scope of their application [82]. To overcome these disadvantages, it is necessary to create covalent or electrostatic bonds between the polymer film and the surface of the substrate. Surface-initiated polymerization (SIP) is the universal way to do this [24] (Fig. 1.3). To perform SIP, the initiator is firstly attached to the surface by electrodeposition [83], self-assembly [24], or by the synthesis of the initiator directly on the surface [84,85]. SIP method can proceed via different polymerization mechanisms depending on the initiator end-group [86]: cationic and anionic polymerization [87], ring-opening polymerization [88], FRP [89], RAFT [85], atom-transfer radical polymerization (ATRP) [90]. The SIP method offers the capability of the film thickness control, uniform coating of the surface, control over composition, high density of grafting [24].

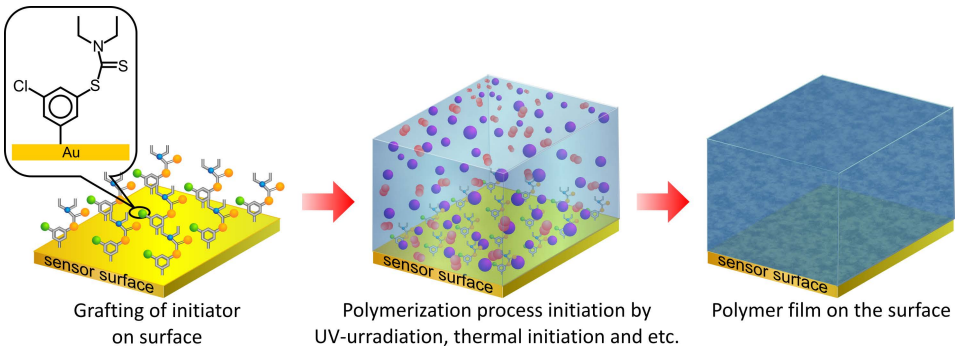

Figure 1.3. Schematic diagram of surface-initiated polymerization.

1.5.2 MIP-sensor for detection of clinically relevant protein

As mentioned above, MIPs can replace the biological receptors used in biosensors for clinical analysis, thereby improving the stability of the sensor to environmental fluctuations and increasing its service life. Also, there is a growing interest in application of MIPs in clinical diagnostics, because the production of MIPs is considered cheaper than obtaining antibodies [14]. Currently, many research groups are focused on the synthesis of MIPs for the detection of clinically relevant proteins. Thus, it was reported that chemosensors based on MIPs successfully detected cancer markers such as breast cancer tumour marker (CA15-3) [18], prostate specific antigen [19,91], carcinoembryonic antigen [92], epithelial ovarian cancer antigen-125 [93]. In addition, successful detection of cardiovascular disease biomarkers (myoglobin [20] and cardiac troponin T [21], clinically-relevant protein such as IgG antibody [22,23], has been reported. As concerns the imprinting of neurotrophic factor (NF) proteins, so far only the selective recognition of another growth factor family protein – vascular endothelial growth factor (VEGF) by hybrid MIP nanoparticles as well as by MIP thin layer on SPR and SPE has been reported [94–96]. Sellergren's group has demonstrated the successful application of MIP receptors for the selective extraction of β-amyloid peptides, a biomarker of Alzheimer's disease [97]. However, it is worth noting that despite the increase in the number of publications dedicated to the use of MIPs for detection of clinically relevant proteins, the MIP capable of selective recognition of a NF protein has still not been reported.

1.6 Neurotrophic factors as target protein

Neurotrophic factors (NFs) are a family of proteins that are secreted by neurons and glial cells and support the survival of nerve cells [98]. They perform an essential function in the development and survival of neurons, as well as in the mature nervous system, they maintain synaptic plasticity and contribute to the formation of long-term memories. The latest studies have confirmed that NFs are associated with the development of various neurodegenerative states, such as Parkinson's, Alzheimer's, and several other mental disorders [6,10,99,100]. Changes in the level of NF concentration in the serum and cerebrospinal fluid may be associated with the stages of development of neurological diseases, which makes NF proteins potential biomarkers for early diagnosis and subsequent neuroprotective treatment. Historically, the first isolated neurotrophic factor in purest form was Nerve growth factor (NGF), the next was discovered the

Brain-derived neurotrophic factor (BDNF) [101]. Also, the NF family includes such proteins as a glial cell-derived neurotrophic factor (GDNF), ciliary neurotrophic factor (CNTF), cerebral dopamine neurotrophic factor (CDNF), mesencephalic astrocyte-derived neurotrophic factor (MANF) and many others.

In this thesis, BDNF and CDNF were selected as model NF proteins for imprinting and a more detailed description of their properties is provided below. BDNF protein performs an important function in the survival of nerve cells by supporting their maturation and growth. It was found that the level of BDNF in the patient's serum was relevant to neurodegenerative disorders such as Huntington's, Parkinson's and Alzheimer's disease [102]. BDNF is a small protein with molecular weight of 27 kDa and isoelectric point (Ip) of 9.43 [103]. BDNF has an oval shape with dimensions of 59x31 Å (Fig. 1.4 a). Considering the use of BDNF as a template molecule for molecular imprinting, the nature and number of available functional groups on the surface of the protein that can subsequently participate in the formation of a complex with functional monomers is of great interest. BDNF contains 6 tyrosines (TYR), 9 serines (SER), 13 threonines (THR) and 2 aspartic acids (ASP) residues, which can form a noncovalent complex with amine groups of a functional monomer (calculated by RasMol 2.7.5.2 software using the Protein Data Bank (pdb) file – 1b8m.pdb). In turn, the hydroxyl groups, carboxylic oxygens and amino groups of a functional monomer can interact noncovalently with asparagine (ASN), glutamine (GLN) and glutamic acid (GLU) residues on the surface of BDNF.

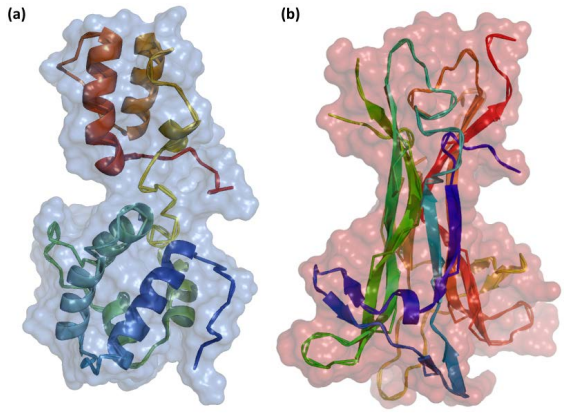

Figure 1.4. 3D structure of the CDNF (4BIT.pdb) (a) and BDNF (1B8M.pdb) (b) proteins.

CDNF has a therapeutic effect in injuries of the spine and neurodegenerative diseases [11,104]. CDNF has molecular weight of 18 kDa. CDNF is a neutral protein with Ip 7.67, has an oval shape with dimensions 58x36 Å (Fig. 1.4 b). CDNF contains the surface accessible amino acid residues: 16 GLU, 6 TYR, 8 SER, 4 GLN, 9 ASP, 4 ASN, 9 THR (calculated by RasMol 2.7.5.2 software using the Protein Data Bank (pdb) file – 1b8m.pdb). CDNF has a 59% similar amino acid sequence to MANF [10].

At present, the level of NFs in serum is determined using classical methods such as western blotting and enzyme-linked immunosorbent assay (ELISA) [105–107]. These are expensive, multi-stage analytical methods requiring a highly qualified analyst and special laboratory conditions. Therefore, there is a great demand for rapid, simple, and less expensive alternatives for detection of NF proteins. Thus, different kinds of biosensors were developed for NF detection: electrochemical sensor with anti-BDNF protein as a

recognition element [108,109], grating-coupled SPR (GC-SPR) sensor with a propeptide as recognition element [110]. However, according to our best knowledge, there is no report on MIP-based sensors for detection NFs.

1.7 Label-free sensing platforms

Label-based assays are widely used for protein detection and are rather informative, but labeling process is usually quite expensive, labour- and time-consuming. Label-free detection technique is based on measuring precisely the chemical and physical characteristics of the molecules [111]. Sensors generate a response directly during or after binding the analyte to the recognition element, without requiring other interactions with the labels providing the signal [112,113]. The advantage of this method is a significant simplification of analysis, reduction in sample preparation time and analysis costs. Therefore, the method of label-free detection is suitable for analysis outside the laboratory, where the possibility of using special devices is limited.

1.7.1 Surface acoustic wave sensor

Surface acoustic wave (SAW) sensors are based on modulation of surface acoustic waves during interaction with material adsorbed onto the sensor surface. The sensor converts the input electrical signal into acoustic waves, which interact with the material. Then the device converts this wave back into an electrical signal. Changes in the amplitude, phase, frequency between the input and output electrical signals are used to determine the properties of the material deposited on the sensor surface [114]. Acoustic waves are transmitted within a limited guide layer, thus only slightly damping in the aquatic environment [115]. The sensitivity of the sensor increases due to changes in the design of the guide layer and the selection of more suitable materials [116]. In order to use the SAW sensor to detect biological molecules, the sensor surface is usually covered by a biolayer that is specific to the analyte. Gold layer makes it possible to functionalize the surface with self-assembled layers of thiols, while the quartz allows the use of silanes functionalization. Schematic diagram of the device SAW sensor is shown in Fig. 1.5 a. There are two interdigital transducers (IDT), the first IDT generates SAW which is propagated through the guide layer. The second IDT detects the modulated SAW and generates an electrical signal. The sensory layers are located on the delay line, which is the distance between two IDTs [117]. The binding of analytes on the modified sensing surface will affect the propagation speed and amplitude of the SAW, and as a result, on the generated output signal (Fig. 1.5 b). As a rule, changes in pressure, temperature, conductivity, dielectric coefficient, and mass can affect the propagation speed of SAW. Changes in the propagation speed v of the SAW will proportionally affect the phase p and resonant frequency f of the SAW [117].

$$\Delta v/v = -\Delta p/p = \Delta f/f \quad (1)$$

SAW sensors operate in the frequency range from 25 to 500 MHz. Increasing the initial resonant frequency can increase the sensitivity of the sensor, but it also contributes to an increase in background noise. Therefore, SAW-based microfluidic systems operate at low frequencies from 10 to 30 MHz. The sensitivity of the sensor also depends on the electromechanical coupling coefficient (K^{-2}) of the piezoelectric material, therefore materials with a higher K^{-2} such as $LiTaO_3$ are preferable for SAW sensors [116]. The use of new sensitive materials, changes in the design of sensors, as well as the integration of

SAW technology with chemical platforms such as thread network or paper-based, increases sensitivity of these methods without loss of sensitivity and portability [118,119].

SAW sensors were applied for detection of cancer biomarker (mammaglobin [120], carcinoembryonic antigen [121], protein PTHrP [122], for the detection of viral diseases (hepatitis B [84], papilloma virus [123], for Immunoglobulin G [23,124] and for many other proteins.

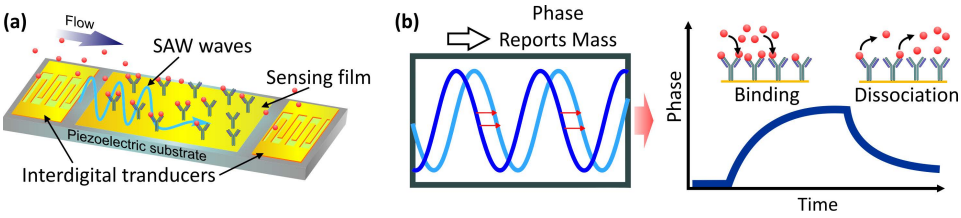

Figure 1.5. *Schematic drawing of SAW sensor design (a) and dependence of signal response to the change in SAW wave pattern on molecular interaction (b).*

1.7.2 Surface plasmon resonance sensor

Surface plasmon resonance (SPR) technology is based on the total internal reflection of a monochromatic polarized light that occurs at the interface between two transparent media with different refractive indices (Fig. 1.6 a). There is an angle of resonance at which a polarized wave will excite plasmons, which are collective oscillations of delocalized electrons. This technique detects changes in the refractive index of a metal substrate produced by any affinity binding interactions between biomolecules, immobilized on the surface of the transducer and the analyte in solution, without the need for labelling of the biomolecule [125].

The angle at which the resonance occurs is extremely sensitive to any change in the refractive index (RI) of the medium adjacent to the metal surface. The energy transfer between the incident beam and excited surface plasmons results in a reduced intensity of the reflected light, which is measured by a photodetector as the SPR signal [126]. A change in the mass on the surface of the sensor chip as a result of binding and/or dissociation of the analyte with the ligand causes a change in the angle of incidence of light due to a change in the refractive index on the surface of the chip (Fig 1.6 b).

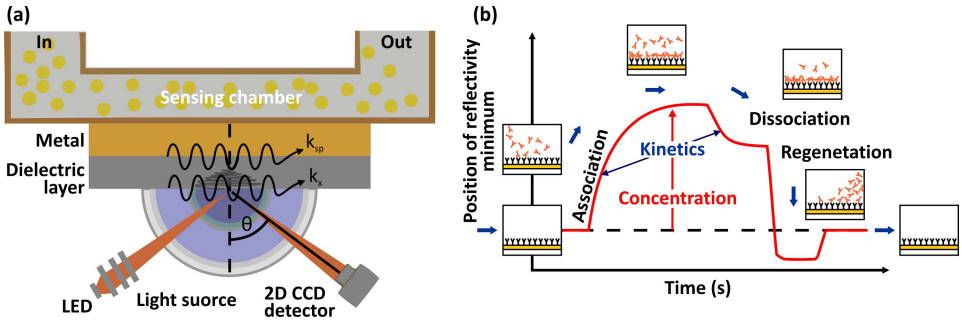

Figure 1.6. A schematic view of the SPR immunoassay technique: basic components of an instrument for SPR biosensing(a), a typical SPR biosensing experiment, showing the optical response versus time (b) [128].

The resonance angle shift can provide information on the amount of bound analyte, the affinity of the analyte for the antibody and the association (or dissociation) kinetics between the antibody and analyte [127]. Changes in the angle of incidence are monitored and recorded in the form of a sensogram, a graph of the response unit (RU or RIU) versus real time, in seconds (1 RU = 0.0001 = 1 μRIU). For most proteins and polymers, a change in 1 RU is approximately equivalent to a change in surface concentration of 1 pg/mm^2.

1.7.3 Screen-printed electrode

Screen-printed electrodes (SPEs) are sensitive disposable electrodes that can be used with portable devices [129]. SPE represents a small platform of non-conductive material (ceramics, alumina, plastic, etc.) with a working, counter and reference electrodes printed on it (Fig. 1.7 a). In the basic technology for the production of SPEs, inkjet printers are used where the particles of carbon-containing materials, silver, etc. are included in the composition of the coloring powder. The composition of the "ink" determines the properties of the electrode. Such electrodes are low in cost and easy to manufacture in bulk in any laboratory. Connected to the measuring device and coated with an analytical solution, the SPE forms an electrochemical cell. Currently, there are many SPE configurations that can be modified to analyze a specific analyte. Multiplex SPE applications have also been developed for the simultaneous detection of various analytes with an array of 8 SPEs and 96 SPEs in a standard 96-well plate [130]. The versatility of SPE allows to modify the sensor in various ways and use a wide range of electrochemical analysis methods, e.g. differential pulse voltammetry (DPV), for the detection of analytes. DPV is a voltammetry method where a series of regular voltage pulses superimposed on the potential linear sweep or stairsteps are used (Fig. 1.7 b).

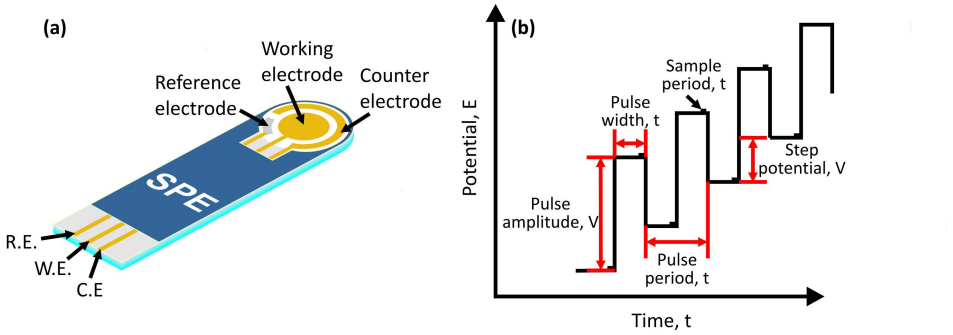

Figure 1.7. Schematic drawing of SPE design (a) and polarogram in DPV (b).

The difference in the current values at the beginning and the end of the pulse is registered. The measured current increases due to the short pulse time, while the differential measurement reduces the influence of background processes.

Protein-MIPs were successful combined with SPEs for detection of many macromolecules such as cardiac biomarker (myoglobin) [20,131], breast cancer biomarker (CA 15-3) [48], epidermal and vascular growth factors [95].

1.8 Theoretical models for analysis of adsorption process on the MIP surface

MIPs are selective adsorbents whose properties can be adjusted by the choice of functional monomers, imprint method, integration with a more sensitive transducer, etc. Therefore, it becomes necessary to evaluate the capability of various MIP films to rebind selectively the target molecule. For this purpose, the response obtained after rebind experiment were analyzed by fitting the experimental data to theoretical models of binding kinetics. Kinetics models of pseudo-first of pseudo-second order reaction allow to determine the value of the sensor response under equilibrium conditions (Q_{eq}) as well as the reaction rate constant (k)

$$Q=Q_{eq}(1-e^{-k1*t}) \quad (2)$$

$$Q=(Q_{eq2}*k2*t)/(1+Q_{eq}*k2*t) \quad (3)$$

where Q is the response upon template rebinding at time t, Q_{eq} is its value at equilibrium, k1 is a pseudo-first order rate constant, k2 is a pseudo-second order rate constant. According to the pseudo-first order kinetics model, the adsorbate binds only to a single active site on the adsorbent surface and the interactions of adsorbate and adsorbent are of physical nature, the rate of occupation of adsorption sites is proportional to the number of unoccupied sites [132]. The pseudo-second order kinetic model is used to describe strongly heterogeneous systems and also in the presence of chemisorption, where the exchange of electrons between the adsorbate and adsorbent occurs [133,134]. The applicability of this model increases with the approaching of the studied system to equilibrium [135].

The ratio between the amount of analyte adsorbed on the MIP surface and its volume concentration under equilibrium conditions at a constant temperature and pressure is described by an adsorption isotherm. The maximum adsorption capacity and the association constant can be determined from fitting parameters of theoretical isotherm models such as Langmuir, Langmuir-Freundlich. The Langmuir model is the most common model for adsorption describing. The theoretical model was developed by Langmuir in 1918 and is based on the assumptions that the adsorbate molecules do not interact with each other and each molecule occupies only one adsorption site on the homogeneous surface of the adsorbent, forming an adsorption monolayer [136].

The Langmuir model is expressed as:

$$Q=Q_{max}C/(K_D+C) \quad (4)$$

where Q and Q_{max} are the responses upon adsorbate rebinding at concentration C and its saturation value, respectively, K_D is the equilibrium dissociation constant.

To describe a heterogeneous adsorption system the Langmuir-Freundlich (LF) isotherm model is widely used. For the first time, this adsorption model was applied for MIPs characterization by Umpleby [137]. LF isotherm is a combination of a homogeneous Langmuir model and a heterogeneous Freundlich model, that makes it possible to analyze various systems at a large range of concentrations. LF describes the relationship between the equilibrium concentration of bound (Q) and free (C) adsorbent in heterogeneous systems:

$$Q=Q_{max}C^m/(K_D+C^m) \quad (5)$$

where *m* is the heterogeneity index, which can take values in the range from 0 to 1 and if values < 1, therefore material is heterogeneous [137].

Based on the calculated values of the equilibrium signals or the values of maximum adsorption, the relative adsorption capacity of MIP can be estimated using the Imprinting Factor (IF), which determines the adsorption capacity of a MIP towards a target relative to the non-imprinted polymer (NIP). IF is a general parameter used to estimate the imprinting effect, as a large value of IF connotes with the availability of more binding sites with high affinity in the resulting polymer, and is defined as [138]:

$$IF = Q_{eq(MIP)}/Q_{eq(NIP)} \quad (6)$$

or,

$$IF = Q_{max(MIP)}/Q_{max(NIP)} \quad (7)$$

where $Q_{eq(MIP)}$, $Q_{max(MIP)}$ and $Q_{max(NIP)}$,$Q_{eq(NIP)}$ equilibrium response and response at saturation of the target molecule on MIP and NIP, respectively.

1.9 Summary of the literature review and objectives of the study

Most modern analytical recognition systems use biological molecules (enzymes, DNA, antibodies), which leads to significant limitations in the design of the biosensor associated with reduced chemical and physical stability of biological receptors. Molecular imprinting technology has been widely recognized as a promising strategy for developing robust molecular recognition materials with high selectivity toward the analyte. Nowadays, MIPs are a promising alternative to natural biological receptors in biosensors providing more stable and low-cost recognition elements.

The importance of a protein for clinical diagnostics is an essential criterion when choosing a target protein for imprinting. The NF proteins, BDNF and CDNF, are potential biomarkers of various neurodegenerative diseases. However, despite the increase in the number of publications dedicated to the use of MIPs for the detection of clinically relevant proteins, the MIP capable of selective recognition of a NF protein has still not been reported. Thus, MIP film capable of selective recognition of a NF protein and coupled as a recognition layer with a label-free platform can provide a prospective solution for preparation of a low-cost robust chemosensor for real-time detection of a NF protein that represents a particular interest for clinical diagnostics.

In terms of effective protein sensing, however, it is required to develop MIP synthesis procedures that (i) do not subsequently hinder mobility and conformation of the large biomolecules in highly reticulated polymeric networks and (ii) allow their intimate integration with a suitable sensor transducer for the direct, label-free detection of molecular recognition events. The surface imprinting approach leading to the formation of polymer with imprinted sites located directly in the surface layer of the MIP films, enabling easy access to the target macromolecules, is a promising way for protein-MIP preparation. SI-C/LR photopolymerization as well as electropolymerization are particularly attractive methods for the synthesis of firmly adherent protein-MIP films directly on the surface of a sensor transducer.

The use of label-free sensor platforms, such as SPR, SAW, or SPE to create a MIP sensor, allows us to study the analytical and selective properties of MIP films without the need of labelling. Moreover, the formation of the MIP sensor based on the portable

sensor platform will allow the development of point-of-care devices capable to carry out the analysis close to a patient's bed.

The main aim of the thesis was to develop synthesis methods employing electro- and photopolymerization approaches to generate MIPs selective to NF proteins, such as CDNF and BDNF, CDNF-MIP and BDNF-MIP, respectively. The methods should allow to generate the MIP films reliably integrated with various label-free sensor platforms, such as SAW, SPR and SPE. Thus, to achieve this aim, the following objectives were specified:

- To adapt the electrochemical surface imprinting approach for formation of a CDNF-MIP film integrated with SAW;
- To develop a SI-C/LR photopolymerization approach for preparation of a protein-MIP film using a model protein. This includes finding: (i) a method for grafting of a photoinitiator on the sensor surface, (ii) optimal ratio of monomer/crosslinker and (iii) UV irradiation power and time;
- To adapt the SI-C/LR photopolymerization approach for formation of BDNF-MIP integrated with SPE;
- To study the capability of CDNF-MIP/SAW and BDNF-MIP/SPE sensor systems to detect selectively a respective target protein from aqueous solutions and synthetic serum.

2 Experimental part

2.1 MIP film formation by electropolymerization

The polymeric matrix for protein recognition was formed by electropolymerization of m-PD directly on SAW sensor surface preliminary modified with the target protein (CDNF) that was immobilized via the linker system having the cleavable S-S bond, DTSSP. The protocol for synthesis of CDNF-MIP and non-imprinted polymer (NIP) films on the sensor surface was adapted from previous work of our group [23]. Thus, preliminary the sensor surface was modified with the target protein (CDNF) immobilized via the linker system having the cleavable S-S bond, DTSSP followed by electropolymerization of mPD conducted at the constant potential (0.6 V versus Ag/AgCl/1M KCl) applied to the sensor surface until defined amount of electrical charge had been passed. To form the molecular imprints the polymer was treated in 0.1 M ethanolic solution of 2-mercaptoethanol to cleave the S-S bond in the linker system and, subsequently, in the aqueous solution of 3 M NaCl and DMSO. The respective reference films i.e those that do not have the molecular imprints of CDNF in the polymer, non-imprinted polymers (NIPs), were prepared by very similar way as CDNF-MIP but excluding the treatment in mercaptoethanol. Thus, the template proteins are still covalently retained in the NIP matrix hindering the possibility to rebind CDNF at this location.

Electropolymerization of m-PD on SAW surface was carried out in the custom-made 5-mL electrochemical cell where a constant potential was applied to the surface of the sensor until a certain amount of electric charge had been reached. The growth of poly(m-phenylenediamine) (Pm-PD) film was controlled precisely by the electrical charge dosage and its thickness was determined by a spectroscopic ellipsometer (SE 850 DUV, Sentech Instruments GmbH, Berlin, Germany). Ellipsometric parameters ψ and Δ were measured from three spots for each sample in ambient air confining the wavelength range between 380 and 850 nm at the angle of incidence of 70°. The spectra were fitted (SpectraRay 3 software) with the optical model containing a one-layer Cauchy layer on the top of the gold and the thicknesses were determined.

2.2 MIP film formation by photopolymerization

The MIP film was synthesized on the surface of the sensors by photopolymerization of a mixture of diethylaminoethyl methacrylate (DEAEM) as a functional monomer and N,N'-Methylenebis(acrylamide) (BAA) as a crosslinker. The formation of polyacrylamide matrix included four basic procedures: 1) modification of the sensor surface with an photoinitiator, 2) template protein immobilization, 3) initiation of photopolymerization by UV irradiation, 4) template removal and MIP film formation.

2.2.1 Modification gold surface by the photoinitiator

In this thesis, a two-stage method for immobilization of the photoinitiator (diethyldithiocarbamate, DEDTC) on a gold surface was developed. The SPR sensor or SPE served as a substrate for photoinitiator immobilization. The first stage is the electrochemical treated in ACN solution containing 1 mM 3.5-DClPD/p-MP, 0.1 M Bu4NBF4 by cyclic voltammetry, ramping the potential between -0.6 V and +0.5 V vs Ag/AgCl/KCl electrode for SPR sensor, and –0.1 V and 0.5 V vs Ag/AgCl/KCl electrode for SPE at a rate of 50 mV/s over two cycles. After that the sensor with grafted 3.5-DClP monolayer was immersed in an ethanolic solution of DEDTC 2 mM at room temperature for overnight. Finally,

the sensor was thoroughly rinsed with pure ethanol and Milli-Q water, dried with a nitrogen flow.

2.2.2 Protein immobilization

Two techniques for protein immobilization on the surface for further synthesis of the MIP film were applied. In addition to the simple and proven method of physical adsorption, methods of covalent immobilization of protein on the glass were applied to create a stamp for microcontact imprinting. The cover glass was modified with epoxy groups by treatment in 5% 3-GPS solution in chloroform. After that, the modified glass was incubated in a special cell with 0.05 mg/mL protein (BSA) solution in PBS buffer at room temperature for 2 h and then washed with MilII-Q water and dried with nitrogen flow.

2.2.3 Microcontact imprinting

Protein-MIP film on modified SPR sensor surface was prepared according to the following procedure. The water solution of monomers was prepared by mixing a 5mM functional monomer (DEAEM) and 20 mM crosslinking monomer (BAA). After that, 10 µL of monomers solution was dropped onto the SPR sensor surface and then cover glass with protein was immersed in this solution drop. Glass distributes over on the sensor surface a drop of the polymerization solution. Then, the all sandwich-structure was irradiated with UV light (300 W/m^2, 365 nm) at room temperature during 15 h under nitrogen atmosphere. Since during photoinitiator free radicals grafted to the sensor surface are formed the polymerization is initiated from the surface. The polymerization process carried out in a custom-made cell, which allows the synthesis of protein-MIP and NIP films at the same time on a single SPR sensor. After the polymerization process, the removal of the protein stamp and extraction of protein was carried in solution containing 0.07 M SDS and 0.2 M NaOH with heating at 80^0C. After removal of the glass from the polymer film surface, SPR sensor was washed with ethanol and then rinsed with Milli-Q water and dried with a nitrogen flow.

2.2.4 Polymerization of acrylamides on SPE surface

The prepolymerization solution was prepared by mixing 12.5 µg/mL BDNF, 2.5 mM functional monomer (DEAEM) and 15 mM cross-linking monomer (BAA) in 0.05 M PBS. The prepolymerization solution (10 µL) was dropped onto the DEDTC-modified SPE sensor and left for 30 min for physical adsorption of the protein on the electrode surface. Before the photopolymerization the SPE with drop of prepolymerization solution was covered with a mask with a hole 20% larger than the diameter of the working electrode. The photopolymerization was carried out directly on the working electrode surface under UV irradiation (500 W/m^2, 365 nm) at room temperature for 30 min. Further, the electrode was alternately immersed in aqueous solution 0.2 M NaOH and 10% acetic acid for 30 min at vortex circulation (600 rpm) to finally remove the protein from the polymer matrix. After that the SPE was washed with MQ and dried under nitrogen flow. NIP film was produced in the same way only the prepolymerization solution was prepared without the addition of BDNF.

2.3 Rebinding and selectivity studies of protein-MIP films

2.3.1 Surface acoustic wave (SAW)

The recognition properties of the synthesized CDNF-MIP films towards CDNF were evaluated by the SAW-based biosensor system (Sam®X, NanoTemper Technologies GmbH, München, Germany), capable of handling two SAW chips with four sensor elements each. The SAW chips, modified with CDNF-MIP and respective reference, NIP films were loaded into the SAW system and equilibrated with running buffer (PBS, pH 7.4) until a stable baseline was established. Then the consecutive injections of the analyte solutions at a flow rate of 25 µL/min in the order from lower to higher concentrations were applied and the signal responses (sensorgrams) were monitored. The association phase lasted 12 min and was interrupted by washing the sensor surface with PBS solution for 20 min (the dissociation phase).

2.3.2 Surface plasmon resonance (SPR)

BSA rebinding on the synthesized BSA-MIP films was studied by SPR. The SPR measurements were performed using a two channels SPR system (SR7500DC, Reichert Technologies Inc., Depew, NY, USA). The modified SPR sensor with BSA-MIP and NIP films was loaded into the system and equilibrated with a degassed PBS buffer solution (pH = 7.4) at a flow rate of 25 µl/min until a constant baseline of SPR sensor response was reached. Subsequently, the various concentrations of the analyte samples (BSA solutions in PBS buffer) were injected into the flow stream by the autosampler (SR7120). The SPR sensor was regenerated by injecting 1% NaOH after each injection of the analyte. The SPR system was controlled SPRAutolink software (v. 1.1.10-G).

2.3.3 Screen-printed electrode (SPE)

The binding affinity and selectivity of the BDNF-MIP films on SPE toward the target protein were determined by means of differential pulse voltammetry (DPV). Measurements were performed in the 1 M KCl solution containing 4 mM redox probe $K_3[Fe(CN)_6]/K_4[Fe(CN)_6]$. The DPV was recorded from 0 V to 0.4 V with pulse amplitude of 0.025 V, width of 0.05 s and 0.001 V step potential. The DPV curves were recorded after 30 minutes incubation of BDNF-MIP- and NIP-modified SPE sensor in solutions with increasing concentration of the analyte. After that, unbound target protein was removed by washing twice in PBS buffer for 5 minutes with a vortex circulation (600 rpm).

3 Result and discussion

3.1 MIP film by electropolymerization

The electrochemical surface imprinting approach was employed in this study to generate CDNF-MIP films with the macromolecular imprints situated at/close to the surface of the polymeric film. According to this approach the polymeric matrix was formed by electropolymerization directly on the sensor surface preliminary modified with the target protein (CDNF) that was immobilized via the linker system having the cleavable S-S bond, DTSSP. The protocol for synthesis of CDNF-MIP films on the sensor surface was adapted from previous work of our group [23].

The CDNF-MIP film was synthesized on the SAW chip by electropolymerization of m-phenylenediamine. The oxidation potential of monomer for coulometric deposition of polymer was selected on the basis of cyclic voltammetry curves for m-phenylenediamine, obtained in the range of potentials from 0 to 0.9 V (Fig. 3.1 a). The potential of 0.6 V, a slightly more positive than the $E_{1/2}$ potential (0.56 V) for the oxidation of m-phenylenediamine [139] was selected for electropolymerization. This made it possible to obtain homogeneous films with a controlled thickness by adjusting the charge passing through the surface of the electrode. Depending on the amount of charge the process of electropolymerization lasted from 0.3 to 7.3 seconds (Fig. 3.2 b), which significantly reduces the effect of electrochemical processes on the conformation of the protein.

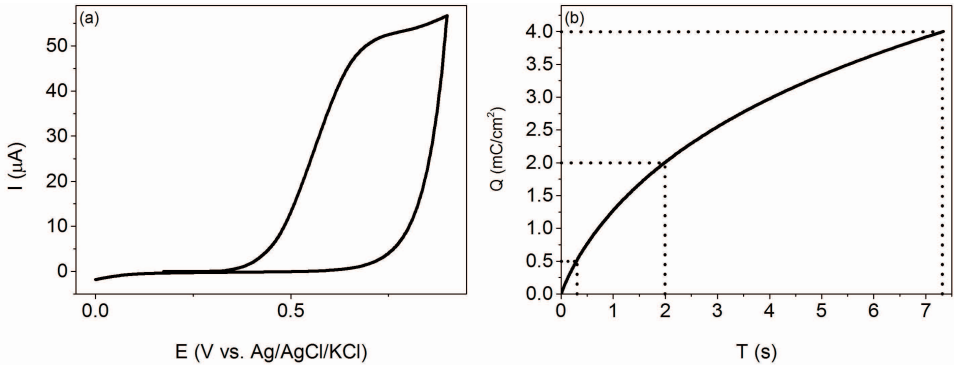

Figure 3.1. Cyclic voltammograms at the scan rate of 50 mV/s (a) and chronocoulometry (b) of 10 mM m-PD in PBS performed on a gold electrode surface modified by 4-ATP/DTSSP/BDNF.

For MIP synthesis by electrochemical surface imprinting approach, the deposition of a polymer with an appropriate thickness is one of the most crucial tasks in order to avoid irreversible entrapment of a macromolecular template and infeasibility of its removal during the subsequent washing out procedures. In order to choose the range of the appropriate thicknesses for the polymer film, which confines, but does not irreversible entrap CDNF, the length of the whole structure containing the linker system and CDNF, was theoretically estimated (Fig. 2, Paper I).

Assuming that covalent attachment of CDNF via the succinimidyl group of DTSSP proceeds predominantly through its lysine residues that are abundant in the protein, the size of the resulting structure with random orientations of CDNF might vary from 5.1 to 7.5 nm. Thus, polymer films confining the immobilized CDNFs till the middle of their possible front dimensions i.e. films with thicknesses between approx. 3.4 and 4.6 nm would be a good starting point in finding an optimal one for CDNF-MIP.

Several polymer films were synthesized in order to study the effect of the amount of electrical charge applied during the in-situ electrodeposition on the thickness of the resulting polymer film. It was found that the film thickness depends linearly on the applied charge value (Fig. 3.2), that made it possible to quite accurately determine the film thickness by controlling the amount of applied charge. The difference in the thicknesses of MIP and NIP films can be associated with a partial loss of short polymer chains during the procedure of removing the template from the matrix. The optimal thickness was elucidated after calculation of the molecular imprinting effect or the imprinting factor (IF) for every pair of CDNF-MIP and NIP characterized by the same thicknesses. The experiments revealed only marginal differences in responses between CDNF-MIP- and NIP-modified sensor elements (Fig. 3a, Paper I) most likely due the intrinsic affinity of PmPD-based matrix to CDNF resulting in significant non-specific binding.

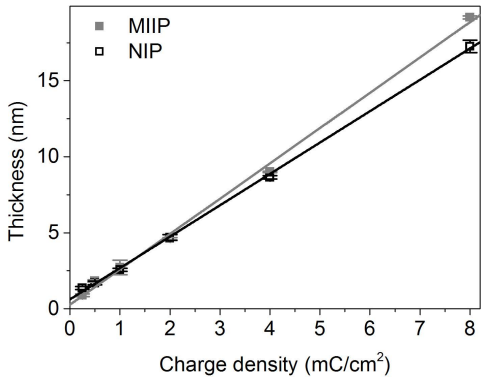

Figure 3.2 The calibration graph representing the dependence of the polymeric thickness of MIP and NIP films, as measured by VIS-ellipsometry, on the amount of the charge consumed during the electropolymerization of m-PD on CDNF-modified gold electrode. The solid lines represent linear regression fits.

In order to reduce the non-specific binding, the CDNF-MIP and NIP films underwent the treatment in 0.01 M PBS solution containing 0.04 mg/mL HSA beforehand the rebinding experiments. Since HSA is significantly larger than CDNF and for this protein, there are no specific binding sites on the CDNF-MIP surface, the HSA can bind to the polymer film only in a non-specific way and suppress nonspecific adsorption of CDNF on both surfaces of the CDNF-MIP film and on NIP film. After pre-treatment in HSA solution, the CDNF-MIP film obtained using a charge of 2 mC/cm^2 corresponding to the thickness of 4.7 nm showed the highest relative rebinding of CDNF as judged by IF of approx. 2.0 (Fig. 3 b, Paper I). At such thickness the polymer confines about the median dimension of CDNF, and, in turn, likely does not hinder its successful extraction to leave behind a selective molecular cavity. The found optimal thickness correlates well with the concept of surface imprinting approach used in this study.

3.2 MIP film by photopolymerization

In this thesis, a SI-C/LR photopolymerization approach for synthesis a protein-MIP film reliably interfaced with a sensor surface was developed. Firstly, BSA as a model protein for imprinting and SPR as a convenient sensor platform were used to proof of concept (Fig. 1, Paper II). In the course of work, the problems of grafting the photoinitiator to the surface, creating a protein stamp, finding an optimal ratio of monomer and crosslinker

in the polymerization medium and UV irradiation power and time were solved. Subsequently, the developed method was adapted for the synthesis of BDNF-MIP films on the SPE surface (Fig. 1, Paper III).

3.2.1 Grafting of the photoinitiator to the gold surface

To apply a method of surface-initiated polymerization the photoinitiator should be attached to the electrode surface (Fig. 1.3). The electrochemical reduction of diazonium salts is widely used to modify the gold surface and allows the grafting of various functional groups on the metal surface, depending on the substituent on the phenyl group [140]. As a result of the modification of the gold surface by 3,5-DClP or p-MP layers, the easily accessible chlorophenyl or maleimide groups, respectively, were attached to the electrode surface. The photoinitiator, DEDTC, was subsequently attached to the gold surface by an electrophilic substitution or addition reaction with pre-deposited layers of 3,5-DClP or p-MP. Under the action of UV light the initiator molecule decomposed into two radicals. The active radicals at the surface were involved in the nucleation of the polymer chain, while the inactive radicals were migrated into the polymerization solution and participated in the chain growth (Paper II).

Analysis of the gold surface with deposited 3,5-DClP/p-MP layers using CV and EIS methods showed an increase in charge transfer resistance, that indicates the formation of thin organic layers on the electrode surface. The XPS data confirmed the successful functionalization of gold by 3,5-DClPDT, p-MPDT electrochemical reduction revealing the presence of Cl and N elements, respectively (Fig. 5, Paper II). The photoinitiator attachment to the functionalized surface was assessed by analyzing the S2p core level region of XPS spectra since the photoinitiator compound contains S=S bond. It can be seen that in the case of photoinitiator grafting through the 3,5-DClP-layer the intensity of the peak at 162 eV is higher compared to the p-MP- modified surfaces. At the same time, the presence of peak at 163.7 eV corresponding to S in the S-S bond in the spectra of p-MP-modified surface can be attributed by the formation of a disulfide bridge between two photoinitiator molecules obviously induced by the UV-light treatment what was not the case for the 3,5-DClP surface functionalization. As a result, the part of initiator can be excluded from the further photopolymerization process. Taking into account all aforesaid, it was decided to select 3,5-DClP as the primary linker for photoinitiator grafting to ensure required surface quality for subsequent formation of the protein-MIP film formation.

3.2.2 Optimization of the photopolymerization conditions

To obtain a highly selective MIP it is essential that the target protein preserves its conformation during the imprinting process. Therefore, the effect of the intensity and duration of UV irradiation on the protein 3D structure was studied by DLS-based particle size analysis and UV-Vis spectroscopy. Analysis of the UV-Vis spectra showed that after UV irradiation with a power of 500 W/m^2 for 3 and 4 hours, a shift of the absorption bands (289.7, 288, and 281 nm) and the appearance of new peaks in the spectra of the BSA solution are observed (Fig. 6 a, Paper II). Changes in the UV-Vis spectra can be explained by conformational changes in the protein structure after UV irradiation, as a result of which the chromophores of aromatic amino acids enter the more polar environment. The DLS analysis of the protein molecular size supported that after 3 h of UV exposure (500 W/m^2), significant changes in the structure of the protein occurred since the amount of BSA molecules in their native monodisperse form (hydrodynamic diameter 7.4 nm) is substantially reduced (Fig. 6 b, Paper II). At the same time, it was

found that irradiation with a lower intensity (300 W/m^2) does not cause such a strong change in the conformation of the protein and its native form remains intact (Fig. 6 c-d, Paper II).

Since the interaction between the protein and the polymer matrix is based on non-covalent interactions it is extremely important to minimize the non-specific interactions between a MIP matrix and a protein that can be achieved, for example, by a proper adjustment of the hydrophilicity of the polymer matrix by optimizing the ratio of monomer/crosslinker. Due to the high content of hydrophobic ethyl groups the DEAEM monomer can lead to the formation of a hydrophobic surface promoting the nonspecific adsorption of a protein, which adversely affect the selectivity of MIP film. In this regard, it is necessary to reduce the influence of hydrophobic non-specific interaction by optimizing the ratio of the hydrophobic monomer, DEAEM, and the hydrophilic cross-linker, BAA. Moreover, the monomer/crosslinker ratio can influence the textural properties of the polymer. Thus, the insufficient numbers of cross-links leads to the formation of a polymer matrix with a low specific area and, as a consequence to a low capacity of MIP, while the excessive numbers of cross-links leads to the formation of very narrow pores and decrease in the number of functional groups resulting in the hindered interaction of the protein with MIP [56]. Therefore, the polymer films were synthesized at different DEAEM/BAA ratios and the contact angles (CA) of the films were measured in order to determine an optimal value of the ratio to produce a polymer of sufficient hydrophilicity. As can be seen in Fig. 3.3, the CA value of the polymer film decreases from 30.7° down to 12.6° along with decreasing monomer/crosslinker ratio, i.e. with increasing the fraction of the more hydrophilic BAA crosslinker. Thus, hydrophilicity of the resulting polymer matrix can be easily manipulated by adjusting the ratio of monomer/crosslinker in the polymerization solution.

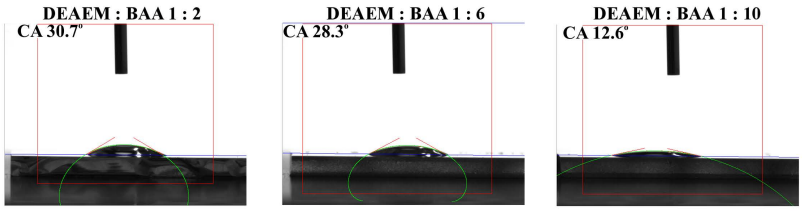

F*igure 3.3 Droplets of ultrapure water on the polymer surfaces prepared with the different DEAEM/BAA ratios.*

3.2.3 Synthesis of BSA-MIP

First, to implement the microcontact imprinting method, a protein stamp was prepared. As a substrate for the formation of the protein stamp, a thin cover glass transmitting ultraviolet radiation in the desired range (340-380 nm) was used. Modification of the cover glass by epoxy groups was implemented with the method of silanization. Silanization is a low-cost, effective, and widely used method for covalent modification of silicon-containing substrates. The technique for covalent immobilization of a protein on a glass surface through the formation of amide ether bonds between amino groups of protein and the epoxy groups of the 3-GPS linker was developed [141]. The quality of protein immobilization (BSA was chosen as a model protein) on an epoxy-silane coverslip was demonstrated using epifluorescence optical microscopy and a fluorescein-BSA isothiocyanate (FITC-BSA) to visualize protein adsorption on the glass surface. The results of epifluorescence optical microscopy showed that the interaction of FITC-BSA with the

glass surface causes a significant and uniform increase (Fig.2, Paper II) in the green fluorescence intensity over the entire glass surface, which indicates the formation of a homogeneous layer of protein on the surface.

The chosen approach for the synthesis of MIP provides the opportunity for the formation of specific binding sites on the surface of the polymer film and is able to prevent complete entrapment of protein in the polymer matrix. Overgrowing of protein by polymer is prevented by a cover glass, on the surface of which target proteins are covalently immobilized. The BSA-MIP film was synthesized on the surface of an SPR chip preliminarily modified by a photoinitiator. To the simultaneous formation of a BSA-MIP film and a non-imprinted film on the surface of a SPR chip, the formation of a protein stamp and subsequent photopolymerization are carried out in specially designed cells for accurately position of cover glass section with and without immobilized protein above the SPR chip surface. The SPR chip previously modified by photoinitiator was placed on the bottom. A drop of the solution containing the functional monomer (DEAEM) and a cross-linker (BAA) was applied on the sensor surface. The cover glass distributed the solution over the surface. The cover glass with the protein monolayer was positioned in such a way that the monolayer was at the bottom. The closed cell design allowed the photopolymerization under nitrogen atmosphere. After polymerization, the sandwich-structure was placed in a solution to separate the protein stamp and the BSA-SPR sensor. Since the protein is covalently immobilized on the cover glass surface, the removal of the protein from the polymer matrix occurred simultaneously with the separation of the sandwich-structure.

3.2.4 Synthesis of BDNF-MIP

The SI-C/LR photopolymerization approach developed for the formation of BSA-MIP was adapted for synthesis of BDNF-MIP film on SPE. However, the approach was modified, since using microcontact imprinting, a quite thick polymer film was formed on the surface, as a result a blocking polymer layer was formed on the electrically conductive surface, which prevented the electrochemical detection of the protein (Fig. 3.4). In this regard, a physical adsorption of the protein on the gold surface modified with the photoinitiator was used. The polymer growth started directly from the photoinitiator-modified gold surface and continued as long as UV radiation was applied. The excessive overgrowing of the polymer around BDNF molecules was prevented by controlling the UV exposure time. To determine the optimal exposure time, the IF for the BDNF-MIP films prepared with different UV exposure times was determined. It was found that the highest IF was obtained for BDNF-MIP film synthesized under UV irradiation of 500 W/m^2 for 30 minutes (Fig. 4, Paper III). As it was previously shown (see section 3.2.3) the irradiation power of 500 W/m^2 during less than 2 h did not result in significant changes in protein conformation.

3.3 Characterization of the protein-MIP films

The prepared protein-MIP films were reliably integrated with the label-free sensor system (SPR, SPE, SAW) that allowed real-time monitoring the events of molecular interaction between the MIP and target protein. The binding parameters of the target molecule with the MIP film were determined by constructing the adsorption isotherms as well as the selectivity of MIP-modified sensors to the target molecule was evaluated.

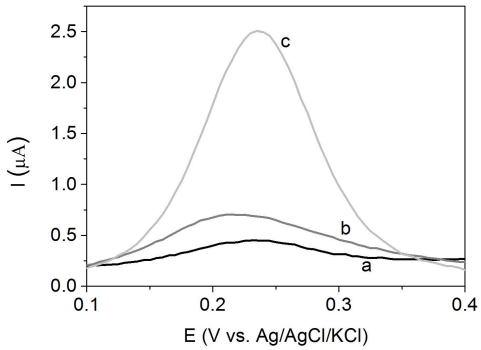

Figure 3.4 Typical DPV curves of the BDNF-MIP modified SPE obtained by combination methods of SI-C/LR photopolymerization and microcontact imprinting irradiated with UV light 300 W/m² at room temperature during 15 h (a); irradiated with UV light 500 W/m² at room temperature during 2 h (b); DPV curves of the BDNF-MIP/SPE obtained by only SI-C/LR photopolymerization with irradiated 500 W/m² at room temperature during 0.5 h (c).

3.3.1 CDNF-MIP interfaced with SAW

The CDNF protein rebinding experiment was performed using SAW sensor platform. The multichannel design of the SAW system made it possible to distinguish the surface of the SAW chip into 4 sections and to synthesize NIP and CDNF-MIP films on one SAW chip. This made available to carry out experiments with NIP and CDNF-MIP films at the same time and thus, avoid the influence of environmental changes on the differences in the response of the CDNF-MIP/SAW and NIP/SAW on the injection of different concentrations of CDNF in PBS. Since the NIP film is a MIP film with a completely occupied specific binding sites by target protein, then only nonspecific protein adsorption is possible on such a surface. Therefore, to reduce the effects of not specific adsorption the binding profiles observed in the association phase for CDNF-MIP surfaces were corrected by subtracting the corresponding binding profiles on the NIP surfaces. After correction of the responses of the CDNF-MIP/SAW sensor, well-defined binding profiles depending on the analyte concentration were obtained, which gave good fit to the pseudo-first order kinetic model with a determination coefficient (R^2) in the range of 0.944-0.994. The binding capacity of CDNF-MIP for CDNF was determined by plotting the dependence of equilibrium response (Q_{eq}) on the concentration of CDNF in PBS solution (Fig. 4, Paper I). The data, fitted to a Langmuir-Freundlich model, showed a dissociation constant (K_D) of 4 μg/mL of CDNF and the response at saturation (Q_{max}) of 2 deg. of MIP.

The selectivity of the CDNF-MIP/SAW to CDNF was evaluated by analyzing the sensor responses upon injections of an interfering protein. MANF was chosen as an interfering protein that has the same molecular weight and is identified to be homologous to CDNF with 59% amino acid identity in human proteins [10]. In order to simulate additional complexity in scenarios for the selectivity testing, the test was carried out in the presence of a constant concentration of mCD48. The CDNF-MIP/SAW demonstrated good selectivity to CDNF as compared to MANF. The difference in the sensor response upon injections of CDNF and MANF increased with increasing the concentration. In the concentration range from 50 ng/mL and above, the responses towards CDNF were four times higher than those towards MANF. Under these conditions the CDNF-MIP/SAW shows a linear response to CDNF in the concentration range from 5 to 50 ng/mL, with limit of detection (LOD) equal 4 ng/mL and limit of quantitation (LOQ) 14 ng/mL.

The selectivity of the CDNF-MIP was further examined by a competitive binding assay performed in a label-free manner. In this assay various concentrations of CDNF or MANF were allowed to compete with the constant concentration of IgG for the binding sites in CDNF-MIP film. The results showed that CDNF inhibited IgG binding on CDNF-MIP better than MANF i.e. bound with CDNF-MIP film more preferentially than MANF (Fig. 6, Paper I). Analysis of the S-shaped dose-response curves showed that the IC50 value was lower in case of CDNF injection than MANF, 0.6 and 0.9 pg/mL, respectively. The normalized response decreased (about 75 %) upon injection of the mixture containing 0.01 ng/mL CDNF, i.e. obviously, the heavier protein (IgG) was replaced with the lighter one (CDNF). Conducting the very same competitive assay with MANF instead of CDNF, resulted in much less inhibition of the response (about 15 %), that is, the replacement of IgG from the recognition sites was less efficient in this case. If both CDNF and MANF competed with IgG in the same solution, then it was still clearly seen that the significant inhibition of the signal was induced namely by the presence of CDNF in the sample rather than the presence of MANF (Fig. 3.5).

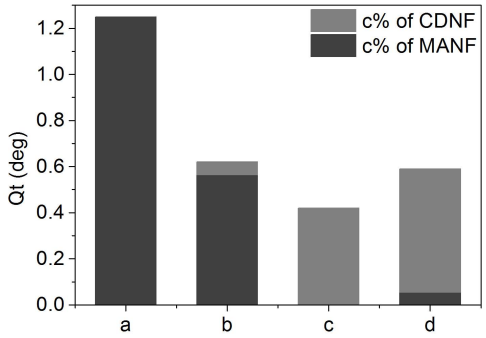

Figure 3.5. Values of Q_{eg} obtained by CDNF-MIP/SAW upon applying the samples containing a fixed concentration of IgG (500 ng/mL) and (a) MANF (10^{-2} ng/mL), (b) MANF (10^{-2} ng/mL)+CDNF (10^{-3} ng/mL), (c) CDNF (10^{-2} ng/mL), (d) CDNF (10^{-2} ng/mL)+MANF (10^{-3} ng/mL).

Thus, CDNF-MIP/SAW could selectively respond to CDNF, confirming that the CDNF specific binding sites were formed in the polymer matrix in the course of the electrochemical surface imprinting approach.

3.3.2 BSA-MIP interfaced with SPR

The protein rebinding experiment on BSA-MIP/SPR was conducted using various concentrations of BSA in PBS buffer. The specificity of interactions was evaluated by comparing the binding profiles for BSA obtained with BSA-MIP/SPR and NIP/SPR under the same conditions. This allowed to correct a non-specific binding component in the BSA-MIP/SPR measured response. Injections of BSA solution caused an increase in the refractive index, due to adsorption of BSA molecules on the BSA-MIP surface, and this process was gradually reaching the equilibrium (association phase). In order to eliminate erroneous environmental influences, the binding profiles observed in the association phase on the BSA-MIP surfaces were corrected by subtracting the corresponding binding profiles on the NIP surfaces. The corrected binding profiles clearly show preferential binding of BSA to BSA-MIP even at a BSA concentration of 2.5 nM (Fig. 7, Paper II). However, during the correction process, it was not possible to completely neutralize the bulk shift effect, which was apparently associated with stronger changes in the refractive index on the BSA-MIP surface than on the NIP surface. It was found that the dependence of equilibrium responses on analyte concentration was well described by the equation

of the Langmuir adsorption isotherm (R^2 = 0.992) (Fig. 8, Paper II). The dissociation constant (K_D) is related to the affinity of the BSA-MIP film towards BSA. Fitting results showed that BSA-MIP/SPR had high binding affinity (K_D = 68.12 nM) and maximum capacity equal 6.7 µRIU. Since the protein adsorption very often takes the form of the Langmuir isotherm, but at the same time, the necessary conditions for applying this adsorption model are not always met, the fitting results were confirmed by calculating the K_D using the *k-observed* plot. The linear response of the BSA-MIP/SPR sensor to BSA injections was found in the range from 2.5 nm to 25 nm. Fitting of practical data to linear regression gives good R^2 = 0.970, which allowed to calculate the LOD and LOQ equal to 5.6 nM and 18.7 nM (or 370 ng/mL and 1.2 µg/mL), respectively.

The selectivity analysis of the BSA-MIP/SPR sensor was performed using competing protein solutions with the same concentration, that included the human serum albumin (HSA) and the Fc fragment of IgG (Fc). As expected, the response of the BSA-MIP/SPR sensor on injection of BSA solution was about 2 times higher than those appeared upon injection of the interfering proteins, indicating that the BSA imprinted SPR sensor showed good selectivity to the target protein. It should be noted that the non-imprinted reference film (NIP) demonstrates only slight differences in binding between BSA, HSA and Fc (Fig. 10, Paper II).

3.3.3 BDNF-MIP interfaced with SPE

The developed SI/C-LR photopolymerization approach was applied to prepare BDNF-MIP/SPE. The analytical performance of the BDNF-MIP was characterized by differential pulse voltammetry (DPV). The DPV curves were recorded after incubation of BDNF-MIP/SPE and NIP/SPE in solutions with increasing concentration of the analyte (from 0.1 to 100 ng/mL of BDNF in PBS buffer). Normalized signals of current were used to plot the intensity of the response of the BDNF-MIP/SPE as a function of the analyte concentration in the solution. The data obtained were in good fit with the theoretical adsorption Langmuir model. The fitting results showed that BDNF-MIP bound the target protein, BDNF, with a dissociation constant K_D of 1.12 ng/mL and had about 5.8 times higher binding capacity than NIP as judged by the respective Q_{max} values (0.92 vs 0.16 a.u.) The detectability of BDNF-MIP/SPE towards BDNF was studied in the presence of a fixed concentration of HSA. Analysis of the regression curve gives the LOD and LOQ values of 6 pg/mL and 20 pg/mL of BDNF, respectively (Fig. 7, Paper III).

The BDNF-MIP/SPE was characterized in terms of its capability to rebind selectively the target protein, BDNF, with respect to the interfering proteins of slightly different size and isoelectric point (pI) such as CDNF, MANF, and mCD48. Selection of CDNF and MANF as interfering analytes was stipulated by their permanent presence in a human serum and thus, they can interfere with the sensor response along with the target protein (BDNF). The third interfering analyte – mCD48 – has the molecular weight and pI value similar to those of BDNF. The selectivity of the sensor was studied in the presence of HSA at a concentration of 0.8 mg/mL, corresponding to a 50-fold dilution of its physiological norm in diluted human serum. For the selectivity study, the concentration of the interfering proteins was selected close to their LOQ value (0.02–0.06 ng/mL). The experimental results confirmed that the BDNF-MIP/SPE had the higher response to BDNF as compared to interfering proteins (Fig. 8, Paper III). When the protein concentration was lower than the LOQ level the BDNF-MIP/SPE did not show a clear preferential binding of the target protein, but at a concentration of 20 pg/mL, this difference became more pronounced and increased with increasing protein concentration.

3.4 Reusability potential of the protein-MIP sensors

The reusability of MIP-based chemosensors can have a big impact on their economic efficiency and decrease the time to market. In this work, CDNF-MIP/SAW, BSA-MIP/SPR and BDNF-MIP/SPE underwent regeneration procedure, which corresponded to that applied for removal of the protein from the polymer matrix after polymerization (Paper I, II, III). The studies showed that the possibility of regeneration of the CDNF-MIP/SAW was limited. After the first regeneration cycle, the intensity of the response of the sensor significantly dropped and at the same time, the standard deviation (SD) increased (Fig. 3.6a). This phenomenon apparently may be associated with the loss of part of the polymer matrix during the regeneration procedure, since the polymer does not have cross-links and, as a result, the m-PD polymer chains stick together only due to π-π interactions. In turn, the protein-MIP obtained by photopolymerization of DEAEM in the presence of the cross-linker (BAA) had improved reusability. BSA-MIP/SPR showed nearly reproducible responses with low relative SD 3.2% even after the 25th regeneration cycle (Fig. 3.6 b).

Thus, the presence of crosslinks in a MIP improves the mechanical stability of the polymer and, as a result, increases the reusability potential of the sensor. However, the protein-MIPs prepared by the similar photopolymerization approach on SPE had only limited reusability. The response of the BDNF-MIP/SPE against BDNF significantly decreased after the first regeneration cycle, nevertheless, the relative SDs of the responses obtained from the freshly prepared and once regenerated sensors were comparable, 4.5% and 3.6%, respectively (Fig. 3.6c). Apparently, this could be associated with the design features of the SPEs that were originally intended for single-time use. Thus, BDNF-MIP/SPE can be regenerated at least once. It is also necessary to take into account that after the regeneration cycle the sensors have to be calibrated again due to change in the sensor's response versus one at the zero cycle.

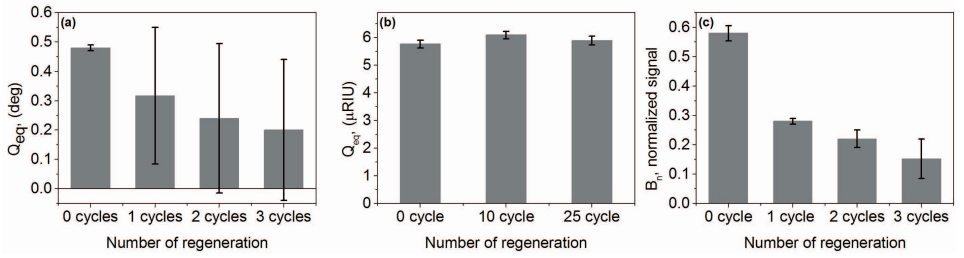

Figure 3.6. Potential reusability of CDNF-MIP, equilibrium responses, Q_{eq}, obtained from the CDNF-MIP/SAW upon injection of 1.25 μg/mL of CDNF in PBS (a); BSA-MIP, equilibrium responses, Q_{eq}, obtained from the BSA-MIP/SPR sensor upon injection of 450 nM BSA in PBS buffer (b); BDNF-MIP, normalized responses of the BDNF-MIP/SPE upon the injection of 2 ng/mL of BDNF in PBS (c).

Conclusions

This thesis firstly reported the preparation of polymer films molecularly imprinted with a neurotrophic factor protein (CDNF-MIP and BDNF-MIP). The developed synthesis methods employing the electro- and photopolymerization techniques allowed the robust integration of the NF-MIP films with the label-free sensor platforms. The following specific conclusions can be drawn from the study:

- The electrochemical surface imprinting approach enabled a simple and rapid preparation of CDNF-MIP directly on SAW sensor surface (CDNF-MIP/SAW).
- The resulting CDNF-MIP bound the target, CDNF, with K_D values of 8 µg/mL and demonstrated notable IF (2.0) with the polymer film thickness of 4.7 nm and after the treatment in HSA solution aiming to suppress the intrinsic affinity of PmPD-based matrix towards CDNF.
- The CDNF-MIP/SAW sensing system could detect CDNF with LOD value of 4 ng/mL in the presence mCD48 as an interfering protein. In the competitive assays the system notably differentiated between CDNF and its homologue – MANF at pg/mL levels in the presence of IgG at sub µg/mL levels.
- The electropolymerized CDNF-MIP film had a limited regeneration capability: the response of CDNF-MIP/SAW was significantly decreased already after the first regeneration cycle.
- The SI-C/LR photopolymerization approach for synthesis of a protein-MIP directly on the sensor surface was developed. The approach based on the combination of SI-C/LR photopolymerization and microcontact imprinting allowed the formation of protein-MIP films robustly interfaced with the sensor transducer.
- The conditions for synthesis of a protein-MIP by SI-C/LR photopolymerization were determined using BSA as a model protein. It was revealed that (i) the photoinitiator (DEDTC) can be easily tethered to a gold sensor surface via 3.5-DClP layer formed by electrochemical reduction of 3.5-DClPDT, (ii) decreasing the ratio of monomer:crosslinker (DEAEM:BAA) increased hydrophilicity of the resulting polymer matrix, (iii) the UV irradiation power - 500 W/m^2 or 300 W/m^2 during 0.5 or 15 hours, respectively - did not significantly affect the protein conformation.
- The BSA-MIPs prepared on SPR by SI-C/LR photopolymerization demonstrated the improved regeneration capability, withstanding at least 25 cycles in an alkaline solution within relative SD 3.2%.
- SI-C/LR photopolymerization was successfully applied to prepare BDNF-MIP on SPE (BDNF-MIP/SPE). BDNF-MIPs demonstrated IF of 5.8 and K_D of ca. 1 ng/mL, but they could be regenerated at least once. The BDNF-MIP/SPE could detect BDNF with LOD value of 6 pg/mL and quantify BDNF with the LOQ value of 20 pg/mL in the presence of HSA as a highly abundant serum protein. Moreover, the sensor was able to discriminate BDNF among analogous molecules, i.e. CDNF and MANF, and a molecule of a similar size, i.e. mCD48.
- The presented synthesis approaches were proved to be suitable for preparation of MIP-sensors capable of selective detection of NF proteins and could be a promising route towards the development of innovative point-of-care diagnostics tools for the early-stage diagnostics of neurological diseases or monitoring therapies.

References

[1] P. Gold, S.O. Freedman, Demonstration of Tumor-Specific Antigens in Human Colonic Carcinomata by Immunological Tolerance and Absorption Techniques, J Exp Med. 121 (1965) 439–462.

[2] N.L. Anderson, The Clinical Plasma Proteome: A Survey of Clinical Assays for Proteins in Plasma and Serum, Clinical Chemistry. 56 (2010) 177–185.

[3] P. Steffen, M. Kwiatkowski, W.D. Robertson, A. Zarrine-Afsar, D. Deterra, V. Richter, H. Schlüter, Protein species as diagnostic markers, Journal of Proteomics. 134 (2016) 5–18.

[4] S.V. Hegarty, G.W. O'Keeffe, A.M. Sullivan, Neurotrophic factors: from neurodevelopmental regulators to novel therapies for Parkinson's disease, Neural Regen Res. 9 (2014) 1708–1711.

[5] A. Cattaneo, N. Cattane, V. Begni, C.M. Pariante, M.A. Riva, The human BDNF gene: peripheral gene expression and protein levels as biomarkers for psychiatric disorders, Transl Psychiat. 6 (2016).

[6] K. Hashimoto, Brain-derived neurotrophic factor as a biomarker for mood disorders: An historical overview and future directions (vol 64, pg 341, 2010), Psychiat Clin Neuros. 64 (2010) 341–357.

[7] C. Laske, E. Stransky, T. Leyhe, G.W. Eschweiler, A. Wittorf, E. Richartz, M. Bartels, G. Buchkremer, K. Schott, Stage-dependent BDNF serum concentrations in Alzheimer's disease, J Neural Transm. 113 (2006) 1217–1224.

[8] D. Lindholm, J. Makela, V. Di Liberto, G. Mudo, N. Belluardo, O. Eriksson, M. Saarma, Current disease modifying approaches to treat Parkinson's disease, Cell Mol Life Sci. 73 (2016) 1365–1379.

[9] S. Sen, R. Duman, G. Sanacora, Serum brain-derived neurotrophic factor, depression, and antidepressant medications: Meta-analyses and implications, Biol Psychiat. 64 (2008) 527–532.

[10] M. Lindahl, M. Saarma, P. Lindholm, Unconventional neurotrophic factors CDNF and MANF: Structure, physiological functions and therapeutic potential, Neurobiol Dis. 97 (2017) 90–102.

[11] H. Zhao, L. Cheng, X.W. Du, Y. Hou, Y. Liu, Z.Q. Cui, L. Nie, Transplantation of Cerebral Dopamine Neurotrophic Factor Transducted BMSCs in Contusion Spinal Cord Injury of Rats: Promotion of Nerve Regeneration by Alleviating Neuroinflammation, Mol Neurobiol Mol Neurobiol. 53 (2016) 187–199.

[12] W.J. Cheong, S.H. Yang, F. Ali, Molecular imprinted polymers for separation science: a review of reviews, J Sep Sci. 36 (2013) 609–628.

[13] L. Ye, K. Mosbach, Molecular imprinting: Synthetic materials as substitutes for biological antibodies and receptors, Chem Mater. 20 (2008) 859–868.

[14] T.S. Bedwell, M.J. Whitcombe, Analytical applications of MIPs in diagnostic assays: future perspectives, Anal Bioanal Chem. 408 (2016) 1735–1751.

[15] K. Haupt, K. Mosbach, Molecularly imprinted polymers and their use in biomimetic sensors, Chem Rev. 100 (2000) 2495–2504.

[16] B.T.S. Bui, K. Haupt, Molecularly imprinted polymers: synthetic receptors in bioanalysis, Anal Bioanal Chem. 398 (2010) 2481–2492.

[17] R. Schirhagl, Bioapplications for Molecularly Imprinted Polymers, Anal Chem. 86 (2014) 250–261.

[18] J.A. Ribeiro, C.M. Pereira, A.F. Silva, M.G.F. Sales, Disposable electrochemical detection of breast cancer tumour marker CA 15-3 using poly(Toluidine Blue) as imprinted polymer receptor, Biosens Bioelectron. 109 (2018) 246–254.
[19] S. Patra, E. Roy, R. Madhuri, P.K. Sharma, Nano-iniferter based imprinted sensor for ultra trace level detection of prostate-specific antigen in both men and women, Biosens Bioelectron. 66 (2015) 1–10.
[20] F.T.C. Moreira, S. Sharma, R.A.F. Dutra, J.P.C. Noronha, A.E.G. Cass, M.G.F. Sales, Protein-responsive polymers for point-of-care detection of cardiac biomarker, Sensor Actuat B-Chem. 196 (2014) 123–132.
[21] B.V.M. Silva, B.A.G. Rodriguez, G.F. Sales, M.D.T. Sotomayor, R.F. Dutra, An ultrasensitive human cardiac troponin T graphene screen-printed electrode based on electropolymerized-molecularly imprinted conducting polymer, Biosens Bioelectron. 77 (2016) 978–985.
[22] M. Bosserdt, J. Erdossy, G. Lautner, J. Witt, K. Kohler, N. Gajovic-Eichelmann, A. Yarman, G. Wittstock, F.W. Scheller, R.E. Gyurcsanyi, Microelectrospotting as a new method for electrosynthesis of surface-imprinted polymer microarrays for protein recognition, Biosens Bioelectron. 73 (2015) 123–129.
[23] A. Tretjakov, V. Syritski, J. Reut, R. Boroznjak, A. Opik, Molecularly imprinted polymer film interfaced with Surface Acoustic Wave technology as a sensing platform for label-free protein detection, Anal Chim Acta. 902 (2016) 182–188.
[24] B. de Boer, H.K. Simon, M.P.L. Werts, E.W. van der Vegte, G. Hadziioannou, “Living” free radical photopolymerization initiated from surface-grafted iniferter monolayers, Macromolecules. 33 (2000) 349–356.
[25] T. Kitto, C. Bodart-Le Guen, N. Rossetti, F. Cicoira, 25 - Processing and patterning of conducting polymers for flexible, stretchable, and biomedical electronics, in: O. Ostroverkhova (Ed.), Handbook of Organic Materials for Electronic and Photonic Devices (Second Edition), Woodhead Publishing, 2019: pp. 817–842.
[26] A. Pietrzyk, W. Kutner, R. Chitta, M.E. Zandler, F. D’Souza, F. Sannicolo, P.R. Mussini, Melamine Acoustic Chemosensor Based on Molecularly Imprinted Polymer Film, Anal Chem. 81 (2009) 10061–10070.
[27] A. Khlifi, S. Gam-Derouich, M. Jouini, R. Kalfat, M.M. Chehimi, Melamine-imprinted polymer grafts through surface photopolymerization initiated by aryl layers from diazonium salts, Food Control. 31 (2013) 379–386.
[28] M. Bompart, K. Haupt, Molecularly Imprinted Polymers and Controlled/Living Radical Polymerization, Aust J Chem. 62 (2009) 751–761.
[29] R.R. Chen, L. Qin, M. Jia, X.W. He, W.Y. Li, Novel surface-modified molecularly imprinted membrane prepared with iniferter for permselective separation of lysozyme, J Membrane Sci. 363 (2010) 212–220.
[30] V.D. Salian, C.J. White, M.E. Byrne, Molecularly imprinted polymers via living radical polymerization: Relating increased structural homogeneity to improved template binding parameters, React Funct Polym. 78 (2014) 38–46.
[31] S. Subrahmanyam, A. Guerreiro, A. Poma, E. Moczko, E. Piletska, S. Piletsky, Optimisation of experimental conditions for synthesis of high affinity MIP nanoparticles, Eur Polym J. 49 (2013) 100–105.
[32] B. Mattiasson, K. Teeparuksapun, M. Hedstrom, Immunochemical binding assays for detection and quantification of trace impurities in biotechnological production, Trends Biotechnol. 28 (2010) 20–27.

[33] S. Ray, G. Mehta, S. Srivastava, Label-free detection techniques for protein microarrays: Prospects, merits and challenges, Proteomics. 10 (2010) 731–748.
[34] M. Espinoza-Castaneda, A. de la Escosura-Muniz, A. Chamorro, C. de Torres, A. Merkoci, Nanochannel array device operating through Prussian blue nanoparticles for sensitive label-free immunodetection of a cancer biomarker, Biosens Bioelectron. 67 (2015) 107–114.
[35] H.V. Tran, B. Piro, S. Reisberg, L. Huy Nguyen, T. Dung Nguyen, H.T. Duc, M.C. Pham, An electrochemical ELISA-like immunosensor for miRNAs detection based on screen-printed gold electrodes modified with reduced graphene oxide and carbon nanotubes, Biosens Bioelectron. 62 (2014) 25–30.
[36] S. Tonello, M. Serpelloni, N.F. Lopomo, E. Sardini, G. Abate, D.L. Uberti, Preliminary Study of a Low-Cost Point-of-Care Testing System Using Screen-Printed Biosensors for Early Biomarkers Detection Related to Alzheimer Disease, Ieee Int Sym Med Mea. (2016) 573–578.
[37] L. Uzun, A.P.F. Turner, Molecularly-imprinted polymer sensors: realising their potential, Biosens Bioelectron. 76 (2016) 131–144.
[38] B. Sellergren, Molecularly imprinted polymers : man-made mimics of antibodies and their applications in analytical chemistry, Elsevier, Amsterdam ; Oxford, 2001.
[39] K. Haupt, Imprinted polymers - Tailor-made mimics of antibodies and receptors, Chem Commun. (2003) 171–178.
[40] M.J. Whitcombe, N. Kirsch, I.A. Nicholls, Molecular imprinting science and technology: a survey of the literature for the years 2004-2011, J Mol Recognit. 27 (2014) 297–401.
[41] T. Ikawa, F. Hoshino, T. Matsuyama, H. Takahashi, O. Watanabe, Molecular-shape imprinting and immobilization of biomolecules on a polymer containing azo dye, Langmuir. 22 (2006) 2747–2753.
[42] H.-G. Elias, An introduction to polymer science, VCH, Weinheim ; Cambridge, 1997.
[43] S. Srinivasan, M.W. Lee, M.C. Grady, M. Soroush, A.M. Rappe, Computational Study of the Self-Initiation Mechanism in Thermal Polymerization of Methyl Acrylate, J Phys Chem A. 113 (2009) 10787–10794.
[44] B.M. Mandal, Fundamentals of Polymerization, WORLD SCIENTIFIC, 2011.
[45] F.K. Li, R.C. Larock, Synthesis, structure and properties of new tung oil-styrene-divinylbenzene copolymers prepared by thermal polymerization, Biomacromolecules. 4 (2003) 1018–1025.
[46] E. Steckhan, ed., Electrochemistry IV, Springer-Verlag, Berlin ; London, 1990.
[47] A. Pietrzyk, S. Suriyanarayanan, W. Kutner, R. Chitta, F. D'Souza, Selective histamine piezoelectric chemosensor using a recognition film of the molecularly imprinted polymer of bis(bithiophene) derivatives, Anal Chem. 81 (2009) 2633–2643.
[48] J.G. Pacheco, M.S.V. Silva, M. Freitas, H.P.A. Nouws, C. Delerue-Matos, Molecularly imprinted electrochemical sensor for the point-of-care detection of a breast cancer biomarker (CA 15-3), Sensor Actuat B-Chem. 256 (2018) 905–912.
[49] Y. Yagci, S. Jockusch, N.J. Turro, Photoinitiated Polymerization: Advances, Challenges, and Opportunities, Macromolecules. 43 (2010) 6245–6260.
[50] D.K. Balta, N. Arsu, Thioxanthone-ethyl anthracene, J Photoch Photobio A. 257 (2013) 54–59.

[51] S. Dadashi-Silab, C. Aydogan, Y. Yagci, Shining a light on an adaptable photoinitiator: advances in photopolymerizations initiated by thioxanthones, Polym Chem-Uk. 6 (2015) 6595–6615.
[52] S.C. Ligon, B. Husar, H. Wutzel, R. Holman, R. Liska, Strategies to Reduce Oxygen Inhibition in Photoinduced Polymerization, Chem Rev. 114 (2014) 557–589.
[53] Z. Altintas, A. Guerreiro, S.A. Piletsky, I.E. Tothill, NanoMIP based optical sensor for pharmaceuticals monitoring (vol 213, pg 305, 2015), Sensor Actuat B-Chem. 277 (2018) 679–679.
[54] M.C. Blanco-Lopez, M.J. Lobo-Castanon, A.J. Miranda-Ordieres, P. Tunon-Blanco, Voltammetric sensor for vanillylmandelic acid based on molecularly imprinted polymer-modified electrodes, Biosens Bioelectron. 18 (2003) 353–362.
[55] Y.X. Wang, Z.H. Chai, Y.J. Sun, M. Gao, G.Q. Fu, Preparation of lysozyme imprinted magnetic nanoparticles via surface graft copolymerization, J Biomat Sci-Polym E. 26 (2015) 644–656.
[56] S. Barral, A. Guerreiro, M.A. Villa-Garcia, M. Rendueles, M. Diaz, S. Piletsky, Synthesis of 2-(diethylamino)ethyl methacrylate-based polymers Effect of crosslinking degree, porogen and solvent on the textural properties and protein adsorption performance, React Funct Polym. 70 (2010) 890–899.
[57] D.X. Yin, M. Ulbricht, Antibody-Imprinted Membrane Adsorber via Two-Step Surface Grafting, Biomacromolecules. 14 (2013) 4489–4496.
[58] K. Matyjaszewski, T.P. Davis, Handbook of radical polymerization, Wiley-Interscience, Hoboken, 2002.
[59] W.A. Braunecker, K. Matyjaszewski, Controlled/living radical polymerization: Features, developments and perspectives (vol 32, pg 93, 2007), Prog Polym Sci. 33 (2008) 165–165.
[60] S. Perrier, P. Takolpuckdee, Macromolecular design via reversible addition–fragmentation chain transfer (RAFT)/xanthates (MADIX) polymerization, Journal of Polymer Science Part A: Polymer Chemistry. 43 (2005) 5347–5393.
[61] G. Moad, E. Rizzardo, S.H. Thang, A RAFT Tutorial., The Strem Chemiker Vol. XXV, No. 1. 56 (2011) 2–10.
[62] G. Moad, E. Rizzardo, S.H. Thang, Radical addition–fragmentation chemistry in polymer synthesis, Polymer. 49 (2008) 1079–1131.
[63] S. Hjerten, J.L. Liao, K. Nakazato, Y. Wang, G. Zamaratskaia, H.X. Zhang, Gels mimicking antibodies in their selective recognition of proteins, Chromatographia. 44 (1997) 227–234.
[64] Y. Ge, A.P. Turner, Too large to fit? Recent developments in macromolecular imprinting, Trends Biotechnol. 26 (2008) 218–224.
[65] A. Rachkov, N. Minoura, Recognition of oxytocin and oxytocin-related peptides in aqueous media using a molecularly imprinted polymer synthesized by the epitope approach, J Chromatogr A. 889 (2000) 111–118.
[66] A. Rachkov, N. Minoura, Towards molecularly imprinted polymers selective to peptides and proteins. The epitope approach, Biochimica et Biophysica Acta (BBA) - Protein Structure and Molecular Enzymology. 1544 (2001) 255–266.
[67] A. Bossi, F. Bonini, A.P. Turner, S.A. Piletsky, Molecularly imprinted polymers for the recognition of proteins: the state of the art, Biosens Bioelectron. 22 (2007) 1131–1137.
[68] D.R. Kryscio, N.A. Peppas, Critical review and perspective of macromolecularly imprinted polymers, Acta Biomater. 8 (2012) 461–473.

[69] H. Shi, W.B. Tsai, M.D. Garrison, S. Ferrari, B.D. Ratner, Template-imprinted nanostructured surfaces for protein recognition, Nature. 398 (1999) 593–597.
[70] G. Lautner, J. Kaev, J. Reut, A. Öpik, J. Rappich, V. Syritski, R.E. Gyurcsányi, Selective artificial receptors based on micropatterned surface-imprinted polymers for label-free detection of proteins by SPR imaging, Advanced Functional Materials. 21 (2011) 591–597.
[71] A. Menaker, V. Syritski, J. Reut, A. Öpik, V. Horváth, R.E. Gyurcsányi, Electrosynthesized surface-imprinted conducting polymer microrods for selective protein recognition, Advanced Materials. 21 (2009) 2271–2275.
[72] A. Tretjakov, V. Syritski, J. Reut, R. Boroznjak, O. Volobujeva, A. Öpik, Surface molecularly imprinted polydopamine films for recognition of immunoglobulin G, Microchimica Acta. 180 (2013) 1433–1442.
[73] P.S. Sharma, A. Pietrzyk-Le, F. D'Souza, W. Kutner, Electrochemically synthesized polymers in molecular imprinting for chemical sensing, Anal Bioanal Chem. 402 (2012) 3177–204.
[74] P.C. Chou, J. Rick, T.C. Chou, C-reactive protein thin-film molecularly imprinted polymers formed using a micro-contact approach, Anal Chim Acta. 542 (2005) 20–25.
[75] H.Y. Lin, C.Y. Hsu, J.L. Thomas, S.E. Wang, H.C. Chen, T.C. Chou, The microcontact imprinting of proteins: The effect of cross-linking monomers for lysozyme, ribonuclease A and myoglobin, Biosens Bioelectron. 22 (2006) 534–543.
[76] C.Y. Wang, Y.C. Chen, D.C. Sheu, T.C. Chou, Molecularly imprinted polymers for the recognition of sodium dodecyl sulfate denatured creatine kinase, J Taiwan Inst Chem E. 43 (2012) 188–194.
[77] K. Manoli, M. Magliulo, M.Y. Mulla, M. Singh, L. Sabbatini, G. Palazzo, L. Torsi, Printable Bioelectronics To Investigate Functional Biological Interfaces, Angew Chem Int Edit. 54 (2015) 12562–12576.
[78] G. Erturk, D. Berillo, M. Hedstrom, B. Mattiasson, Microcontact-BSA imprinted capacitive biosensor for real-time, sensitive and selective detection of BSA, Biotechnol Rep (Amst). 3 (2014) 65–72.
[79] B. Osman, L. Uzun, N. Besirli, A. Denizli, Microcontact imprinted surface plasmon resonance sensor for myoglobin detection, Mat Sci Eng C-Mater. 33 (2013) 3609–3614.
[80] B.G. Knecht, A. Strasser, R. Dietrich, E. Martlbauer, R. Niessner, M.G. Weller, Automated microarray system for the simultaneous detection of antibiotics in milk, Anal Chem. 76 (2004) 646–654.
[81] G. Erturk, M. Hedstrom, M.A. Tumer, A. Denizli, B. Mattiasson, Real-time prostate-specific antigen detection with prostate-specific antigen imprinted capacitive biosensors, Anal Chim Acta. 891 (2015) 120–129.
[82] G.K. Jennings, E.L. Brantley, Physicochemical Properties of Surface-Initiated Polymer Films in the Modification and Processing of Materials, Advanced Materials. 16 (2004) 1983–1994.
[83] R. Ahmad, A. Mocaer, S. Gam-Derouich, A. Lamouri, H. Lecoq, P. Decorse, P. Brunet, C. Mangeney, Grafting of polymeric platforms on gold by combining the diazonium salt chemistry and the photoiniferter method, Polymer. 57 (2015) 12–20.
[84] H.J. Lee, K. Namkoong, E.C. Cho, C. Ko, J.C. Park, S.S. Lee, Surface acoustic wave immunosensor for real-time detection of hepatitis B surface antibodies in whole blood samples, Biosens Bioelectron. 24 (2009) 3120–3125.

[85] A. Zengin, G. Karakose, T. Caykara, Poly(2-(dimethylamino)ethyl methacrylate) brushes fabricated by surface-mediated RAFT polymerization and their response to pH, Eur Polym J. 49 (2013) 3350–3358.
[86] A. Olivier, F. Meyer, J.M. Raquez, P. Damman, P. Dubois, Surface-initiated controlled polymerization as a convenient method for designing functional polymer brushes: From self-assembled monolayers to patterned surfaces, Prog Polym Sci. 37 (2012) 157–181.
[87] R. Ahmad, Polymer brushes by anionic and cationic Surface-Initiated Polymerization (SIP), Adv Polym Sci. 197 (2006) 107–136.
[88] C. Slugovc, The ring opening metathesis polymerisation toolbox, Macromol Rapid Comm. 25 (2004) 1283–1297.
[89] N. Tsubokawa, M. Satoh, Surface grafting of polymers onto glass plate: Polymerization of vinyl monomers initiated by initiating groups introduced onto the surface, J Appl Polym Sci. 65 (1997) 2165–2172.
[90] T. Farhan, W.T.S. Huck, Synthesis of patterned polymer brushes from flexible polymeric films, Eur Polym J. 40 (2004) 1599–1604.
[91] P. Jolly, V. Tamboli, R.L. Harniman, P. Estrela, C.J. Allender, J.L. Bowen, Aptamer-MIP hybrid receptor for highly sensitive electrochemical detection of prostate specific antigen, Biosens Bioelectron. 75 (2016) 188–195.
[92] Y.T. Wang, Z.Q. Zhang, V. Jain, J.J. Yi, S. Mueller, J. Sokolov, Z.X. Liu, K. Levon, B. Rigas, M.H. Rafailovich, Potentiometric sensors based on surface molecular imprinting: Detection of cancer biomarkers and viruses, Sensor Actuat B-Chem. 146 (2010) 381–387.
[93] S. Viswanathan, C. Rani, S. Ribeiro, C. Delerue-Matos, Molecular imprinted nanoelectrodes for ultra sensitive detection of ovarian cancer marker, Biosens Bioelectron. 33 (2012) 179–183.
[94] A. Cecchini, V. Raffa, F. Canfarotta, G. Signore, S. Piletsky, M.P. MacDonald, A. Cuschieri, In Vivo Recognition of Human Vascular Endothelial Growth Factor by Molecularly Imprinted Polymers, Nano Lett. 17 (2017) 2307–2312.
[95] M. Johari-Ahar, P. Karami, M. Ghanei, A. Afkhami, H. Bagheri, Development of a molecularly imprinted polymer tailored on disposable screen-printed electrodes for dual detection of EGFR and VEGF using nano-liposomal amplification strategy, Biosens Bioelectron. 107 (2018) 26–33.
[96] Y. Kamon, T. Takeuchi, Molecularly Imprinted Nanocavities Capable of Ligand-Binding Domain and Size/Shape Recognition for Selective Discrimination of Vascular Endothelial Growth Factor Isoforms, ACS Sens. 3 (2018) 580–586.
[97] J.L. Urraca, C.S. Aureliano, E. Schillinger, H. Esselmann, J. Wiltfang, B. Sellergren, Polymeric complements to the Alzheimer's disease biomarker beta-amyloid isoforms Abeta1-40 and Abeta1-42 for blood serum analysis under denaturing conditions, J Am Chem Soc. 133 (2011) 9220–9223.
[98] Y.S. Levy, Y. Gilgun-Sherki, E. Melamed, D. Offen, Therapeutic potential of neurotrophic factors in neurodegenerative diseases, Biodrugs. 19 (2005) 97–127.
[99] M.H. Voutilainen, U. Arumae, M. Airavaara, M. Saarma, Therapeutic potential of the endoplasmic reticulum located and secreted CDNF/MANF family of neurotrophic factors in Parkinson's disease, Febs Lett. 589 (2015) 3739–3748.
[100] R.L. Watts, D.G. Standaert, J.A. Obeso, Movement disorders, 3rd ed., McGraw-Hill Medical, New York, 2012.

[101] D.K. Binder, H.E. Scharfman, Brain-derived neurotrophic factor, Growth Factors. 22 (2004) 123–131.
[102] M.P. Mattson, S. Maudsley, B. Martin, BDNF and 5-HT: a dynamic duo in age-related neuronal plasticity and neurodegenerative disorders, Trends Neurosci. 27 (2004) 589–594.
[103] S. Bathina, U.N. Das, Brain-derived neurotrophic factor and its clinical implications, Arch Med Sci. 11 (2015) 1164–1178.
[104] H.J. Huttunen, M. Saarma, CDNF Protein Therapy in Parkinson's Disease, Cell Transplant. (2019) 963689719840290.
[105] B. Elfving, P.H. Plougmann, G. Wegener, Detection of brain-derived neurotrophic factor (BDNF) in rat blood and brain preparations using ELISA: Pitfalls and solutions, J Neurosci Meth. 187 (2010) 73–77.
[106] K. Mlyniec, B. Budziszewska, B. Holst, B. Ostachowicz, G. Nowak, GPR39 (Zinc Receptor) Knockout Mice Exhibit Depression-Like Behavior and CREB/BDNF Down-Regulation in the Hippocampus, Int J Neuropsychoph. 18 (2015).
[107] H. Soya, T. Nakamura, C.C. Deocaris, A. Kimpara, M. Iimura, T. Fujikawa, H. Chang, B.S. McEwen, T. Nishijima, BDNF induction with mild exercise in the rat hippocampus, Biochem Bioph Res Co. 358 (2007) 961–967.
[108] M. Bockaj, B. Fung, M. Tsoulis, W.G. Foster, L. Soleymani, Method for Electrochemical Detection of Brain Derived Neurotrophic Factor (BDNF) in Plasma, Anal Chem. 90 (2018) 8561–8566.
[109] Y.K. Yoo, J. Lee, J. Kim, G. Kim, S. Kim, J. Kim, H. Chun, J.H. Lee, C.J. Lee, K.S. Hwang, Ultra-sensitive detection of brain-derived neurotrophic factor (BDNF) in the brain of freely moving mice using an interdigitated microelectrode (IME) biosensor, Sci Rep-Uk. 6 (2016).
[110] K. Tawa, M. Satoh, K. Uegaki, T. Hara, M. Kojima, H. Kumanogoh, H. Aota, Y. Yokota, T. Nakaoki, M. Umetsu, H. Nakazawa, I. Kumagai, Rapid and Sensitive Detection of Brain-Derived Neurotrophic Factor with a Plasmonic Chip, Jpn J Appl Phys. 52 (2013).
[111] R.L. Rich, D.G. Myszka, Survey of the 2009 commercial optical biosensor literature, J Mol Recognit. 24 (2011) 892–914.
[112] R. Karlsson, P.S. Katsamba, H. Nordin, E. Pol, D.G. Myszka, Analyzing a kinetic titration series using affinity biosensors, Anal Biochem. 349 (2006) 136–147.
[113] A.J. Qavi, A.L. Washburn, J.Y. Byeon, R.C. Bailey, Label-free technologies for quantitative multiparameter biological analysis, Anal Bioanal Chem. 394 (2009) 121–135.
[114] T.M.A. Gronewold, Surface acoustic wave sensors in the bioanalytical field: Recent trends and challenges, Anal Chim Acta. 603 (2007) 119–128.
[115] I. Sayago, D. Matatagui, M.J. Fernandez, J.L. Fontecha, I. Jurewicz, R. Garriga, E. Munoz, Graphene oxide as sensitive layer in Love-wave surface acoustic wave sensors for the detection of chemical warfare agent simulants, Talanta. 148 (2016) 393–400.
[116] K. Lange, B.E. Rapp, M. Rapp, Surface acoustic wave biosensors: a review, Anal Bioanal Chem. 391 (2008) 1509–1519.
[117] D.B. Go, M.Z. Atashbar, Z. Ramshani, H.C. Chang, Surface acoustic wave devices for chemical sensing and microfluidics: a review and perspective, Anal Methods-Uk. 9 (2017) 4112–4134.

[118] S. Ramesan, A.R. Rezk, K.W. Cheng, P.P.Y. Chan, L.Y. Yeo, Acoustically-driven thread-based tuneable gradient generators, Lab Chip. 16 (2016) 2820–2828.
[119] A.R. Rezk, A. Qi, J.R. Friend, W.H. Li, L.Y. Yeo, Uniform mixing in paper-based microfluidic systems using surface acoustic waves, Lab Chip. 12 (2012) 773–779.
[120] O. Tigli, L. Bivona, P. Berg, M.E. Zaghloul, Fabrication and Characterization of a Surface-Acoustic-Wave Biosensor in CMOS Technology for Cancer Biomarker Detection, Ieee T Biomed Circ S. 4 (2010) 62–73.
[121] S.M. Li, Y. Wan, Y. Su, C.H. Fan, V.R. Bhethanabotla, Gold nanoparticle-based low limit of detection Love wave biosensor for carcinoembryonic antigens, Biosens Bioelectron. 95 (2017) 48–54.
[122] V. Crivianu-Gaita, M. Aamer, R.T. Posaratnanathan, A. Romaschin, M. Thompson, Acoustic wave biosensor for the detection of the breast and prostate cancer metastasis biomarker protein PTHrP, Biosens Bioelectron. 78 (2016) 92–99.
[123] Y.X. Wang, M. Chen, L.Q. Zhang, Y. Ding, Y. Luo, Q.H. Xu, J.F. Shi, L. Cao, W.L. Fu, Rapid detection of human papilloma virus using a novel leaky surface acoustic wave peptide nucleic acid biosensor, Biosens Bioelectron. 24 (2009) 3455–3460.
[124] K. Saha, F. Bender, E. Gizeli, Comparative study of IgG binding to proteins G and A: Nonequilibrium kinetic and binding constant determination with the acoustic waveguide device, Anal Chem. 75 (2003) 835–842.
[125] J.C. Homola, ed., Surface plasmon resonance based sensors, Springer-Verlag Berlin Heidelberg, 2006.
[126] F.A. Tanious, B. Nguyen, W.D. Wilson, Biosensor-surface plasmon resonance methods for quantitative analysis of biomolecular interactions, Method Cell Biol. 84 (2008) 53–77.
[127] D.R. Shankaran, K.V.A. Gobi, N. Miura, Recent advancements in surface plasmon resonance immunosensors for detection of small molecules of biomedical, food and environmental interest, Sensor Actuat B-Chem. 121 (2007) 158–177.
[128] C.T. Campbell, G. Kim, SPR microscopy and its applications to high-throughput analyses of biomolecular binding events and their kinetics, Biomaterials. 28 (2007) 2380–2392.
[129] Z. Taleat, A. Khoshroo, M. Mazloum-Ardakani, Screen-printed electrodes for biosensing: a review (2008-2013), Microchim Acta. 181 (2014) 865–891.
[130] P. Yanez-Sedeno, S. Campuzano, J.M. Pingarron, Multiplexed Electrochemical Immunosensors for Clinical Biomarkers, Sensors-Basel. 17 (2017).
[131] V.V. Shumyantseva, T.V. Bulko, L.V. Sigolaeva, A.V. Kuzikov, P.V. Pogodin, A.I. Archakov, Molecular imprinting coupled with electrochemical analysis for plasma samples classification in acute myocardial infarction diagnostic, Biosens Bioelectron. 99 (2018) 216–222.
[132] W. Plazinski, W. Rudzinski, A. Plazinska, Theoretical models of sorption kinetics including a surface reaction mechanism: A review, Advances in Colloid and Interface Science. 152 (2009) 2–13.
[133] J. Faccini, S. Ebrahimi, D.J. Roberts, Regeneration of a perchlorate-exhausted highly selective ion exchange resin: Kinetics study of adsorption and desorption processes, Sep Purif Technol. 158 (2016) 266–274.
[134] W. Rudzinski, W. Plazinski, On the applicability of the pseudo-second order equation to represent the kinetics of adsorption at solid/solution interfaces: a theoretical analysis based on the statistical rate theory, Adsorption. 15 (2009) 181–192.

[135] W. Plazinski, J. Dziuba, W. Rudzinski, Modeling of sorption kinetics: the pseudo-second order equation and the sorbate intraparticle diffusivity, Adsorption. 19 (2013) 1055–1064.
[136] R.A. Latour, The Langmuir isotherm: A commonly applied but misleading approach for the analysis of protein adsorption behavior, J Biomed Mater Res A. 103 (2015) 949–958.
[137] R.J. Umpleby, S.C. Baxter, Y.Z. Chen, R.N. Shah, K.D. Shimizu, Characterization of molecularly imprinted polymers with the Langmuir-Freundlich isotherm, Anal Chem. 73 (2001) 4584–4591.
[138] T. Muhammad, Z. Nur, E.V. Piletska, O. Yimit, S.A. Piletsky, Rational design of molecularly imprinted polymer: the choice of cross-linker, Analyst. 137 (2012) 2623–2628.
[139] J.A. McCleverty, ed., Comprehensive coordination chemistry II : from biology to nanotechnology, Elsevier Pergamon, Amsterdam ; London, 2004.
[140] X. Zhang, F. Rösicke, V. Syritski, G. Sun, J. Reut, K. Hinrichs, S. Janietz, J. Rappich, Influence of the para-Substitutent of benzene diazonium salts and the solvent on the film growth during electrochemical reduction, Zeitschrift Fur Physikalische Chemie. 228 (2014) 557–573.
[141] M. Schaeferling, S. Schiller, H. Paul, M. Kruschina, P. Pavlickova, M. Meerkamp, C. Giammasi, D. Kambhampati, Application of self-assembly techniques in the design of biocompatible protein microarray surfaces, Electrophoresis. 23 (2002) 3097–3105.

Acknowledgements

This research was carried out at the Laboratory of Biofunctional Materials, Department of Materials and Environmental Technology, Tallinn University of Technology.

First, I want to sincerely appreciate my supervisors, Dr. Vitali Syritski and Prof. Andres Öpik, for their great consistent patience and guidance through all the stages of the writing of the thesis. Also, to Dr. Jekaterina Reut, who has spent tireless efforts in making this thesis write-up of good success, through advice, editing and proofreading of the work.

I wish to thank Prof. Malle Krunks, Head of the Department of Materials and Environmental Technology, for giving me the possibility to carry out this doctoral thesis, for support, useful remarks and discussions.

I would like to express my gratitude to Dr. Mati Danilson for the XPS measurements, and Dr. Ilona Oja Acik for the contact angle measurements. I would like to thank Dr. Jörg Rappich who kindly offered facilities of Helmholtz-Zentrum Berlin für Materialien und Energie GmbH to fabricate the cells used in this thesis for photopolymerization. I also want to thank Icosagen AS and Prof. Mart Ustav personally, for kindly providing the NF proteins. I would like to thank Prof. Mart Saarma for support in working with NF proteins. I want to thank Dr. Andreas Furchner from Leibniz-Institut für Analytische Wissenschaften – ISAS – e. V. for the VIS ellipsometry measurements

In addition, I would like to thank my colleagues Dr. Roman Borozнjak, Dr. Aleksei Tretjakov, and every single member whom I worked with in the Department of Materials and Environmental Technology.

I am grateful to the financial support from the Estonian Ministry of Education and Research under the Estonian Research Council grants (PUT150 and PRG307), Tallinn University of Technology in the frame of the Development project (grant SS425), and European Social Fund's Doctoral Studies and Internationalization Program (DoRa8).

This work has been partially supported by Graduate School of Functional materials and technologies receiving funding from the European Regional Development Fund in University of Tartu, Estonia, project 2014-2020.4.01.16-0027.

Abstract

Photo- and Electropolymerization Approaches for Molecular Imprinting of a Neurotrophic Factor Protein

Nowadays, healthcare is facing an increasing demand for fast and reliable analytical methods suitable for achieving appropriate selectivity with low limit of detection while being low-cost, portable, and capable of in situ real-time monitoring. Most of the current biosensing systems utilize labile biological recognition elements that offer high selectivity towards a target analyte, but limit the shelf life of the device and increase cost and analysis time. Thus, there is a growing interest in the replacement of biological receptors with synthetic analogues such as molecularly imprinted polymers (MIPs) – materials with antibody-like ability to bind and discriminate between molecules. The main benefits of MIPs are related to their synthetic nature, i.e. excellent chemical and thermal stability coupled with their reproducible and cost-effective fabrication. The surface imprinting approach leading to the formation of polymer with imprinted sites located directly in the surface layer of the MIP films, enabling easy access to the target macromolecules, is a promising way for protein-MIP preparation. SI-C/LR photopolymerization as well as electropolymerization are particularly attractive methods for the synthesis of firmly adherent protein-MIP films directly on the surface of a sensor transducer.

The importance of a protein for clinical diagnostics is an essential criterion when choosing a target protein for imprinting. For example, neurotrophic factor (NF) proteins, were found to be associated with a number of neurological diseases such as Alzheimer's, Parkinson's and mental disorders. Serum concentration of a specific NF protein could thus be a potential biomarker for early-stage diagnosis of these conditions. However, despite the increased number of publications dedicated to the use of MIPs for the detection of clinically relevant proteins, the MIP capable of selective recognition of a NF protein has still not been reported.

The thesis is aimed at the development of synthesis methods to generate a MIP film capable of selective recognition of a NF protein and coupled as a recognition layer with a label-free platform. Two clinically relevant NF-proteins: CDNF and BDNF, were used as target molecules for molecular imprinting to generate CDNF-MIP and BDNF-MIP, respectively. The developed synthesis methods employing the electro- and photopolymerization techniques allowed the robust integration of the NF-MIP films with the label-free sensor platform.

The electrochemical surface imprinting approach was adapted for the preparation of CDNF-MIP directly on SAW sensor surface, CDNF-MIP/SAW. Such MIPs bound the target, CDNF, with K_D values of 8 µg/mL and demonstrated notable IF (2.0) with the polymer film thickness of 4.7 nm and after the treatment in HSA solution aiming to suppress the intrinsic affinity of PmPD-based matrix towards CDNF. The CDNF-MIP/SAW sensing system could detect CDNF with LOD value of 4 ng/mL in the presence mCD48 as an interfering protein. In the competitive assays the system notably differentiated between CDNF and its homologue - MANF at pg/mL levels in the presence of IgG at sub µg/mL levels.

Unfortunately, the electropolymerized CDNF-MIP demonstrated a limited regeneration capability. In order to improve the MIP reusability a synthesis approach based on the combination of SI-C/LR photopolymerization and microcontact imprinting allowing the formation of protein-MIP films robustly interfaced with the label-free sensor platforms was developed. Preliminary, the approach was applied for imprinting BSA as a model

protein to form BSA-MIP film interfaced with SPR as a well-established sensor technique. It was revealed that (i) the photoinitiator (DEDTC) could be easily tethered to a gold sensor surface via 3,5-DClP layer preliminary formed by electrochemical reduction of 3,5-DClPDT; (ii) decreasing the ratio of monomer:crosslinker (DEAEM:BAA) increased hydrophilicity of the resulting polymer matrix; (iii) UV-irradiation power of 500 W/m^2 or 300 W/m^2 applied for 0.5 or 15 hours, respectively, did not significantly affect the protein conformation. The model sensor system, BSA-MIP/SPR, demonstrated the improved regeneration capability i.e. withstanding at least 25 regeneration cycles.

Further, by means of the SI-C/LR photopolymerization, BDNF-MIP was formed on SPE. Although, the resulting BDNF-MIPs against BDNF demonstrated the improved IF of 5.8 and K_D of ca. 1 ng/mL, they still could be regenerated at least once. Nevertheless, BDNF-MIP/SPE sensor system with the help of DPV could detect and quantify BDNF in the presence of HSA with LOD and LOQ values of 6 and 20 pg/mL, respectively. Moreover, the system was able to discriminate BDNF among analogous molecules, i.e. CDNF and MANF, and a molecule of a similar size, i.e. mCD48.

In summary, synthesis of the polymer films molecularly imprinted with NF proteins, BDNF and CDNF, was first reported in the thesis. The presented synthesis methods were proved to be suitable for preparation of MIP-sensors capable of selective detection of NF proteins and could be a promising route towards the development of innovative point-of-care diagnostics tools for the early-stage diagnostics of neurological diseases or monitoring therapies.

Kokkuvõte

Foto- ja elektropolümerisatsiooni meetodid neurotroofsete tegurite molekulaarseks jäljendamiseks

Tänapäeva kliinilises diagnostikas on kasvav vajadus kiirete ja usaldusväärsete analüütiliste meetodite järele, mis oleksid analüüsitavate sihtmolekulide suhtes kõrge selektiivsusega, suure tundlikkusega ja samal ajal suhteliselt odavad reaalajas sihtmolekuli kontsentratsiooni muutuste jälgimiseks. Enamik sel eesmärgil kasutatavad biosensoreid põhinevad täna ebastabiilsetel bioloogiliselt tundlikel elementidel nagu DNA, antikehad või ensüümid, mis võivad siduda erinevaid sihtmolekule küll efektiivselt ja spetsiifiliselt, kuid samal ajal on nende eluiga lühike ja hind suhteliselt kõrge. Seega on ilmne vajadus ülalnimetatud bioloogiliste retseptorite asendamiseks sünteetilistega, milleks sobivad näiteks molekulaarselt jäljendatud polümeerid (MIP), millede antikehadele sarnased omadused võimaldavad siduda erinevaid sihtmolekule sama efektiivselt. Tänaseks on MIP süsteemides kasutatud sensormaterjalid võrreldes biosensoritega näidanud mitmeid positiivseid omadusi nagu keemiline ja termiline stabiilsus, tehnoloogia reprodutseeritavus ning odav hind.

Suurte molekulide nagu proteiinide molekulaarseks jäljendamiseks kasutatakse nn. “pindmiste mälupesade“ loomist MIP kile pinnale, mis võimaldab makromolekulide paremat liikumist ja suuremat mälupesade arvu. Käesolev doktoritöö ongi pühendatud proteiinide molekulaarse jäljendamise võimaluste uurimisele vahetult sensori pinnal eeskätt keskendudes pindpolümerisatsiooni tehnoloogiale kontrollitud/elav-radikaalse fotopolümerisatsiooni ja elektropolümerisatsiooni meetoditel.

Kliinilises diagnostikas on erinevatel proteiinidel oluline roll ja seepärast ka vajadus nende kiireks ja täpseks määramiseks, mille üheks võimaluseks on molekulaarse jäljendamise tehnoloogia kasutamine. Näiteks seostatakse neurotroofseid tegureid mitmete neurodegeneratiivsete haigustega sealhulgas Alzheimeri ja Parkinsoni tõvega. Seega Alzheimeri ja Parkinsoni tõvega seotud neurotroofsete tegurite jälgimine võiks anda kasulikku teavet nende haiguste diagnoosil juba varajases staadiumis. Seni on aga kirjanduses molekulaarse jäljendamise tehnoloogia kasutamise kohta neurotroofsete tegurite hindamisel väga vähe teavet. Ja siit tulenebki käesoleva doktoritöö peamine eesmärk uurida erinevate sünteesi meedotide kasutamise võimalusi neurotroofsete tegurite molekulaarseks jäljendamiseks ning sidumiseks erinevate märgisevabade sensorplatvormidega. Jäljendatavateks neurotroofseteks teguriteks on valitud CDNF ja BDNF kui kirjanduse andmetel mitmete neurodegeneratiivsete haigustega seotud potentsiaalsed biomarkerid.

Neurotroofse teguri CDNF molekulaarseks jäljendamiseks akustilise laine põhimõttel (SAW) töötava sensori pinnale kasutati elektrokeemilist polümerisatsiooni. Molekulaarselt jäljendatud 4,7 nm paksuse CDNF-MIP/SAW kilele määrati polümeer-sihtmolekul dissotsiatsiooni konstandi K_D väärtuseks 8 µg/mL ja sihtmolekuli sidumise efektiivsust iseloomustava teguri IF väärtuseks 2,0. Mittespetsiifilise adsorptsioooni vähendamiseks käsitleti CDNF-MIP kilet ka HSA lahusega. CDNF-MIP/SAW sensori sihtmolekuli avastamispiiriks LOD määrati 4 ng/mL konkureeriva proteiini mCD48 juuresolekul. Selektiivsuse uurimine konkureeriva sidumise meetodil konstantsel IgG kontsentratsioonil (500 ng/mL) näitas, et CDNF-MIP/SAW sensor on võimeline eristama sihtmolekuli CDNF tema homoloogsest valgust MANF. Elektropolümerisatsiooni meetodil sünteesitud CDNF-MIP kile puuduseks oli aga liiga väike korduvkasutatavus.

Selle puuduse minimiseerimiseks uuriti pindmist kontrollitud elav-radikaal fotopolümerisatsiooni mikrokontaktmeetodil sensori pinnal, kasutades mudelproteiinina BSA-d ja sensorina pinnaplasma resonantsi (SPR) põhimõtet. Fotopolümerisatsiooni kasutamine näitas, et fotoinitsiaator DEDTC seondub hästi sensori kullast elektroodiga 3.5-DCIP vahekihi abil, mis kanti elektroodi pinnale 3.5-DClPDT ühendi elektrokeemilisel redutseerimisel. Vähendades monomeeri ja ristsildade moodustaja suhet (DEAEM:BAA) suurenes polümeeri maatriksi hüdrofiilsus. UV kiirguse intensiivsustel 500 W/m^2 kuni 300 W/m^2 vastavalt 0,5 ja 15 tunni jooksul käsitlemine ei muutnud märkimisväärselt valgu struktuuri. Mudelsensor BSA-MIP/SPR, mis valmistati pindmise elav-radikaal fotopolümerisatsiooni metodil oli ka omadustelt väga stabiilne 25 regenereerimistsükli järel.

Seejärel kasutati analoogilist tehnoloogiat neurotroofse teguri BDNF molekulaarseks jäljendamiseks sõeltrükitud elektrokeemilisele elektroodile (SPE). Kuigi fotopolümeriseeritud BDNF-MIP kile sihtmolekuli sidumisomadusi iseloomustavate parameetrite väärtused IF 5,8 ja K_D 1,12 ng/mL olid võrreldes elektropolümerisatsioonil saadud parameetritega paremad, säilitas BDNF-MIP kile stabiilsed sidumisomadused ainult ühe regeneererimistsükli järel. Siiski, fotopolümerisatsiooni teel valmistatud BDNF-MIP/SPE sensoril oli HSA vesilahuses väga hea avastamispiir 6 pg/mL ja määramispiir 20 pg/mL. BDNF-MIP/SPE oli märkimisväärselt selektiivsem sihtmolekuli BDNF suhtes konkureerivate molekulide CDNF, MANF ja mCD48 juuresolekul.

Kokkuvõttes on käesolevas doktoritöös esmakordselt sünteesitud neurotroofsete teguritega BDNF ja CDNF molekulaarselt jäljendatud polümeerkiled. Doktoritöös analüüsitud sünteesi meetodid sobisid hästi MIP sensorite valmistamiseks neurotroofsete tegurite selektiivseks määramiseks ning on rakendatavad potentsiaalselt kliinilise diagnostika vajadusteks ka laiemalt. Doktoritöö loob head eeldused patsiendimanuste testide (PoCT) arendamiseks neurodegeneratiivsete haiguste varajaseks diagnoosiks ja jälgimiseks.

Appendix

Publication I

A. Kidakova, R. Boroznjak, J. Reut, A. Öpik, M. Saarma and V. Syritski, Molecularly imprinted polymer-based SAW sensor for label-free detection of cerebral dopamine neurotrophic factor protein, Sensors and Actuators B: Chemical, 308, (2020), 127708.

Sensors & Actuators: B. Chemical 308 (2020) 127708

Contents lists available at ScienceDirect

Sensors and Actuators B: Chemical

journal homepage: www.elsevier.com/locate/snb

Molecularly imprinted polymer-based SAW sensor for label-free detection of cerebral dopamine neurotrophic factor protein

Anna Kidakova[a], Roman Borozznjak[a], Jekaterina Reut[a], Andres Öpik[a], Mart Saarma[b], Vitali Syritski[a,*]

[a] Department of Materials and Environmental Technology, Tallinn University of Technology, Ehitajate tee 5, 19086, Tallinn, Estonia
[b] Institute of Biotechnology, HiLIFE, University of Helsinki, P.O.Box 56, Viikinkaari 5D, FI-00014, Finland

ARTICLE INFO

Keywords:
Molecularly imprinted polymer
Electrochemical polymerization
m-Phenylenediamine
CDNF
Surface acoustic wave sensor
Neurodegenerative diseases

ABSTRACT

In this study we report on a surface acoustic wave (SAW) sensor modified with a molecularly imprinted polymer (MIP) film that selectively recognizes the cerebral dopamine neurotrophic factor (CDNF) protein, a potential biomarker for early-stage diagnosis and/or the follow-up of neuroprotective therapies. CDNF-MIP as a synthetic recognition element was prepared by a simple electrochemical surface imprinting approach allowing its reliable interfacing with SAW sensor. The optimal thickness of the MIP layer as well as a suitable pretreatment method were adjusted to improve the recognition capacity and selectivity of the resulting CDNF-MIP sensor. The 4.7 nm thick CDNF-MIP layers treated in 0.04 mg/ml HSA solution demonstrated the highest relative rebinding towards CDNF. The selectivity of the sensor was studied by the carefully designed competitive binding experiments, which revealed that the sensor can sense CDNF confidently in a label-free manner starting from 0.1 pg/ml. We anticipate that the findings can be a premise for fabricating the desired cost-effective research or diagnostics tools in the field of neurodegenerative diseases.

1. Introduction

In clinical diagnostics, the research in the discovery and detection of biomarkers of human diseases, neurological and mental disorders has become of great demand due to the increase in the prevalence of these diseases over the last decades and the urgent need for their early stage diagnosis [1]. For example, neurotrophic factor (NTFs) proteins are a family of proteins secreted from neurons and glial cells, and supporting the survival of neurons [2]. NTFs were found to be associated with a number of neurological diseases (NDs) such as Alzheimer's, Parkinson's and mental disorders and have been tested in clinical trials of several neurodegenerative diseases [3–6].

Cerebral dopamine neurotrophic factor (CDNF), and mesencephalic astrocyte derived neurotrophic factor (MANF) form a new family of unconventional NTFs that have been shown to be promising candidates for the treatment of Alzheimer's and Parkinson's [6–9]. In animal models of Parkinson's disease these NTFs can support the survival of neurons and regenerated neuronal axons opening a possibility for the development of disease modifying treatments. CDNF is currently tested in phase I-II clinical study on Parkinson's disease patients in three Scandinavian medical centres [10]. The abnormal levels of NTFs in the blood may be associated with a number of NDs [11], mental disorders [3] and diabetes [12]. Serum and/or cerebrospinal fluid (CSF) concentration of a specific NTF could therefore be a potential biomarker for early-stage diagnosis and/or the follow-up of neuroprotective therapies.

Today, ELISA is one of the most commonly used immunological assays, applicable in both research and diagnostics, providing a quantitative detection of specific proteins, including NTFs, in serum samples [13]. In spite of its high specificity and low limit of detection (LOD) [14], ELISA suffers from several disadvantages such as laborious, lengthy procedure, the use expensive bioassay kits, low reliability and reproducibility in serum samples because of the cross-reaction with other antibodies.

To address these issues valuable alternatives to the traditional detection methods e.g. based on label-free sensor platform have been intensively studied [15]. The sensors based on the acoustic wave transduction mechanism seem to be a prospective for diagnostics purposes since they combine direct detection, simplicity in handling, real-

Abbreviations: CDNF, cerebral dopamine neurotrophic factor; CDNF-MIP, polymer film with molecular imprints of CDNF; HSA, human serum albumin; IgG, Immunoglobulin G; MANF, mesencephalic astrocyte-derived neurotrophic; mCD48, mouse recombinant cluster of differentiation 48; MIP, molecularly Imprinted polymer; NIP, non-imprinted polymer; NTF, neurotrophic factor; PBS, phosphate buffer saline; SAW, surface acoustic wave sensor

* Corresponding author.
E-mail address: vitali.syritski@taltech.ee (V. Syritski).

https://doi.org/10.1016/j.snb.2020.127708
Received 8 July 2019; Received in revised form 4 December 2019; Accepted 11 January 2020
Available online 18 January 2020

time monitoring, and good sensitivity with a more reduced cost. Thus, Surface Acoustic Wave sensors (SAW) being fully compatible with large-scale fabrication and multiplexing technologies may provide substantial advantages in biosensing where electron transfer processes are hindered [16]. However, the reported label-free biosensing systems mostly utilize labile biological recognition elements (e.g. enzymes, DNA, antibodies) [17,18]. Moreover, applications for label-free sensing of NTF-proteins are very scarce [19,20].

Coupling label-free sensor platforms with synthetic recognition elements that avoid the disadvantages associated with the use of biological receptors in order to provide a reproducible and fast analysis of a biological sample, is of great importance. Molecular imprinting is one of the state-of-the-art techniques to generate robust synthetic molecular recognition materials with antibody-like ability to bind and discriminate between molecules [21]. The technique can be defined as the process of template-induced formation of specific molecular recognition sites in a polymer matrix material. The main benefits of these polymers, so-called Molecularly Imprinted Polymers (MIPs), are related to their synthetic nature, i.e., excellent chemical and thermal stability associated with reproducible, cost-effective fabrication. MIP receptors have been shown to be a promising alternative to natural biological receptors in biosensors providing more stable and low-cost recognition elements [22,23].

It should be noted that robust interfacing of a MIP with a sensor platform capable of responding upon interaction between the MIP and a binding analyte is a key aspect in the design of a MIP-based sensor. Recently, the use of an electrosynthesis approach for the facile integration of MIPs with label-free sensor platforms was reported [24–27].

The application of MIP-based sensors for diagnostics has been extensively studied. Thus, the detection of cancer biomarkers - prostate specific antigen [28], epithelial ovarian cancer antigen-125 [29], carcinoembryonic antigen [30], cardiovascular disease biomarkers - myoglobin [31] and cardiac troponin T [32] by MIP-modified sensors have been reported. In addition, MIP receptors for selective extraction of Alzheimer's disease biomarker, β-amyloid peptides, has been studied by Sellergren's group [33]. As concerns the imprinting of NTFs, so far only the selective recognition of another growth factor family protein - vascular endothelial growth factor (VEGF-A) by hybrid MIP nanoparticles as well as by MIP thin layer on SPR and screen-printed electrodes (SPE) has been reported [34–36]. Very recently, our group demonstrated the preparation of a photopolymerized MIP film integrated to a SPE and capable of selective recognition of brain-derived neurotrophic factor [37].

In this study, we report for the first time on the fabrication of MIP-based SAW sensor for label-free detection of CDNF. In this sensor, CDNF-MIP prepared by a surface imprinting approach, was utilized as a synthetic recognition element firmly interfaced with SAW sensing surface in the course of a simple electrochemical synthesis. As compared to electrochemical detection, we reported previously, the use of a mass-sensitive transducer such as SAW benefits from the absence of necessity to employ a redox pair as an electrochemical indicator as well as for ensuring the sufficient electrical conductivity at the electrode/solution interface for reliable and fast sensing of CDNF.

2. Experimental

2.1. Chemical and materials

Sodium chloride (NaCl), 4-aminothiophenol (4-ATP), 2-mercaptoethanol, m-phenylenediamine (mPD), dimethyl sulfoxide (DMSO), human serum albumin (HSA), and sodium dodecyl sulfate (SDS) were purchased from Sigma-Aldrich. Human recombinant Cerebral Dopamine Neurotrophic Factor (CDNF, 18.5 kDa, calculated pI 7.68), human recombinant mesencephalic astrocyte-derived neurotrophic factor (MANF, 18.1 kDa, calculated pI 8.55), and mouse recombinant mCD48 (cluster of differentiation 48, 22.2 kDa, pI 9.36) were provided by Icosagen AS (Tartu, Estonia). 3,3′-dithiobis [sulfosuccinimidylpropionate] (DTSSP) was purchased from Thermo Fisher Scientific Inc. Glycerol, sulfuric acid, hydrogen peroxide, and ammonium hydroxide were purchased from Lach-ner, S.R.O. All chemicals were of analytical grade or higher and were used as received without any further purification. Ultrapure Milli-Q water (resistivity 18.2 MΩ cm at 25 °C, EMD Millipore) was used for the preparation of all aqueous solutions. Phosphate buffered saline (PBS) solution (0.01 M, pH 7.4) was used to prepare synthesis and analyte solutions.

2.2. Preparation of CDNF-MIP sensor

The technological basis for a CDNF-MIP sensor was a label-free SAW system (SamX, NanoTemper Technologies GmbH, München, Germany). SAW system uses a pair of Love-wave sensor chips manufactured from ST-cut quartz substrates. Every sensor chip has four sensor elements (sensing surface 5 × 1.2 mm per sensor element). The shear-horizontal acoustic waves in the elements are generated by radio-frequency (RF) signal (between 147 and 150 MHz) applied to the input interdigital transducers (IDTs). The waves concentrated within the gold-coated SiO_2 guiding layer are converted back to an RF signal upon arriving to the output IDTs. The phase shift of RF signals measured by a Vector Network Analyzer is proportional to the mass loading on a sensing surface of the chip. The sensing surface of the sensor chips was modified with CDNF-MIP as a synthetic recognition layer using an electrochemical surface imprinting approach. The protocol for synthesis of CDNF-MIP was adapted from our previous work [26] (Fig. 1). Thus, firstly the sensor surface was modified with the target protein (CDNF) immobilized via 4-ATP/DTSSP linker system having the cleavable S—S bond, followed by electropolymerization of mPD conducted at the constant potential (0.6 V versus Ag/AgCl/1 M KCl) applied to the sensor surface until defined amount of electrical charge had been passed.

Poly(m-phenylenediamine) (PmPD) film thicknesses were determined by a spectroscopic ellipsometer (SE 850 DUV, Sentech Instruments GmbH, Berlin, Germany). Ellipsometric parameters ψ and Δ were measured from three spots for each sample in ambient air confining the wavelength range between 380 and 850 nm at the angle of incidence of 70°. The spectra were fitted (SpectraRay 3 software) with the optical model containing a one-layer Cauchy layer on the top of the gold and the thicknesses were determined.

To form the molecular imprints the polymer was treated in 0.1 M ethanolic solution of 2-mercaptoethanol to cleave the S—S bond in the linker system and, subsequently, in the aqueous solution of 3 M NaCl and DMSO. The respective reference films i.e those that do not have the molecular imprints of CDNF in the polymer, non-imprinted polymers (NIPs), were prepared by very similar way as CDNF-MIP, but excluding the treatment in mercaptoethanol. Thus, the template proteins are still covalently retained in the NIP matrix hindering the possibility to rebind CDNF at this location.

2.3. Rebinding and selectivity studies

The sensor chips, modified with CDNF-MIP and the respective reference, NIP layers (Fig. S1), were loaded into SAW system and equilibrated with the degassed running buffer solution (PBS, pH 7.4) at a flow rate of 25 µl/min until a stable baseline was established. The temperature of the running solutions and the chips was controlled with Peltier element with +/-0.01 °C precision and kept constant at 22 °C. Then the consecutive injections of the analyte solutions in order from lower to higher concentrations were applied (from 50 ng/ml to 33.75 µg/ml of CDNF on PBS buffer) and the phase-shift responses versus time (sensorgrams) were recorded. The details of kinetics analysis of the sensorgrams are given in section S1 of SI. The selectivity of the CDNF-MIP sensor was studied with the help of a kinetic titration series, where the solution of either CDNF or an interfering homologous

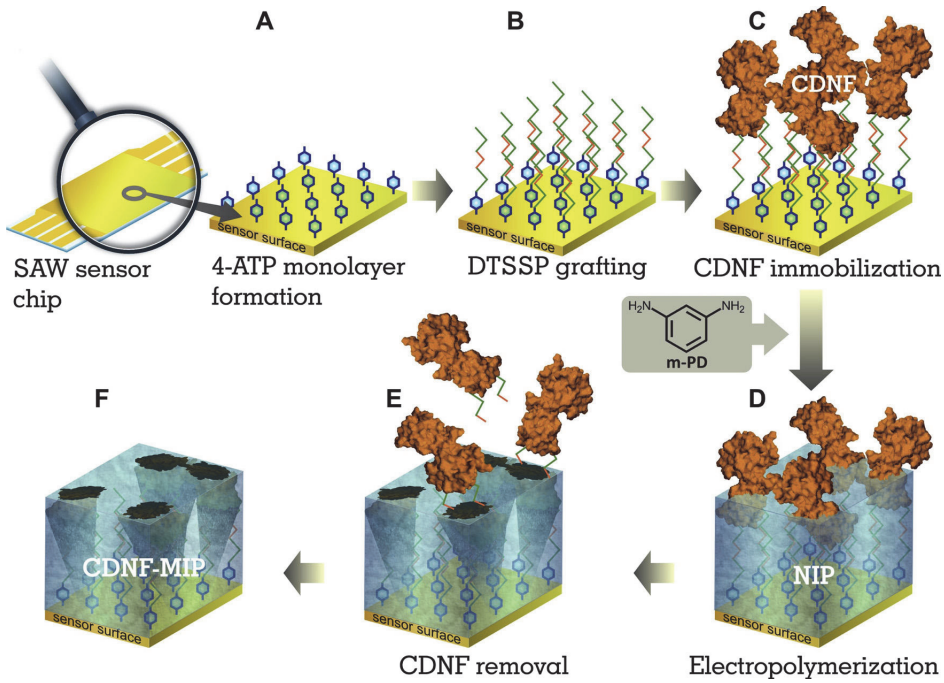

Fig. 1. The surface imprinting strategy for synthesis of the CDNF-MIP layer on the gold sensing surface of the SAW chip using the electropolymerization approach.

protein MANF in order from a low to a high concentration (from 5 ng/ml to 300 ng/ml) were sequentially injected onto the sensor elements. The respective solution were prepared in PBS buffer and contained the constant concentration of mCD48 (1.25 μg/ml). The selectivity was assessed by comparison of the residual responses at infinite dissociation which appeared after washing the sensor surface with running PBS buffer solution for 25 min (see section S2). In the competitive binding assays [38,39], the various concentrations (from 10^{-6} to 10^{-2} ng/ml) of either CDNF or MANF (competitor) were allowed to compete in PBS buffer with the constant amount of IgG (500 ng/ml) for the binding sites in CDNF-MIP. Additionally, the samples having different ratios of CDNF to MANF (10^{-2}:10^{-3} ng/ml or 10^{-3}:10^{-2} ng/ml) and IgG (500 ng/ml) were applied to assess the ability of the sensor to discriminate between CDNF and MANF (see section S2).

3. Results and discussion

3.1. Optimization of CDNF-MIP sensor preparation

The molecular imprinting strategy used in this study employs the bottom-up approach [26] in order to generate the macromolecular imprints resided on at/close to the surface of the polymeric film. Thus, for such MIP, the deposition of a polymer with an appropriate thickness is one of the most crucial tasks in order to avoid irreversible entrapment of a macromolecular template and infeasibility of its removal during the subsequent washing out procedures. The effect of polymer thickness on the performance of the resulting macromolecular-MIP has been already demonstrated in our previous study [26]. Thereby, we began to design CDNF-MIP paying special attention to the careful choice of an optimal thickness of the polymer matrix. In order to choose the range of the appropriate thicknesses for the polymer film, which confines, but does not irreversible entrap CDNF, the length of the whole structure containing the linker system and CDNF, was theoretically estimated (Fig. 2). Assuming that covalent attachment of CDNF via the succinimidyl group of DTSSP proceeds predominantly through its lysine residues that are abundant in the protein, the size of the resulting structure with random orientations of CDNF might vary from ca. 5.1–7.5 nm. Thus, polymer films confining the immobilized CDNFs till the middle of their possible front dimensions i.e. films with thicknesses between approx. 3.4 and 4.6 nm would be a good starting point in finding an optimal one for CDNF-MIP.

The correlation between the amount of electrical charge applied during the *in-situ* electrodeposition of the polymer and the thicknesses of the resulting CDNF-MIP films is presented in Fig. 2. As it can be seen, the thicknesses for CDNF-MIP varied linearly (R^2 = 0.998) across the applied electric charge range. This makes prediction of the thickness in the range of ca. 3 nm–8 nm quite certain in a convenient way by controlling the applied charge. The optimal thickness was elucidated after calculation of the molecular imprinting effect or the imprinting factor (*IF*) for every pair of CDNF-MIP and NIP characterized by the same thicknesses:

$$IF = Q_{eq(MIP)}/Q_{eq(NIP)} \quad (1)$$

where $Q_{eq(MIP)}$ and $Q_{eq(NIP)}$ are phase-shift responses at the equilibrium upon injection of a particular concentration of CDNF onto CDNF-MIP- and NIP-modified sensor elements, respectively. Thus, among the CDNF-MIPs having thicknesses ranging between 0.5 and 9 nm, one with PmPD generated by 1 mC/cm^2 (ca. 2.3 nm) demonstrated the highest *IF* (1.2) (Fig. 3a). It should be noted that there was significant non-specific binding on NIPs resulting in marginal differences in responses between CDNF-MIP- and NIP-modified sensor elements. This makes values of *IFs* not prominent enough to justify confidently that 2.3 nm thick polymer would be an optimal one for CDNF-MIP. In order to reduce the non-specific binding, the CDNF-MIP and NIP films were underwent the treatment in 0.01 M PBS solution containing 0.04 mg/ml HSA beforehand the rebinding experiments.

Although the treatment with HSA significantly suppressed the response amplitudes, the noticeable difference between CDNF-MIP- and

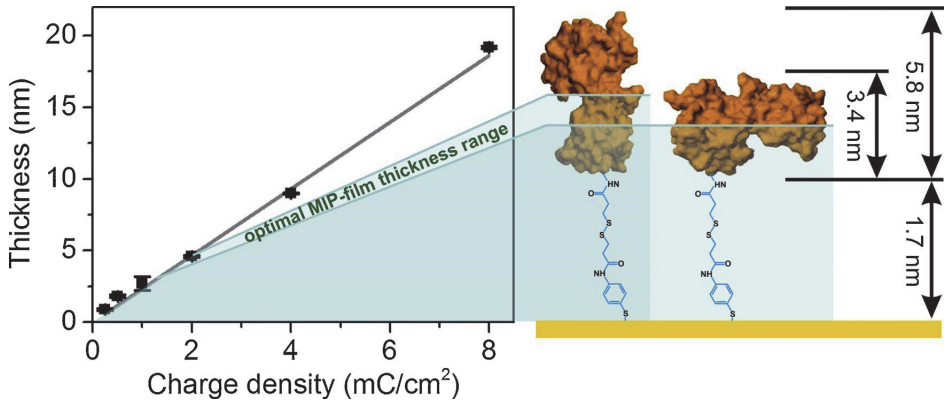

Fig. 2. The calibration graph representing the dependence of the polymeric thickness of MIP films, as measured by VIS-ellipsometry, on the amount of the charge consumed during the electropolymerization of *m*-PD on CDNF-modified gold electrode. The solid lines represent linear regression fits. The drawing on the right hand of the figure demonstrates an approximation of the heights of the linker-CDNF structure immobilized on a planar surface.

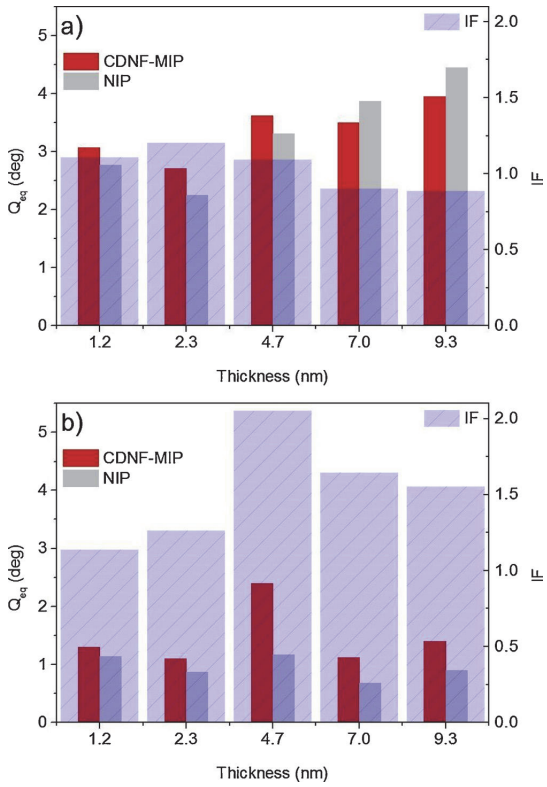

Fig. 3. Effect of the polymer thickness of CDNF-MIP and NIP films on the responses of the SAW sensors and the respective imprinting factors measured upon injection of 1.25 µg/mL of CDNF in PBS: a) without blocking of non-specific adsorption b) after blocking in 0.1 M PBS buffer (pH 7.4) containing 0.04 mg/ml HSA.

NIP-modified sensor elements was achieved (Fig. 3b). This also affected the ranking of the optimal polymer thicknesses. After the treatment in HSA, CDNF-MIPs with thickness of 4.7 nm (2 mC/cm^2) had the highest relative rebinding of CDNF as judged by *IF*equal to about 2 (Fig. 3b). The found optimal thickness correlates well with the concept of surface imprinting approach used in this study. At such thickness the polymer confines about the median dimension of CDNF, and, in turn, likely does not hinder its successful extraction to leave behind a selective molecular cavity. Thus, the use of electrochemical polymerization for protein-MIP is a very sophisticated method to generate precisely such ultrathin polymer matrices by just control the applied electrochemical charge.

3.2. Rebinding studies

The CDNF-MIP sensors were characterized in terms of their capability to rebind CDNF by monitoring and comparing its binding kinetics on CDNF-MIP and NIP surfaces. Since, according to the applied synthesis strategy, the template proteins were not removed from NIP, we considered the NIP as the CDNF-MIP with completely occupied specific binding sites and, analysing the obtained binding profiles, assumed that during the rebinding process (i) such a NIP surface exhibited only nonspecific protein adsorption and (ii) on the respective CDNF-MIP surface the nonspecific adsorption could occur to the same extent. Thus, in order to reference out the contribution of nonspecific interactions in the response signals, the binding profiles on the CDNF-MIP were corrected by subtracting the corresponding binding profiles observed on the NIP surfaces.

After the correction, the responses of the CDNF-MIP sensor demonstrated well pronounced analyte concentration-dependent binding profiles and allowed fitting them to the pseudo-first order kinetics model (Eq. S1) (Fig. S2). This model has been previously successfully applied for description of binding kinetics on MIPs [40]. In this study, the model still gave a decent fit to the experimental kinetics data with a coefficient of determination (R^2) in the range of 0.944-0.994 (Table S1) and allowed predicting the equilibrium responses (Q_{eq}) at every injected concentration of CDNF.

We examined two binding isotherm models to describe Q_{eq} vs concentration data: Langmuir (L) and Langmuir–Freundlich (LF) (Fig. 4). While L model assumes that a monolayer of adsorbate is formed on a homogeneous surface of the adsorbent [41], LF model, being a continuous distribution model, can be applied for modelling a more complex interaction between the molecule and the surface of the adsorbent with the participation of binding sites having different levels of affinity [42]. As expected, the LF model provided somewhat better agreement with the binding isotherm data than the L model (coefficient of correlation 0.990 and 0.975, respectively (Table S2)). As has been shown previously, most MIPs often behave as heterogeneous systems, and thus

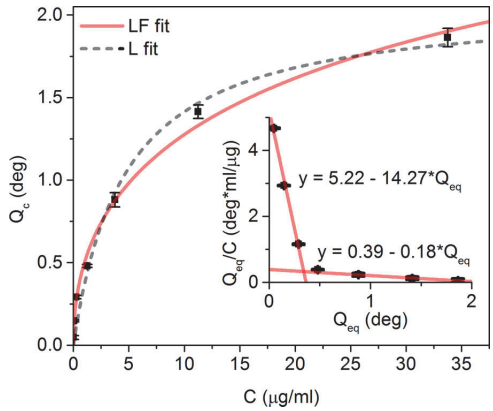

Fig. 4. The adsorption isotherm of CDNF measured by CDNF-MIP sensor. The dashed lines represent fits to the Langmuir (gray, dash) and Langmuir-Freundlich (red, solid) adsorption models. Insert: the Scatchard plot with limiting slopes estimates by means of linear regression. For interpretation of the references to colour in this figure legend, the reader is referred to the web version of this article.)

the LF model would be more universally applicable to their characterization, since it takes into account heterogeneity of binding sites and is able to model binding behavior in a wider concentration range up to saturation [42,43]. Additionally, the Scatchard plot i.e the experimental binding isotherm in the Q_{eq}/C vs. Q_{eq} format, clearly shows the heterogeneity of the binding sites (Fig. 4, insert). Two separate straight line parts on the curve of the isotherm indicate that there are sites with different affinities. The flat and steep lines describes the sites with low and high affinity, respectively [42].

The heterogeneity of the current CDNF-MIPs can be explained by the fact that CDNF imprints were formed by CDNFs randomly oriented towards the sensor surface. Indeed, to form the CDNF-MIP, CDNFs were initially immobilized on the surface through the covalent interaction of primary amines of the lysine side chain of CDNF with the active group of DTSSP. Since the primary amines are located over the entire surface of CDNF, it could be immobilized with different orientations to the surface leading to the formation of the imprinted sites with different binding energy in the course of the subsequent imprinting process.

3.3. Selectivity studies

Several binding assays were carried out in order to assess the feasibility and selectivity of detecting CDNF by CDNF-MIP sensor. In the first test, CDNF-MIP sensor was investigated in terms of its capability to rebind the target protein, CDNF with respect to a protein having a very similar structure [4], same size, but a slightly different pI such as MANF and can be thus, a suitable pair to assess the selectivity of the prepared CDNF-MIP layer. The test was carried out in the presence of mCD48 having pI value higher than CDNF and MANF in order to cause an additional nonspecific background and thus somewhat simulate additional complexity in scenarios for the selectivity testing.

As it can be seen, although the sensor is responsive to every applied injection, the sharp rises appear only upon injection of the solutions containing CDNF (Fig. 5a). During the dissociation stages the responses do not returned back to the baseline, but are gradually shifted to higher values indicating that a part of protein molecules remained bound to the sensor surface. Taking into account such behavior, we analyzed the sensor responses by calculating the residual binding values at dissociation stage, Q_{res} (see Section S2 and Table S3 in SI for details) and compared these values between CDNF and MANF injection series in order to assess the capability of the sensor to distinguish the respective

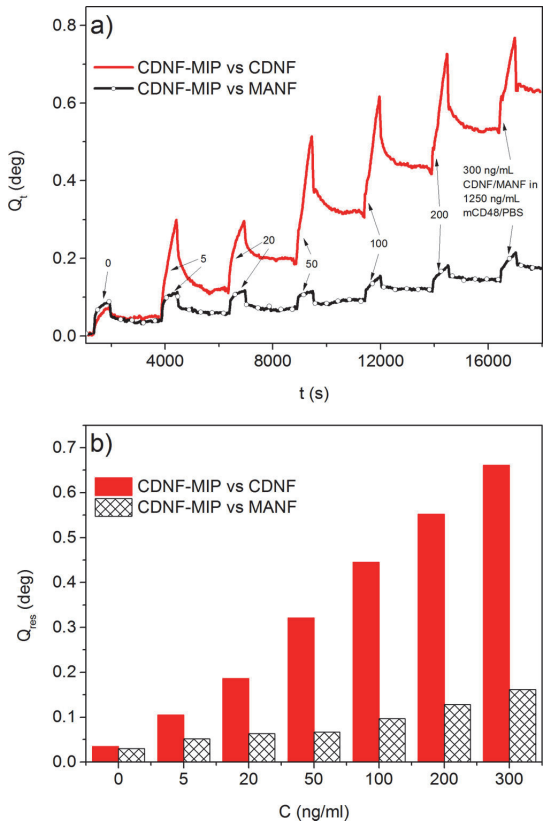

Fig. 5. (a) The NIP-corrected sensorgrams of CDNF-MIP sensor measured by the kinetic titration method upon injections of different concentrations of CDNF (red line) or MANF (black line, empty dot) in the presence of 1.25 μg/ml mCD48 and (b) the corresponding residual responses at infinite dissociation derived from Eq. S4 (see section S2). For interpretation of the references to colour in this figure legend, the reader is referred to the web version of this article.)

proteins (Fig. 5b). The noticeable increase of Q_{res} in favour of CDNF containing mixtures can be observed already after the first concentration applied (5 ng/ml) eventually reaching 4-fold difference after the final injection (300 ng/mL). A possible explanation for this phenomenon could be the higher affinity of the CDNF-MIP surface towards CDNF molecules that remain bound to CDNF-MIP at much higher extent than MANF molecules. Under the given assay conditions, the CDNF-MIP sensor shows a linear response to CDNF in the concentration range from 5 to 50 ng/ml, with limit of detection (LOD) and limit of quantitation (LOQ) of 4.2 ng/ml and 14 ng/ml (Fig. S3).

To further examine selectivity of the CDNF-MIP sensor, we designed a label-free binding assay, where various concentrations of either CDNF or MANF were allowed to compete with the constant amount of IgG for the binding sites in CDNF-MIP. Specifically, in the assay, we looked into the inhibition of non-specific binding of a relatively massive protein such as IgG on the surface of the CDNF-MIP caused by the increasing concentration of competing protein in the applied mixture.

The optimal concentration of IgG in the assay was selected by plotting the binding isotherm of non-specific adsorption of IgG on the surface of the CDNF-MIP. As it can be seen, adsorption of IgG is linear versus the concentration in the range of 31.25–1000 ng/ml, but tends to saturate afterwards (Fig. S4). Therefore, the concentration of 500 ng/ml

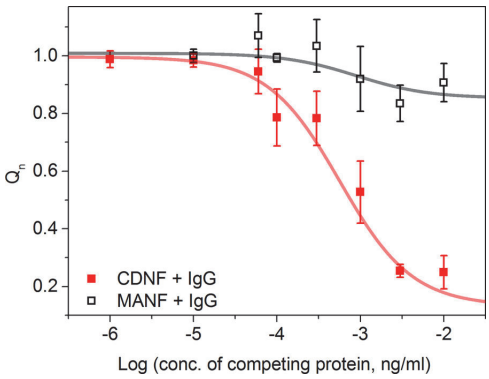

Fig. 6. Competitive binding of IgG measured by CDNF-MIP sensor as a function of the competing protein concentration (ng/ml). The binding was conducted in PBS buffer solution containing a fixed concentration of IgG (500 ng/ml) and increasing concentration of the competing protein, either CDNF or MANF, in the range of 10^{-6} to 10^{-2} ng/ml. The sensor responses were normalized to the response upon injection of IgG (500 ng/ml).

IgG was selected for the following binding assays as one could provide a noticeable effect on the competitive replacement of IgG on the CDNF-MIP surface. The concentrations above 500 ng/ml might be redundant and can hinder observing the effect.

Although, little is known about the nature of protein recognition sites in MIPs, it was reasonable to expect that in the given competitive binding assays CDNF-MIP sensor was going to be more responsive to CDNF i.e. the mixtures containing CDNF and IgG would evoke stronger inhibitions of IgG binding than those containing MANF and IgG. As demonstrated by Fig. 6, indeed the normalized response, Q_n, decreased (about 75 %) upon injection of the mixture containing 0.01 ng/ml CDNF, i.e. obviously, the heavier protein (IgG) is replaced with the lighter one (CDNF). Conducting the very same competitive assay with MANF instead of CDNF, resulted in much less inhibition of the response (about 15 %), that is, the replacement of IgG from the recognition sites is less efficient in this case. If both CDNF and MANF competed with IgG in the same solution then it was still clearly seen that the significant inhibition of the signal was induced namely by the presence of CDNF in the sample rather than the presence of MANF (Fig. S5).

The competitive binding assay data are fitted by three parameter dose response curves revealing IC50 values for CDNF and MANF assays with a marginal difference: 0.6 versus 0.9 pg/ml, respectively (see Section S2 and Table S4). Nevertheless, taking into account the high similarity in the three-dimensional structures of CDNF and MANF [44,45] and the fact that CDNF was identified to be homologous to MANF with 59 % amino acid identity in human proteins [4], the given assay still supports clearly that CDNF-MIP surface preferentially binds CDNF than MANF. The limit of detection in this assay, calculated as the analyte concentration causing a 20 % inhibition (IC_{20}), corresponded to 0.1 pg/ml. However, even 10 pg/ml concentration of MANF is unable to cause such significant inhibition to CDNF binding response. The found LOD is significantly below the CDNF concentrations found in human serum [46].

4. Conclusions

We have demonstrated the possibility of using a MIP-based synthetic receptor to build a SAW sensor capable of detecting a neurotrophic factor protein, CDNF, in label-free manner. The electrochemical surface imprinting approach enabled a simple and rapid preparation of the polymeric matrix possessing the selectivity to CDNF, i.e. CDNF-MIP, directly on the sensor surface. We found that the thickness of the polymer matrix is critical and should be precisely adjusted in order to achieve the notable imprinting effect in the resulting CDNF-MIPs. Polymers with thicknesses, confining about the median dimension of a macromolecule, thus likely provide its successful extraction and leaving behind a molecular cavity capable of efficient and selective rebinding. Moreover, intrinsic affinity of PmPD-based matrix to CDNF was needed to be suppressed in order to properly assess imprinting effect. Nevertheless, the presence of intrinsic affinity in the resulting CDNF-MIP would not likely necessarily disturb the sensor response, but could be considered for designing competitive assays, where the target protein displaces interfering one from the MIP-modified sensor surface. As demonstrated, the prepared CDNF-MIP sensor clearly differentiated between CDNF and its homologue - MANF even in the presence of IgG in the test solution showing a response at sub pg/ml range.

We anticipate that our results provide guidelines for synthesis of MIPs applicable for detection of other essential NFs. These NF-selective MIPs can work well as synthetic recognition layers with other label-free sensing platforms such as surface plasmon resonance and quartz crystal microbalance, where accumulated mass is measured at the surface of their transducers. Further study is needed to investigate the sensor capability detecting CDNF in complex matrixes as body fluids. If this works the adaptation of our results to portable sensor platforms will pave the way for the much-needed cost-effective research or diagnostics tools in the field of neurodegenerative diseases. Efforts along those lines are currently in progress to validate detection of CDNF in body fluids of real patient samples that have been verified with CDNF and MANF ELISAs.

Declaration of Competing Interest

The authors declare that they have no known competing financial interests or personal relationships that could have appeared to influence the work reported in this paper.

Acknowledgements

This work was supported by the Estonian Research Council grant (PRG307) and by the Jane and Aatos Erkko Foundation. The authors thank Dr. Andreas Furchner from Leibniz-Institut für Analytische Wissenschaften – ISAS – e. V. for the VIS ellipsometry measurements. The authors thank Icosagen AS and prof. Mart Ustav personally, for kindly providing the neurotrophic factor proteins.

Appendix A. Supplementary data

Supplementary material related to this article can be found, in the online version, at doi:https://doi.org/10.1016/j.snb.2020.127708.

References

[1] World Health Organization, Neurological Disorders: Public Health Challenges, World Health Organization, Geneva, Switzerland, 2006http://whqlibdoc.who.int/publications/2006/9241563362_eng.pdf.
[2] Y.S. Levy, Y. Gilgun-Sherki, E. Melamed, D. Offen, Therapeutic potential of neurotrophic factors in neurodegenerative diseases, BioDrugs Clin. Immunother. Biopharm. Gene Ther. 19 (2005) 97–127.
[3] K. Hashimoto, Brain-derived neurotrophic factor as a biomarker for mood disorders: an historical overview and future directions, Psychiatry Clin. Neurosci. 64 (2010) 341–357, https://doi.org/10.1111/j.1440-1819.2010.02113.x.
[4] M. Lindahl, M. Saarma, P. Lindholm, Unconventional neurotrophic factors CDNF and MANF: structure, physiological functions and therapeutic potential, Neurobiol. Dis. 97 (2017) 90–102, https://doi.org/10.1016/j.nbd.2016.07.009.
[5] M. Saarma, P. Lindholm, U. Arumäe, Neurotrophic factors, Mov. Disord. (2012) 129–140.
[6] M.H. Voutilainen, U. Arumae, M. Airavaara, M. Saarma, Therapeutic potential of the endoplasmic reticulum located and secreted CDNF/MANF family of neurotrophic factors in Parkinson's disease, FEBS Lett. 589 (2015) 3739–3748, https://doi.org/10.1016/j.febslet.2015.09.031.
[7] D. Lindholm, J. Mäkelä, V. Di Liberto, G. Mudò, N. Belluardo, O. Eriksson, M. Saarma, Current disease modifying approaches to treat Parkinson's disease, Cell.

Mol. Life Sci. 73 (2016) 1365–1379, https://doi.org/10.1007/s00018-015-2101-1.
[8] P. Lindholm, M.H. Voutilainen, J. Lauren, J. Peranen, V.M. Leppanen, J.O. Andressoo, M. Lindahl, S. Janhunen, N. Kalkkinen, T. Timmusk, R.K. Tuominen, M. Saarma, Novel neurotrophic factor CDNF protects and rescues midbrain dopamine neurons in vivo, Nature 448 (2007) 73–77, https://doi.org/10.1038/nature05957.
[9] Y.A. Sidorova, M. Saarma, Glial cell line-derived neurotrophic factor family ligands and their therapeutic potential, Mol. Biol. 50 (2016) 521–531, https://doi.org/10.1134/s0026893316040105.
[10] H.J. Huttunen, M. Saarma, CDNF protein therapy in Parkinson's disease, Cell Transplant. (2019), https://doi.org/10.1177/0963689719840290 963689719840290.
[11] M. Ventriglia, R. Zanardini, C. Bonomini, O. Zanetti, D. Volpe, P. Pasqualetti, M. Gennarelli, L. Bocchio-Chiavetto, Serum brain-derived neurotrophic factor levels in different neurological diseases, Biomed Res. Int. 2013 (2013) 901082, , https://doi.org/10.1155/2013/901082.
[12] E. Galli, T. Härkönen, M.T. Sainio, M. Ustav, U. Toots, A. Urtti, M. Yliperttula, M. Lindahl, M. Knip, M. Saarma, P. Lindholm, Increased circulating concentrations of mesencephalic astrocyte-derived neurotrophic factor in children with type 1 diabetes, Sci. Rep. 6 (2016) 29058, https://doi.org/10.1038/srep29058.
[13] B. Elfving, P.H. Plougmann, G. Wegener, Detection of brain-derived neurotrophic factor (BDNF) in rat blood and brain preparations using ELISA: pitfalls and solutions, J. Neurosci. Methods 187 (2010) 73–77, https://doi.org/10.1016/j.jneumeth.2009.12.017.
[14] S. Zhang, A. Garcia-D'Angeli, J.P. Brennan, Q. Huo, Predicting detection limits of enzyme-linked immunosorbent assay (ELISA) and bioanalytical techniques in general, Analyst 139 (2014) 439–445, https://doi.org/10.1039/c3an01835k.
[15] S. Ray, G. Mehta, S. Srivastava, Label-free detection techniques for protein microarrays: prospects, merits and challenges, Proteomics 10 (2010) 731–748, https://doi.org/10.1002/pmic.200900458.
[16] K. Chang, Y. Pi, W. Lu, F. Wang, F. Pan, F. Li, S. Jia, J. Shi, S. Deng, M. Chen, Label-free and high-sensitive detection of human breast cancer cells by aptamer-based leaky surface acoustic wave biosensor array, Biosens. Bioelectron. 60 (2014) 318–324, https://doi.org/10.1016/j.bios.2014.04.027.
[17] M. Espinoza-Castaneda, A. de la Escosura-Muniz, A. Chamorro, C. de Torres, A. Merkoci, Nanochannel array device operating through Prussian blue nanoparticles for sensitive label-free immunodetection of a cancer biomarker, Biosens. Bioelectron. 67 (2015) 107–114, https://doi.org/10.1016/j.bios.2014.07.039.
[18] H.V. Tran, B. Piro, S. Reisberg, L. Huy Nguyen, T. Dung Nguyen, H.T. Duc, M.C. Pham, An electrochemical ELISA-like immunosensor for miRNAs detection based on screen-printed gold electrodes modified with reduced graphene oxide and carbon nanotubes, Biosens. Bioelectron. 62 (2014) 25–30, https://doi.org/10.1016/j.bios.2014.06.014.
[19] A.E. Kennedy, K.S. Sheffield, J.K. Eibl, M.B. Murphy, R. Vohra, J.A. Scott, G.M. Ross, A surface plasmon resonance spectroscopy method for characterizing small-molecule binding to nerve growth factor, J. Biomol. Screen. 21 (2016) 96–100, https://doi.org/10.1177/1087057115607814.
[20] K.S. Sheffield, R. Vohra, J.A. Scott, G.M. Ross, Using surface plasmon resonance spectroscopy to characterize the inhibition of NGF-p75(NTR) and proNGF-p75(NTR) interactions by small molecule inhibitors, Pharmacol. Res. 103 (2016) 292–299, https://doi.org/10.1016/j.phrs.2015.12.005.
[21] K. Mosbach, Molecular imprinting, Trends Biochem. Sci. 19 (1994) 9–14.
[22] K. Haupt, K. Mosbach, Molecularly imprinted polymers and their use in biomimetic sensors, Chem. Rev. 100 (2000) 2495–2504.
[23] L. Ye, K. Mosbach, Molecular imprinting: synthetic materials as substitutes for biological antibodies and receptors, Chem. Mater. 20 (2008) 859–868, https://doi.org/10.1021/cm703190w.
[24] A.G. Ayankojo, A. Tretjakov, J. Reut, R. Boroznjak, A. Öpik, J. Rappich, A. Furchner, K. Hinrichs, V. Syritski, Molecularly imprinted polymer integrated with a surface acoustic wave technique for detection of sulfamethizole, Anal. Chem. 88 (2016) 1476–1484, https://doi.org/10.1021/acs.analchem.5b04735.
[25] A. Tretjakov, V. Syritski, J. Reut, R. Boroznjak, O. Volobujeva, A. Öpik, Surface molecularly imprinted polydopamine films for recognition of immunoglobulin G, Microchim. Acta. 180 (2013) 1433–1442, https://doi.org/10.1007/s00604-013-1039-y.
[26] A. Tretjakov, V. Syritski, J. Reut, R. Boroznjak, A. Öpik, Molecularly imprinted polymer film interfaced with Surface Acoustic Wave technology as a sensing platform for label-free protein detection, Anal. Chim. Acta 902 (2016) 182–188, https://doi.org/10.1016/j.aca.2015.11.004.
[27] P.S. Sharma, A. Pietrzyk-Le, F. D'Souza, W. Kutner, Electrochemically synthesized polymers in molecular imprinting for chemical sensing, Anal. Bioanal. Chem. 402 (2012) 3177–3204, https://doi.org/10.1007/s00216-011-5696-6.
[28] P. Jolly, V. Tamboli, R.L. Harniman, P. Estrela, C.J. Allender, J.L. Bowen, Aptamer-MIP hybrid receptor for highly sensitive electrochemical detection of prostate specific antigen, Biosens. Bioelectron. 75 (2016) 188–195, https://doi.org/10.1016/j.bios.2015.08.043.
[29] S. Viswanathan, C. Rani, S. Ribeiro, C. Delerue-Matos, Molecular imprinted nanoelectrodes for ultra sensitive detection of ovarian cancer marker, Biosens. Bioelectron. 33 (2012) 179–183, https://doi.org/10.1016/j.bios.2011.12.049.
[30] Y.T. Wang, Z.Q. Zhang, V. Jain, J.J. Yi, S. Mueller, J. Sokolov, Z.X. Liu, K. Levon, B. Rigas, M.H. Rafailovich, Potentiometric sensors based on surface molecular imprinting: detection of cancer biomarkers and viruses, Sens. Actuators B-Chem. 146 (2010) 381–387, https://doi.org/10.1016/j.snb.2010.02.032.
[31] V.V. Shumyantseva, T.V. Bulko, L.V. Sigolaeva, A.V. Kuzikov, A.I. Archakov, Electrosynthesis and binding properties of molecularly imprinted poly-o-phenylenediamine for selective recognition and direct electrochemical detection of myoglobin, Biosens. Bioelectron. 86 (2016) 330–336, https://doi.org/10.1016/j.bios.2016.05.101.
[32] B.V.M. Silva, B.A.G. Rodríguez, G.F. Sales, M.D.P.T. Sotomayor, R.F. Dutra, An ultrasensitive human cardiac troponin T graphene screen-printed electrode based on electropolymerized-molecularly imprinted conducting polymer, Biosens. Bioelectron. 77 (2016) 978–985, https://doi.org/10.1016/j.bios.2015.10.068.
[33] J.L. Urraca, C.S.A. Aureliano, E. Schillinger, H. Esselmann, J. Wiltfang, B. Sellergren, Polymeric complements to the Alzheimer's disease biomarker β-Amyloid isoforms Aβ1–40 and Aβ1–42 for blood serum analysis under denaturing conditions, J. Am. Chem. Soc. 133 (2011) 9220–9223, https://doi.org/10.1021/ja202908z.
[34] A. Cecchini, V. Raffa, F. Canfarotta, G. Signore, S. Piletsky, M.P. MacDonald, A. Cuschieri, In vivo recognition of human vascular endothelial growth factor by molecularly imprinted polymers, Nano Lett. 17 (2017) 2307–2312, https://doi.org/10.1021/acs.nanolett.6b05052.
[35] Y. Kamon, T. Takeuchi, Molecularly imprinted nanocavities capable of ligand-binding domain and Size/Shape recognition for selective discrimination of vascular endothelial growth factor isoforms, ACS Sens. 3 (2018) 580–586, https://doi.org/10.1021/acssensors.7b00622.
[36] M. Johari-Ahar, P. Karami, M. Ghanei, A. Afkhami, H. Bagheri, Development of a molecularly imprinted polymer tailored on disposable screen-printed electrodes for dual detection of EGFR and VEGF using nano-liposomal amplification strategy, Biosens. Bioelectron. 107 (2018) 26–33, https://doi.org/10.1016/j.bios.2018.02.005.
[37] A. Kidakova, J. Reut, R. Boroznjak, A. Öpik, V. Syritski, Advanced sensing materials based on molecularly imprinted polymers towards developing point-of-care diagnostics devices, Proc. Est. Acad. Sci. 68 (2019) 158–167, https://doi.org/10.3176/proc.2019.2.07.
[38] A.P. Davenport, F.D. Russell, Radiolig and binding assays: theory and practice, Curr. Dir. Radiopharm. Res. Dev. Stephen J Mather, 1996, pp. 169–178 http://public.ebookcentral.proquest.com/choice/publicfullrecord.aspx?p=3102748.
[39] Y. Gao, X. Li, L.-H. Guo, Development of a label-free competitive ligand binding assay with human serum albumin on a molecularly engineered surface plasmon resonance sensor chip, Anal. Methods 4 (2012) 3718–3723, https://doi.org/10.1039/C2AY25780G.
[40] A. Kidakova, J. Reut, J. Rappich, A. Öpik, V. Syritski, Preparation of a surface-grafted protein-selective polymer film by combined use of controlled/living radical photopolymerization and microcontact imprinting, React. Funct. Polym. 125 (2018) 47–56.
[41] R.A. Latour, The Langmuir isotherm: a commonly applied but misleading approach for the analysis of protein adsorption behavior, J. Biomed. Mater. Res. A 103 (2015) 949–958, https://doi.org/10.1002/jbm.a.35235.
[42] R.J. Umpleby, S.C. Baxter, A.M. Rampey, G.T. Rushton, Y.Z. Chen, K.D. Shimizu, Characterization of the heterogeneous binding site affinity distributions in molecularly imprinted polymers, J. Chromatogr. B-Anal. Technol. Biomed. Life Sci. 804 (2004) 141–149.
[43] R.J. Umpleby, S.C. Baxter, M. Bode, J.K. Berch, R.N. Shah, K.D. Shimizu, Application of the Freundlich adsorption isotherm in the characterization of molecularly imprinted polymers, Anal. Chim. Acta 435 (2001) 35–42.
[44] M. Hellman, U. Arumäe, L. Yu, P. Lindholm, J. Peränen, M. Saarma, P. Permi, Mesencephalic astrocyte-derived neurotrophic factor (MANF) has a unique mechanism to rescue apoptotic neurons, J. Biol. Chem. 286 (2011) 2675–2680, https://doi.org/10.1074/jbc.M110.146738.
[45] V. Parkash, P. Lindholm, J. Peränen, N. Kalkkinen, E. Oksanen, M. Saarma, V.-M. Leppänen, A. Goldman, The structure of the conserved neurotrophic factors MANF and CDNF explains why they are bifunctional, Protein Eng. Des. Sel. 22 (2009) 233–241, https://doi.org/10.1093/protein/gzn080.
[46] E. Galli, A. Planken, L. Kadastik-Eerme, M. Saarma, P. Taba, P. Lindholm, Increased serum levels of mesencephalic astrocyte-derived neurotrophic factor in subjects with Parkinson's disease, Front. Neurosci. 13 (2019), https://doi.org/10.3389/fnins.2019.00929.

Anna Kidakova graduated from Astrakhan State Technical University in 2007. She received her MSc (2014) in material sciences from TalTech. She is currently a PhD student at the Laboratory of Biofunctional Materials of TalTech. Her research interest includes the development of molecularly imprinted polymer-based sensors for point-of care application.

Roman Boroznjak received his MSc (2007) in organic chemistry and PhD (2017) in natural and exact sciences from TalTech. His research interests include computational modelling and rational design of molecularly imprinted polymers.

Jekaterina Reut is currently a research scientist at the Department of Material and Environmental Technology in TalTech. She received her PhD (2004) in the field of electrically conducting polymers from TalTech. Her research interest is in the area of the design and synthesis of molecularly imprinted polymers for biosensing applications.

Andres Öpik received his PhD in chemistry from the University of Tartu in 1980. He is currently Professor of physical chemistry at the Department of Material and Environmental Technology in TalTech. His main research field is material science and technology: investigation of the physical and chemical properties and possibilities of practical applications of different electronic materials such as electrically conductive polymers and inorganic semiconductive compounds. Currently his research interests include the development of novel functional materials based on molecularly imprinted polymers for biomedical diagnostics.

Mart Saarma received his PhD in 1975 in Molecular Biology at the University of Tartu. Currently he is the head of the Laboratory of Molecular Neuroscience at the Institute of Biotechnology, HiLIFE, University of Helsinki. He is investigating the structure, biology and therapeutic potential of neurotrophic factors. His group has characterized several new GDNF family receptors and novel neurotrophic factor CDNF that is in Phase I—II clinical trials on Parkinson's disease patients.

Vitali Syritski received his PhD in Chemistry at Tallinn University of Technology in 2004. Currently he is the head of the Laboratory of Biofunctional Materials in the Department of Material and Environmental Technology at TalTech. His present research interests include molecularly imprinted technology and electrochemical analysis. In particular, he has focused on development of chemical and biosensors for accurate and fast detection of disease biomarkers and environmental contaminants.

Publication II

A. Kidakova, J. Reut, J. Rappich, A. Öpik, V. Syritski, Preparation of a surface-grafted protein-selective polymer film by combined use of controlled/living radical photopolymerization and microcontact imprinting, React. Funct. Polym. 125 (2018) 47–56.

Reactive and Functional Polymers 125 (2018) 47–56

Contents lists available at ScienceDirect

Reactive and Functional Polymers

journal homepage: www.elsevier.com/locate/react

Preparation of a surface-grafted protein-selective polymer film by combined use of controlled/living radical photopolymerization and microcontact imprinting

Anna Kidakova[a], Jekaterina Reut[a], Jörg Rappich[b], Andres Öpik[a], Vitali Syritski[a,*]

[a] Department of Materials and Environmental Technology, Tallinn University of Technology, Ehitajate tee 5, 19086 Tallinn, Estonia
[b] Helmholtz-Zentrum Berlin für Materialien und Energie GmbH, Institut für Silizium-Photovoltaik, Kekulestr. 5, 12489 Berlin, Germany

ARTICLE INFO

Keywords:
Molecularly imprinted polymers
Microcontact imprinting
Photopolymerization
Protein imprinting
Bovine serum albumin
Controlled/living radical polymerization
SPR sensor

ABSTRACT

In this study, we describe a strategy for the formation of a molecularly imprinted polymer (MIP) capable of selective rebinding of protein-sized molecules and interfaced with a planar sensing surface. The strategy is based on the synergistic use of the surface-initiated controlled/living radical (C/LR) photopolymerization and microcontact imprinting approach aiming at design of a protein-responsive polymer for biosensing application. Bovine serum albumin (BSA), 2-(diethylamino)ethyl methacrylate, bis-acrylamide were used as a model protein, a functional monomer and a cross-linker, respectively, to prepare the BSA-MIP film. The optimal parameters of C/LR photopolymerization such as the method for photoinitiator attachment to the sensor surface, monomer:cross-linker molar ratio, polymerization time, were determined. The BSA-MIP film were studied in terms of their recognition capability and selectivity towards the target protein (BSA) through the analysis of the responses of the BSA-MIP modified SPR sensors upon interaction with BSA and interfering proteins, human serum albumin (HSA) and Fc-fragment of immunoglobulin G (Fc). It was found that BSA-MIP adsorbed BSA with the dissociation constant (KD) in the nanomolar range (68 nM) and shows more than two times higher adsorption capacity as compared to HSA and Fc, even though their molecular sizes were similar. Also, BSA-MIP could be perfectly regenerated in the alkaline solution showing nearly reversible responses (loss of 2.4%) even after the 25th regeneration cycle. The presented simple synthesis strategy could be potentially employed for the preparation of protein-MIP films on a planar sensor transducer allowing to develop sensing systems for detection of clinically relevant proteins.

1. Introduction

The concept of molecular imprinting has been widely recognized as a promising strategy for synthesis of robust molecular recognition materials with high selectivity towards the analyte [1]. Molecular imprinting can be defined as the process of template-induced formation of specific molecular recognition sites in a polymer matrix material. In this process, a mixture of functional monomers is polymerized around a chosen target molecule acting as a template. Removal of the templates from the formed polymer leaves behind binding sites that are capable of selectively recognizing of the template molecules or similar structures. The main benefits of these, so-called Molecularly Imprinted Polymers (MIPs), are related to their synthetic nature, i.e., excellent chemical and thermal stability associated with reproducible, cost-effective fabrication. Therefore, MIPs have received much interest and are successfully applied in different areas such as artificial antibody mimics [2], materials separation [3] and drug delivery [4]. MIPs have been reported to be a promising alternative to biological receptors in biosensors providing more stable and low-cost recognition elements [5]. Bulk imprinting is the simplest approach to macromolecular imprinting. The advantage of this approach is that the 3D–binding sites are formed for the whole protein. However, a significant disadvantage is the diffusional limitations, as the polymer matrix surrounding the protein from all sides and prevents protein washing from the matrix [2]. To solve this problem Shi and coworkers proposed to precipitate the protein on the surface of mica before the polymerization [6]. Thus, the growth of the polymer matrix is limited to the surface of protein stamp and the resulting specific cavities are located very close to the surface of the polymer. Nowadays, surface imprinting of proteins has become the most common used approach [7–9]. One of the prospective approaches to produce protein-MIP films with surface-confined binding sites is microcontact imprinting [10,11]. An important advantage of the

* Corresponding author.
E-mail address: vitali.syritski@ttu.ee (V. Syritski).

https://doi.org/10.1016/j.reactfunctpolym.2018.02.004
Received 6 September 2017; Received in revised form 1 February 2018; Accepted 7 February 2018
Available online 14 February 2018

microcontact imprinting is that very little or no template molecules remain "trapped" in the polymer matrix after completion of the polymerization resulting in a MIP-film with more homogeneous binding sites [12].

In addition to the above mentioned techniques, the development of MIPs for biosensing application requires a perfect interfacing between the recognition element and the sensor transducer. Popular methods of polymer film preparation on a solid surface such as spin-casting, dip-coating, polyelectrolyte deposition and plasma deposition result in physically adsorbed polymer films, which exhibit non-covalent interactions (hydrophobic or electrostatic interactions, van der Waals forces) with the surface. This gives a relatively weak adhesion, making these films not steady to external factors (solvents, high temperature, mechanical actions) and limits the scope of their application [13]. Surface initiated polymerization is an universal way to overcome these disadvantages by creating covalent bonding between the polymer film and the surface [14]. To perform surface initiated polymerization an initiator is firstly attached to the substrate surface using different techniques [14,15]. This method offers the capability of the film thickness control, uniform coating of surface, control over composition, and high density of grafting [14]. Surface initiated polymerization can proceed via different polymerization mechanisms depending on the initiator end-group [16]: free-radical polymerization (FRP) [17], cationic and anionic polymerization [18], atom-transfer radical polymerization (ATRP) [19], ring-opening polymerization [20] and reversible addition fragmentation chain transfer (RAFT) polymerization [21].

Photopolymerization seems to be suitable methods for in situ MIP film synthesis providing the possibility of good control of both film thickness and inner morphology [22]. A wide range of photoinitiators allows realizing photopolymerization by various mechanisms, including the controlled/living radical polymerization (C/LRP) method, which allows the control of the composition and thickness of the MIP films. Salian and co-workers showed the improvement in network homogeneity and imprinting efficiency in weakly cross-linked MIP networks prepared by C/LRP in comparison with FRP [23]. C/LRP extended the reaction-controlled regime of the polymerization reaction and formed more homogeneous polymer chains and networks with smaller mesh sizes. The RAFT polymerization is the most versatile process among C/LRP techniques. Effective chain transfer agents for the reversible attachment mechanism fragmentation are different dithioesters, dithiocarbamates, trithiocarbamates, and xanthates [24]. RAFT process initiators are called iniferters (initiator–transfer agent–terminator) [25]. The RAFT mechanism is widely used for the synthesis of MIP-particles [26–30], MIP-fibers [31] as well as MIP films directly on the sensor surface [32,33]. RAFT approach has been successfully applied for imprinting of small molecules [23,29] as well as macromolecules such as proteins [34].

The aim of the study is to develop a strategy for the preparation of a protein-imprinted polymer film (protein-MIP) directly on the surface of a planar sensor by the combination of the controlled/living radical photopolymerization initiated from the surface and microcontact molecular imprinting. Bovine serum albumin (BSA), 2-(diethylamino)ethyl methacrylate, bis-acrylamide were used as a model protein, a functional monomer and a cross-linker, respectively to prepare the BSA-MIP films. The optimal parameters of C/LRP, such as the method for photoinitiator attachment to the sensor surface, monomer/cross-linker molar ratio and polymerization time, were determined. The prepared BSA-MIP films were studied in terms of their recognition capability and selectivity towards the target protein (BSA) through the analysis of the responses of the BSA-MIP modified SPR sensors upon interaction with BSA and interfering proteins, human serum albumin (HSA) and Fc-fragment of immunoglobulin G (Fc).

2. Experimental

2.1. Chemicals and materials

3,5-dichlorophenyl diazonium tetrafluoroborate (3,5-DClPDT), sodium diethyldithiocarbamate (NaDEDTC), acetonitrile (ACN), (3-glycidyloxypropyl)trimethoxysilane (3-GPS), *N,N′*-methylenebis(acrylamide) (BAA), diethylaminoethyl methacrylate (DEAEM), bovine serum albumin (BSA, 66 kDa), human serum albumin (HSA, 66.5 kDa) and sodium dodecyl sulfate (SDS) were obtained from Sigma-Aldrich. Tetrabutylammonium tetrafluoroborate (Bu_4NBF_4, ⩾99.0%,) was obtained from Fluka. Fc-fragment of immunoglobulin G (Fc, 50 kDa) was obtained from Icosagen AS (Estonia). All chemicals were of analytical grade or higher and were used as received without any further purification. *para*-Maleimidophenyl diazonium tetrafluoroborate (p-MPDT) was synthesized from *N*-(4-aminophenyl)maleimide (TCI Europa) and identified by nuclear magnetic resonance spectroscopy in CD_3-CN (8.55 doublet, 2H; 8.12 doublet, 2H; 7.07 singlet, 2H). Ultrapure water (resistivity 18.2 MΩ·cm, Millipore, USA) was used for the preparation of all aqueous solutions. Phosphate buffered saline (PBS) solution (0.01 M, pH 7.4) was used to prepare analyte solutions.

2.2. Synthesis of BSA-MIP

The BSA-MIPs were synthesized directly on the SPR sensor surface using the following main stages (Fig. 1): (a) covalent immobilization of BSA on the surface of a glass slide via 3-GPS, (b) modification of the gold surface of the sensor by the iniferter, DEDTC, and coating by the mixture of the functional and crosslinking monomers (DEAEM and BAA) (c) bringing the BSA-modified glass slide into contact with the DEDTC-modified SPR sensor and initiation of polymerization by UV-irradiation, (d) detaching the glass slide from the SPR sensor leaving behind BSA imprints on the polymer surface.

2.2.1. Immobilization of BSA on a glass slide

A cover glass slide (22 × 22 mm) was cleaned in a base piranha solution (3:1 volume ratio of 30% NH_4OH and 30% H_2O_2) for 30 min with heating up to 60 °C and rinsed abundantly with ultrapure water. The cleaned glass slide was transferred to ethanol for 10 min and then dried with a nitrogen flow. The glass slide was immersed in 5% 3-GPS chloroform solution for 30 min. After the reaction, the glass slide was rinsed by chloroform to remove any unbound 3-GPS molecules and dried with nitrogen and stored in an oven at 180 °C for 2 h. Finally, the epoxy-silane modified glass slide was incubated in PBS buffer solution containing 0.05 mg/ml BSA for 2 h at room temperature, washed with water and dried under nitrogen flow. Quality of protein immobilization on the glass slide was evaluated by epifluorescent microscopy and contact angle (CA) measurements. The epifluorescent imaging was performed via a 20× plan fluorite objective (Plan Fluor Epi BD, NA0.45, WD4.5 mm) using a Peltier-cooled charge-coupled device camera (DS-5Mc) attached to a research microscope (Eclipse LV100D, Nikon Instruments, Japan) equipped with a fluorescence illumination system (Lumen 200, Prior Scientific Inc., USA). NIS-Elements imaging software was used to analyze the fluorescent images calculating the mean pixel intensity in a region of interest. CA measurements were performed at room temperature using a drop shape analyzer (DSA25, Krüss GmbH, Germany). A drop of water (7 μl) was semi-automatically placed onto the polymer surface using Hamilton syringe and the contact angles indicating the wetting ability of the materials were calculated automatically.

2.2.2. Modification of the gold surface of the sensor by the iniferter

The gold surface of SPR sensor served as a substrate for iniferter (DEDTC) grafting. The sensor surface was treated by an UV ozone cleaner (PSD Pro Series, Novascan Technologies, Inc., USA) for 30 min followed by rinsing with ultrapure water and drying with a nitrogen

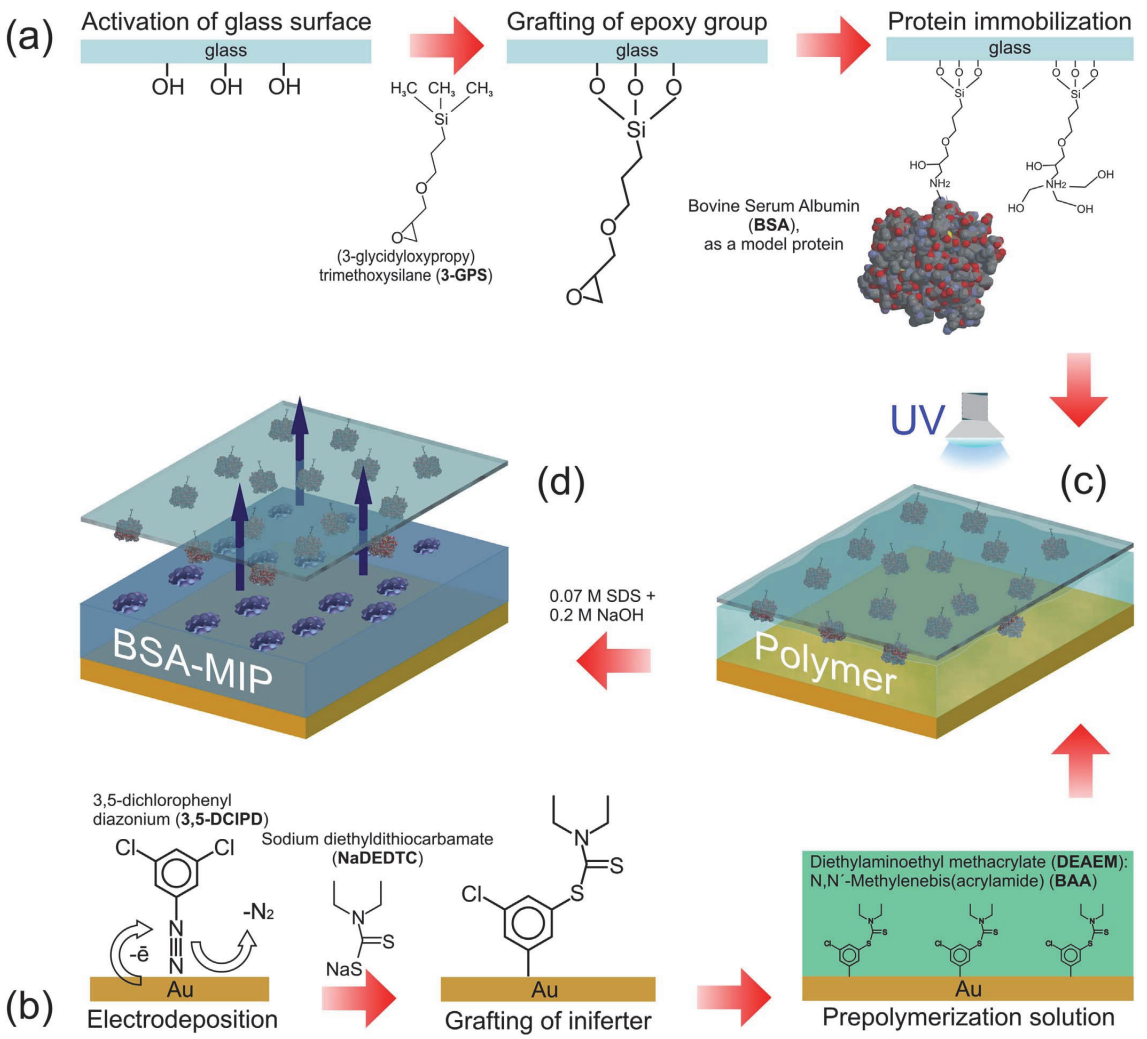

Fig. 1. Fabrication of the protein-MIP by the surface initiated living radical photopolymerization combined with the microcontact imprinting approach: (a) a target protein is covalently immobilized on a glass substrate, (b) a gold substrate with the previously surface-grafted iniferter layer is coated by the monomers solution, (c) the substrates are brought into contact to form a confined space for the protein and the monomers, the polymerization is initiated by UV-irradiation, (d) the glass substrate is removed resulting in molecular imprints of the target protein on the polymer surface.

flow. Then the surface was electrochemically treated in ACN solution containing 1 mM 3,5-DClPDT or p-MPDT and 0.1 M Bu_4NBF_4 by cyclic voltammetry, ramping the potential between −0.6 V and +0.5 V at a rate of 50 mV/s over two cycles. After the electrochemical reduction of the diazonium salts the sensor surface was washed with tetrahydrofuran (THF) to remove the physisorbed loosely bound layer [35] and then with ultrapure water, and finally dried under a nitrogen flow. The charge transfer blocking behavior of the deposited organic layers was investigated by electrochemical impedance spectroscopy (EIS) and cyclic voltammetry (CV). The electrochemical measurements were conducted with an electrochemical workstation (Reference 600, Gamry Instruments, USA) in the conventional three-electrode configuration. The sensor surface served as a working electrode, while a platinum wire and Ag/AgCl/KCl electrode were used as a counter and a reference electrode, respectively. EIS and CV measurements were performed in the 1 M KCl solution containing 4 mM redox probe $K_3[Fe(CN)_6]/K_4[Fe(CN)_6]$. For CV measurements the potential was swept between 0 and 0.5 V at a scan rate of 50 mV/s. For each electrode, three potential scans were applied. EIS measurements were performed in frequency range between 100 kHz and 0.1 Hz with an amplitude of 10 mV. Each electrode measurement was repeated 3 times. The EIS spectra were fitted to an equivalent electrical circuit using Echem Analyst software (Gamry Instruments, USA).

After that, the sensor with grafted 3,5-DClP layer was immersed in an ethanolic solution of NaDEDTC 2 mM overnight at room temperature. In the case of a sensor with grafted p-MP layer, a drop (80 µl) of 2 mM NaDEDTC aqueous solution was put onto the sensor surface and irradiated with UV light for 15 min. Finally, the sensor was thoroughly rinsed with ethanol and ultrapure water, and dried with a nitrogen flow. The DEDTC-modified gold surface was characterized by X-ray photoelectron spectroscopy (XPS) (AXIS Ultra DLD, Kratos Analytical Ltd., England) with monochromatic single anode Al Kα (1486.6 eV) X-

ray source. Vision 2.2.10 software was used for the analysis of spectra. The samples were washed with water, dried with N_2 stream and kept in a vacuum chamber overnight to remove adsorbed components of air from the surface prior to analysis.

2.2.3. Controlled/living radical photopolymerization

BSA-MIP film on the DEDTC-modified SPR sensor surface was prepared by the C/LRP under UV-irradiation. Preliminary, the optimal monomer:cross-linker molar ratio was determined by the contact angle (CA) measurements of the polymer films synthesized at different monomer:cross-linker molar ratio (1:2, 1:6, 1:10). A drop of water (10 µl) was semi-automatically placed onto the polymer surface using Hamilton syringe and the contact angles indicating the wetting ability of the materials were calculated automatically. Then, the solution of monomers was prepared by mixing 5 mM functional monomer (DEAEM) and 30 mM cross-linking monomer (BAA) aqueous solutions and 10 µl of the solution was dropped onto the DEDTC-modified SPR sensor and covered by the cover glass with immobilized protein. Subsequently, the all sandwich-structure was irradiated with UV light (300 W/m^2, 365 nm) at room temperature during 15 h under nitrogen atmosphere. The polymerization process was carried out in a special cell, which allows the synthesis of BSA-MIP and a reference polymer, non-imprinted polymer (NIP), simultaneously on the SPR sensor. After the polymerization process, the polymer embedding BSA was confined between the glass slide and the SPR sensor. To separate the slide from the sensor with the polymer, a solution containing 0.07 M SDS and 0.2 M NaOH and heated up to 80 ^{0}C was used. During the separation stage the removal of BSA from the polymer proceeds simultaneously, since the protein has been covalently attached to the glass slide (stage A), leaving behind BSA-imprints on the polymer surface. The polymer film was characterized by infrared spectroscopic ellipsometry. An aperture of ∅5 mm was used for the measurements. The spectra were recorded with a resolution of 4 cm^{-1} and an angle of incident of 70°. The surface morphology of the NIP and MIP film was characterized by high-resolution scanning electron microscope (HR-SEM Zeiss Merlin) equipped with an In-Lens SE detector for topographic imaging. Measurements were made at operating voltage of 3.00 kV.

The influence of the UV irradiation time on the BSA stability was studied by the dynamic light scattering (DLS)-based particle size analysis and UV–Vis spectroscopy. The DLS measurements were made by a particle analyzer (ZetaSizer NanoS, Malvern Instruments Ltd., England). The instrument uses a light source having the wavelength of 633 nm and measures the scattered light at a fixed angle of 175°. Aqueous solution of BSA (1 mg/ml, 70 µl) was placed into a plastic microcuvette (p/n 759200, BrandTech Scientific, INC., USA). UV–Vis absorption spectra of the aqueous solution containing 1 mg/ml BSA were recorded in 1 cm quartz cuvettes with the UV-2401PC spectrophotometer (Shimadzu Corporation, Japan) in the wavelength range from 270 to 310 nm.

2.3. Rebinding, reusability and selectivity study of BSA-MIP

The synthesized BSA-MIPs were characterized in terms of their affinity and selectivity to rebind BSA by monitoring the molecular binding events with the SPR system (SR7500DC, Reichert Technologies Inc., Depew, NY, USA). The BSA-MIP- and NIP-modified SPR sensor was loaded into the system and equilibrated with a degassed PBS buffer solution (pH 7.4) at a flow rate of 25 µl/min until a constant baseline was reached. The solutions with increasing concentration of the analyte (from 2.5 to 1350 nM of BSA in PBS buffer) were subsequently injected into the flow stream by an autosampler and the changes in the refractive index upon binding of the analyte on the sensor surface were recorded. The association phase lasted 12 min and was interrupted by washing the sensor surface with PBS solution for 20 min (the dissociation phase), after that the regeneration of BSA-MIP and NIP films were conducted using 0.2 M NaOH for 12 min. The binding profiles observed in the association phase on the BSA-MIP surfaces were corrected by subtracting the respective binding profiles on the NIP surfaces. Kinetic analysis of the corrected binding profiles was performed by fitting the data to the pseudo-first order kinetic model to determine equilibrium signals (Q_{eq}) at a particular analyte concentration. The binding isotherms were generated using Q_{eq} values. The values of the dissociation constant (K_D) and the maximum binding response at saturation (Q_{max}) were derived from fitting the binding isotherm to Langmuir (L) and Langmuir-Freundlich (LF) adsorption models. Additionally, the K_D value was estimated from the analysis of the plot of k_{obs} vs applied analyte concentration (see the Supplementary Information), where k_{obs} is the observed association rate constant derived from the kinetic analysis of the binding profiles in the association phase. The study of the reusability of the BSA-MIPs were performed by repeated injection of 450 nM BSA solution after each regeneration. The selectivity of the BSA imprinted film towards the template molecules was studied by injecting 450 nM solutions of other proteins, HSA and Fc fragment of IgG (Fc).

3. Results and discussion

When synthesizing a MIP for sensing of macromolecules such as proteins, it is essential that the synthesis strategy (i) prevents the entrapment of protein in the polymer matrix during polymerization process, (ii) forms a polymer with imprinted sites located at or close to the surface, enabling easy access to the target protein molecules and (iii) leads to robust interfacing of the MIP with the surface of a sensor i.e. efficient transduction of the binding event of this macromolecular analyte by the MIP into useful analytical signals. To address the above mentioned requirements we combined the microcontact molecular imprinting approach, which avoids overgrowing the polymer around a macromolecular template, and the surface initiated C/LR photopolymerization, which attaches covalently this polymer to a sensor surface (see Fig. 1).

3.1. Immobilization of BSA on a glass surface

Before BSA immobilization the glass surface was modified by 3-GPS in order to introduce the epoxy groups on the surface allowing the covalent attachment of protein through the formation of amide and ether bonds with the amino and hydroxyl groups of the protein, respectively [36]. The success of glass modification by 3-GPS was confirmed by the contact angle measurements demonstrating increase of CA value from 7.4° (glass surface with OH– groups) to 51.5° (glass surface with epoxy groups) (Fig. S1). The immobilization of BSA onto the epoxy-silane modified glass slide was demonstrated using the epi-fluorescence optical microscopy and a fluorescent derivative of the BSA, fluorescein isothiocyanate-BSA (FITC-BSA) to visualize adsorption of the protein onto the surface of the glass. Fluorescence images of the 3-GPS modified glass slide before and after its incubation in the FITC-BSA solution are presented in Fig. 2. As can be seen, the interaction of the

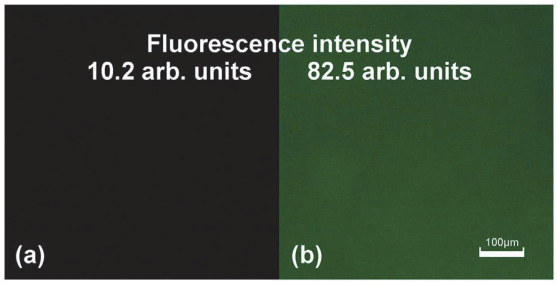

Fig. 2. Fluorescence microscopy images of the 3-GPS modified glass before (a) and after (b) incubation in the FITC-BSA solution.

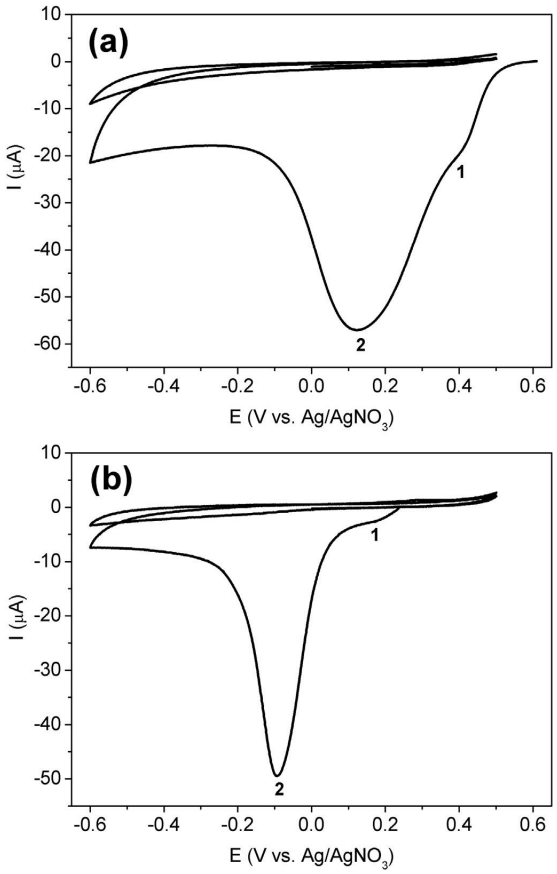

Fig. 3. Cyclic voltammograms recorded on the bare gold electrodes in ACN solution containing 0.1 M Bu_4NBF_4 and (a) 1 mM 3,5-DClPDT or (b) 1 mM p-MPDT, scan rate 50 mV/s.

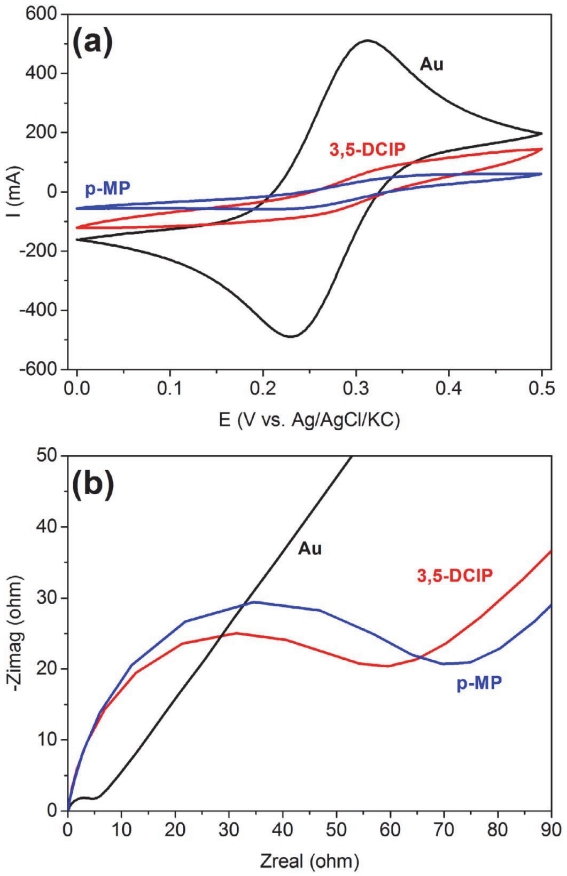

Fig. 4. (a) Cyclic voltammogram at scan rate 50 mV/s and (b) Nyquist plot for the bare gold (Au) and 3,5-DClP and p-MP-modified gold electrodes recorded in the aqueous solution containing 4 mM $K_3[Fe(CN)_6]/K_4[Fe(CN)_6]$ and 1 M KCl.

FITC-BSA with the glass surface caused substantial and uniform increase (10.2 vs 82.5 arb. units) in green fluorescence intensity across the glass surface indicating thus the formation of a homogeneous layer of the protein on the surface.

3.2. Modification of a gold sensor surface by the iniferter

Among a great number of surface modification techniques, electrochemical reduction of organic diazonium salt is a well-known technique to graft organic molecules onto metal surfaces that has considerable promise due to the high stability of the covalently attached layers and the versatility of the chemistry [37,38]. Different functional groups can be introduced to the surface depending on the substituent on the phenyl group of aryldiazonium salt [39]. In this study two different substituted phenyl groups: 3,5-dichlorophenyl (3,5-DClP) and *p*-maleimidophenyl (p-MP) were preliminary grafted to the SPR-sensor surface by electrochemical reduction of the corresponding diazonium salts, in order to find an optimal functionalization for subsequent covalent attachment of the iniferter (DEDTC). During the first cycle of electrodeposition of 3,5-DClP, there are two distinct reduction peaks around 0.4 V and 0.12 V (Fig. 3a). The different crystallographic orientations present on the polycrystalline gold substrates influence the electrodeposition of diazonium salts [40]. Thus, the reduction peaks observed in Fig. 3a very likely correspond to deposition of 3,5-DClP on Au111 and Au100 facets, respectively [40,41]. The second cycle shows only charging current without 3,5-DClPDT reduction, indicating the formation of a blocking layer, which prevents further transfer of electrons from the electrode surface to the diazonium species in the solution [42]. The similar behavior can be seen during the electrochemical grafting of p-MP, but the respective reduction current peaks of p-MPDT on Au111 and Au100 facets appear at 0.19 V and −0.1 V (Fig. 3b).

The charge transfer blocking behavior of the 3,5-DClP and p-MP layers were investigated by EIS and CV studying barrier properties of the layers to transfer electrons from/to electroactive redox species as $[Fe(CN)_6]^{3-/4-}$. Fig. 4a compares the electrochemical responses of the bare gold and 3,5-DClP- or p-MP-modified electrodes. While the well-defined current peaks of the $[Fe(CN)_6]^{3-/4-}$ redox system can be clearly seen on the bare Au electrode, they are significantly suppressed after the electrochemical grafting of the substituted phenyl groups confirming the insulating nature of the depositing organic monolayers. The charge transfer resistance estimated from the width of the semicircle in the Nyquist plot increased from 2 Ω cm^{-2} for the bare gold electrode to 25 Ω cm^{-2} and 35 Ω cm^{-2}, for 3,5-DClP- and p-MP-modified electrodes, respectively (Fig. 4b). The increase in the charge transfer resistance is the direct consequence of the partial passivation of the gold electrode that blocks the ability of the redox probe to access the surface of the working electrode.

The XPS data additionally confirmed the successful

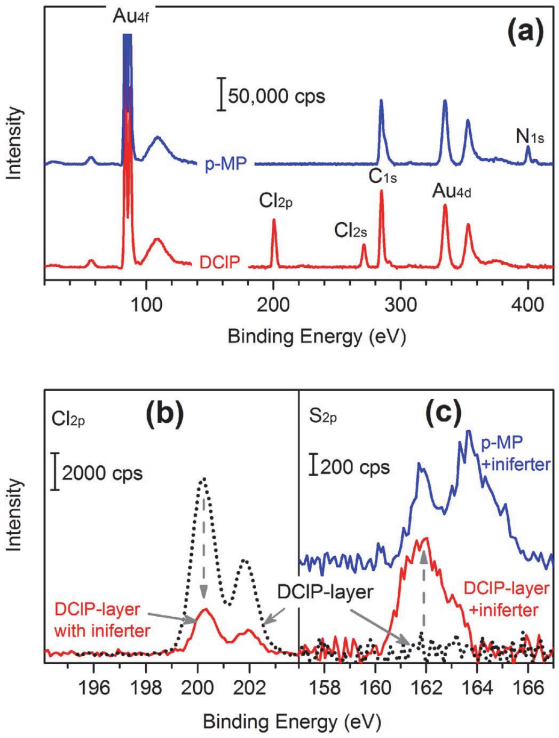

Fig. 5. (a) XP survey spectra of 3,5-DClP- and p-MP-modified gold surfaces, XP core level spectra in the Cl2p (b) and S2p (c) binding energy regime for the 3,5-DClP layer (dotted lines) and 3,5-DClP with iniferter attached (red solid lines) and the p-MP layer with grafted iniferter (blue solid line in c).

functionalization of the gold electrode by either 3,5-DClP or p-MP layer by the presence of Cl2p and Cl2s, and the N1 s related signals in the overview spectra (Fig. 5a) located at about 200, 271, and 400.5 eV, respectively. Attachment of the iniferter to the 3,5-DClP- and p-MP-modified surfaces by electrophilic substitution was assessed by analyzing the respective Cl2p and the S2p core level regions. The Cl2p signal of the 3,5 DClP surface is strongly reduced (Fig. 5b) due to the exchange of the Cl by the S-C from the iniferter as shown in the sketch of Fig. 1b. Additionally, for both functional molecules the signal due to S2p core level develops after the treatment with the iniferter (Fig. 5c). These observations lead to the assumption that the iniferter is grafted onto both functionalized surfaces. However, the 3,5-DClP functionalized surface shows a more homogeneous and more intense signal in the S2p core level range at 162 eV which is most probably due to binding of S to C (Fig. 5c). Grafting the iniferter onto the p-MP layer (blue solid line in Fig. 5c) shows obviously two different S-related bonds, one formed to the C of the maleimide group at about 162 eV and a second signal at around 163.7 eV. This core level signal seems to be most likely due to disulfide bridge formation of two iniferter molecules obviously induced by the UV-light treatment what was not the case for the 3,5-DClP surface functionalization. Consequently, we used the surface modification with 3,5-DClP for the grafting of the iniferter to the surface of the SPR-sensor to ensure a well-defined surface finishing for the subsequent BSA-MIP film formation.

3.3. Fabrication of BSA-MIP film

The effect of intensity and time of UV irradiation on the structure of BSA was studied in order to optimize the time of the photopolymerization and to minimize a possible damage of the protein during the UV irradiation. With increased time of exposure to UV irradiation of 500 W/m^2 starting from 2 h and more, a shift of the absorption bands (289.7, 288 and 281 nm) and the appearance of new peaks in the spectra of the BSA solution can be clearly observed (Fig. 6a). These changes in UV–Vis spectra can be explained by alteration in the environment around the aromatic amino acid chromophore happening in a course of conformational changes of the protein (e.g. partial unfolding). The DLS analysis of the protein molecular size supported that after 3 h of UV exposure (500 W/m^2), significant changes in the structure of the protein occurred since the amount of the BSA molecules in their native monodisperse form (hydrodynamic diameter 7.4 nm) is substantially reduced (Fig. 6b). Although, power of UV-irradiation of 500 W/m^2 caused the significant conformational changes of BSA appeared already after 2 h of exposure, UV treatment with weaker intensity (300 W/m^2) did not produce such detrimental changes in BSA during up to 15 h (Fig. 6c, d). Therefore, UV irradiation with the intensity of 300 W/m^2 for 15 h was further applied to perform the photopolymerization.

The specific interaction between a MIP matrix and a target protein is based on the non-covalent interactions such as van der Waals, ionic and hydrogen bonding occurring in the recognition cavities of the MIP. At the same time due to the presence of a huge amount of functional groups in the protein molecule there is a high probability of increasing of nonspecific interactions between protein and MIP matrix that may lead to poor selectivity and cross-reactivity. Therefore, it is extremely important to minimize the non-specific interactions between a MIP matrix and a protein that can be achieved, for example, by a proper adjustment of the hydrophilicity of the polymer matrix by optimizing the ratio of monomers and/or monomer/cross-linker with hydrophilic and hydrophobic groups. Moreover, the monomer/cross-linker ratio can influence the textural properties of the polymer. Thus, the insufficient numbers of cross-links leads to the formation of a polymer matrix with a low specific area and, as a consequence to a low capacity of MIP, while the excessive numbers of cross-links leads to the formation of very narrow pores and decrease in the number of functional groups resulting in the hindered interaction of the protein with MIP [43]. Due to the high content of hydrophobic ethyl groups the DEAEM monomer can lead to the formation of a hydrophobic surface promoting the nonspecific adsorption of protein, which adversely affect the selectivity of MIP film. In this regard, it is necessary to reduce the influence of hydrophobic non-specific interaction by optimizing the ratio of the hydrophobic monomer, DEAEM, and the hydrophilic cross-linker, BAA. Therefore, the polymer films were synthesized at different DEAEM/BAA ratios and the contact angles (CA) of the films were measured in order to determine an optimal value of the ratio to produce a polymer of sufficient hydrophilicity. As can be seen in Fig. S2, the CA value of the polymer film decreases with decreasing monomer/cross-linker ratio, i.e. with increasing the fraction of the more hydrophilic BAA crosslinker. This leads to a highly hydrophilic surface formation at the ratio of 1:10 (CA = 12.6°). However, the highly hydrophilic surface can cause the strong repulsion of the hydrophobic parts of the protein. This behavior would prevent partly the interaction of the protein with the MIP film surface. Therefore, the monomer/cross-linker ratio of 1:6 was selected in this study for preparation of BSA-MIP.

The IRSE spectrum of the polymer film (see Fig. S3) showed characteristic vibrational modes of amide and carboxyl groups with each monomer containing only one of these groups (see Fig. S4). The specific absorption band amide I for the amide group of BAA are clearly visible at about 1675 cm^{-1} [44] whereas the characteristic carboxyl stretching of DEAEM is displayed at about 1730 cm^{-1} [45]. This observation points to the polymer formation by BAA and DEAEM.

3.4. BSA rebinding study

The BSA-MIP and the respective NIP were synthesized directly on

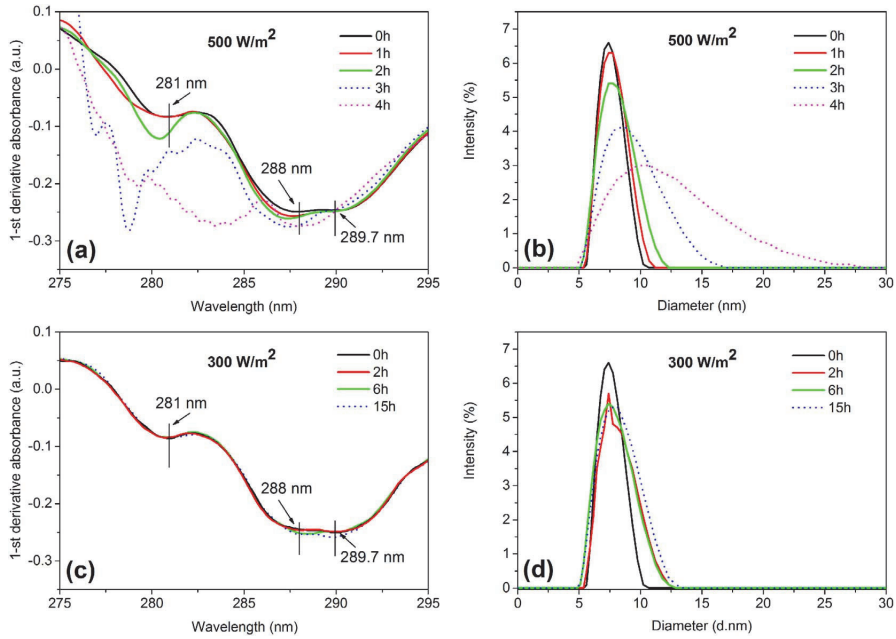

Fig. 6. Effect of UV irradiation time on stability of BSA in the PBS solution. The first derivative of the UV–Vis absorption spectra of the BSA solution (a, c) and the size-intensity ratio (DLS) of the BSA molecules (b, d).

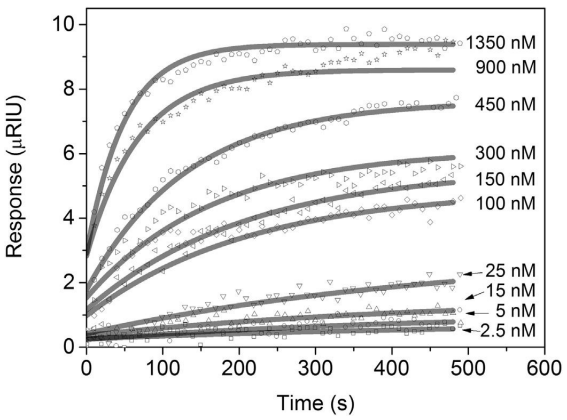

Fig. 7. Typical sensorgrams of the BSA-MIP modified SPR sensor upon injections of the different concentration of BSA in PBS buffer. The responses were corrected by subtraction of the respective NIP signal.

the same SPR sensor providing thus a possibility to correct properly the non-specific binding component of measured response on the BSA-MIP modified surface. After the correction of the responses of the BSA-MIP-modified SPR sensor (see Section 2.3), there were well pronounced analyte concentration-dependent binding profiles obtained (Fig. 7). These profiles actually reflect preferential binding of BSA to BSA-MIP rather that to NIP, since the morphology of the BSA-MIP and NIP films were almost identical, as demonstrated by SEM micrographs (Fig. S5). It should be noted that bulk shift effects were not completely compensated after the applied correction. These effects, very likely caused by mismatch of the refractive indices of the running buffer and the sample solutions, were still higher on the BSA-MIP than NIP-modified sensor areas. In order to further correct the contribution of the bulk shifts into the response signals we introduced the shared *BS* constant in the pseudo-first order kinetics model used to analyze the corrected binding profiles observed in the association phase on the BSA-MIP surface (Eq. (1)) [46]. Thus, by fitting the binding profiles to the kinetics model given in Eq. (1), it was possible to predict the equilibrium responses (Q_{eq}) at every injected concentration of BSA:

$$Q = Q_{eq}(1 - e^{-kobs \cdot t}) + BS \quad (1)$$

where Q is the response upon BSA rebinding at time t, Q_{eq} is its value at equilibrium, k_{obs} is the observed association rate constant, BS is a bulk shift. The kinetics parameters obtained by the fitting of the responses at all applied concentration are listed in the Table S1. As can be seen the pseudo-first order kinetics model gave goodness-of-fit to the experimental data with the coefficient of determination (R^2) in the range of 0.648–0.964. Subsequently, the Q_{eq} values derived from Eq. (1) were used to plot the binding isotherm. Analytical isotherm models such as Langmuir (Eq. (2)) and Langmuir-Freundlich (Eq. (3)) are widely used for modeling binding events on MIPs [47]. In the present study, we as well, applied the same models in order to estimate the equilibrium dissociation constant (K_D) of the prepared BSA-MIP:

$$Q = Q_{max}C/(K_D + C) \quad (2)$$

$$Q = Q_{max}C^m/(K_D + C^m) \quad (3)$$

where Q and Q_{max} are the responses upon BSA rebinding at concentration C and its saturation value, respectively. K_D is the equilibrium dissociation constant, m is the heterogeneity index, which value ranges from 0 to 1 and increases as heterogeneity decreases. The results of fitting are presented in Fig. 8 and the calculated values of Q_{max}, K_D, m, and R^2 are summarized in Table 1. As can be seen both Langmuir and Langmuir-Freundlich models yielded quite similar Q_{max} and K_D values for BSA-MIP, however, according to R^2, it seems that the Langmuir-Freundlich model had offered somewhat better agreement with the binding isotherm data than the Langmuir model (0.998 versus 0.992, respectively). Many studies have already shown that most MIPs had

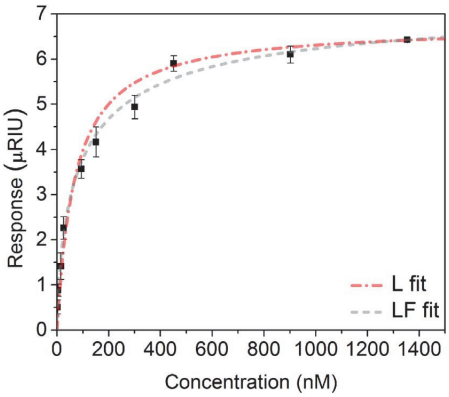

Fig. 8. The binding isotherms of BSA to the BSA-MIP-modified SPR sensor. The responses were corrected by subtraction of the respective NIP signal and fitted to the Langmuir (L) and Langmuir-Freundlich (LF) isotherm models.

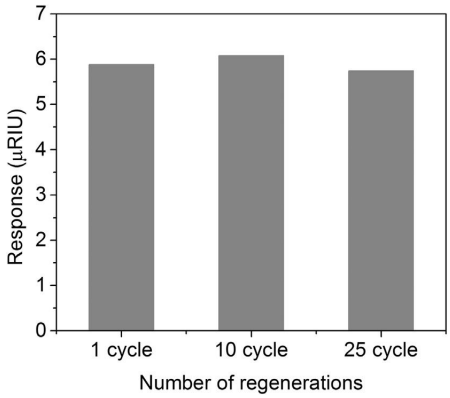

Fig. 9. Potential reusability of the BSA-MIP: equilibrium responses, *Qeq*, of the BSA-MIP and NIP-modified SPR sensors upon injection of 450 nM BSA solution in PBS after 1, 10 and 25 regeneration cycles.

Table 1
The binding parameters of the BSA-MIP obtained by fitting of the binding isotherms to Langmuir (L) and Langmuir–Freundlich (LF) model. k_{obs} analysis is presented in Fig. S6.

	LF	L	k_{obs} analysis
K_D (nM)	24.14 ± 4.12	68.12 ± 11.54	67.12 ± 4.3
Qmax (μRIU)	7.4 ± 0.24	6.7 ± 0.07	
m	0.7 ± 0.05	1	
R^2	0.998	0.992	0.988

often heterogeneous binding sites and thus, Langmuir-Freundlich model was more universally applicable in characterizing MIPs because it took into account heterogeneity information and was able to model binding behavior over the wider concentration range up to saturation [48–50]. Indeed, in the given imprinting strategy, orientation of the template molecules (BSA) before the polymerization was not controlled as BSA was immobilized on the glass slide via covalent interaction between the amino and/or hydroxyl groups of the protein and the epoxy groups of the 3-GPS. These amino and/or hydroxyl groups are distributed over the entire surface of BSA, and have the same reactivity [51]. As a result, BSA may be immobilized with multiple orientations on the glass slide leading to formation of the imprinted sites with different binding energy in course of the subsequent microcontact imprinting process. It should be noted that the difference in the fits obtained by Langmuir and Langmuir-Freundlich models was marginal and obviously the given BSA-MIP could be well characterized by the simpler Langmuir model. Additionally, K_D values derived from the latter is very same to that determined by the k_{obs} plot analysis (Fig. S6) 68 nM and 67 nM, respectively (Table 1).

Under the optimal conditions, the BSA-MIP sensor shows a pseudo-linear response to BSA in the concentration range from 2.5 to 25 nM, with limit of detection (LOD) and limit of quantitation (LOQ) of 5.6 nM and 18.7 nM determined, respectively, as 3 and 10 times of the standard deviation (SD) divided by the slope of the regression line (Fig. S7) [52].

We expect that the similar analytical performance of the MIPs applying the same strategy could be achieved in detection of the other albumin family proteins e.g. HSA and subsequently these materials would be potentially suitable to employ in sensing systems for clinical detection of elevated HSA level e.g. in urine where albumin concentration higher than 380 nM (25 mg/L) can be an early indicator of kidney damage [53].

3.5. Reusability and selectivity studies

Since, the possibility to regenerate and repeatedly use a protein-MIP based sensor would be a significant advantage over a conventional antibody based biosensor, we examined the ability of the prepared BSA-MIP to withstand the regeneration procedure. The treatments in solutions efficiently disrupting possible multiple hydrogen and electrostatic bonds between the protein and the MIP surface were assessed to refresh the surface of the BSA-MIP. It was found that the BSA-MIP modified sensor could be perfectly regenerated in NaOH showing nearly reversible responses (2.4% decrease in the response) even after the 25th regeneration cycle (Fig. 9, Fig. S8). The BSA-MIP was further characterized in terms of its capability to rebind selectively the target protein, BSA, with respect to its analogue, i.e. human serum albumin (HSA, pI 5.67) as well as a protein with slightly different size and pI, such as Fc fragment of IgG (pI 7.12). A quick assessment of the selectivity of the BSA-MIP-sensor was conducted under non-competitive conditions by comparison of the equilibrium responses arising upon interaction with an interfering protein and the target protein. As can be seen in Fig. 10, the obtained responses show that the target molecule gives about 2 times higher binding signal than those appeared upon injection of the HSA and Fc. It is worth noting that the very same, but the non-imprinted reference film (NIP) demonstrates only marginal differences in binding between BSA and interfering proteins - HSA and Fc.

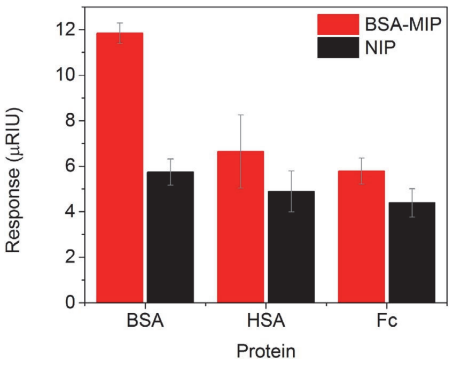

Fig. 10. The selectivity test of the BSA-MIP towards BSA, Fc and HSA conducted under non-competitive conditions through injection of 450 nM solutions of the respective proteins in PBS onto the BSA-MIP and NIP-modified SPR sensors. The equilibrium responses, *Qeq*, of the BSA-MIP and NIP-modified SPR sensors were compared.

4. Conclusions

In this study, we have described a new synthesis strategy to prepare protein-MIP films by combined use of the microcontact imprinting and the surface-initiated C/LR photopolymerization. The strategy took advantage of the microcontact imprinting by providing a protein molecule to be confined into the polymer matrix avoiding, at same time, its complete entrapment. Furthermore, the surface initiated C/LR photopolymerization allowing the formation of a covalently attached polymer film with controlled thickness directly on a sensor surface providing thus the perfect interfacing between the recognition element and a sensor transducer such as a SPR sensor. Using this synthesis strategy, the polymethacrylate-based thin film having molecular imprints of BSA (BSA-MIP) was successfully interfaced directly with the SPR sensor. The film adsorbed BSA with K_D values in the nanomolar range (68 nM) and with about two times higher adsorption capacity as compared to HSA and Fc, even though their molecular size and shape were similar to BSA. The BSA-MIP modified SPR sensor had pseudo-linear range between 2.5 nM and 25 nM and LOD of 5.6 nM. The BSA-MIP film could be perfectly regenerated in the alkaline solution showing nearly reversible responses with a loss of only 2.4% even after the 25th regeneration cycle. Although further research is required in this field, we think that the presented simple synthesis strategy offers a prospective solution for the development of MIP-based sensing systems for detection of clinically relevant proteins associated with a number of diseases, for example, kidney diseases and cancer.

Acknowledgements

This work was supported by the Estonian Research Council grant (PUT150). The authors thank Dr. Mati Danilson for the XPS measurements, Dr. Olga Volobueva for SEM imaging, and Dr. Karsten Hinrichs for the IRSE measurement.

Supplementary data

Supplementary data to this article can be found online at https://doi.org/10.1016/j.reactfunctpolym.2018.02.004.

References

[1] M.J. Whitcombe, N. Kirsch, I.A. Nicholls, Molecular imprinting science and technology: a survey of the literature for the years 2004–2011, J. Mol. Recognit. 27 (6) (2014) 297–401.
[2] K. Haupt, K. Mosbach, Molecularly imprinted polymers and their use in biomimetic sensors, Chem. Rev. 100 (2000) 2495–2504.
[3] M.R. Younis, S.Z. Bajwa, P.A. Lieberzeit, W.S. Khan, A. Mujahid, A. Ihsan, A. Rehman, Molecularly imprinted porous beads for the selective removal of copper ions, J. Sep. Sci. 39 (4) (2016) 793–798.
[4] G. Cirillo, O.I. Parisi, M. Curcio, F. Puoci, F. Iemma, U.G. Spizzirri, N. Picci, Molecularly imprinted polymers as drug delivery systems for the sustained release of glycyrrhizic acid, J. Pharm. Pharmacol. 62 (5) (2010) 577–582.
[5] M. Cieplak, W. Kutner, Artificial biosensors: how can molecular imprinting mimic biorecognition? Trends Biotechnol. 34 (2016) 922–941.
[6] H. Shi, W.B. Tsai, M.D. Garrison, S. Ferrari, B.D. Ratner, Template-imprinted nanostructured surfaces for protein recognition, Nature 398 (6728) (1999) 593–597.
[7] D.R. Kryscio, N.A. Peppas, Critical review and perspective of macromolecularly imprinted polymers, Acta Biomater. 8 (2) (2012) 461–473.
[8] A. Menaker, V. Syritski, J. Reut, A. Öpik, V. Horvath, R.E. Gyurcsanyi, Electrosynthesized surface-imprinted conducting polymer microrods for selective protein recognition, Adv. Mater. 21 (22) (2009) 2271–2275.
[9] A. Tretjakov, V. Syritski, J. Reut, R. Boroznjak, O. Volobujeva, A. Öpik, Surface molecularly imprinted polydopamine films for recognition of immunoglobulin G, Microchim. Acta 180 (15–16) (2013) 1433–1442.
[10] P.C. Chou, J. Rick, T.C. Chou, C-reactive protein thin-film molecularly imprinted polymers formed using a micro-contact approach, Anal. Chim. Acta 542 (1) (2005) 20–25.
[11] G. Erturk, M. Hedstrom, B. Mattiasson, A sensitive and real-time assay of trypsin by using molecular imprinting-based capacitive biosensor, Biosens. Bioelectron. 86 (2016) 557–565.
[12] B. Osman, L. Uzun, N. Besirli, A. Denizli, Microcontact imprinted surface plasmon resonance sensor for myoglobin detection, Mat Sci Eng C-Mater 33 (7) (2013) 3609–3614.
[13] G.K. Jennings, E.L. Brantley, Physicochemical properties of surface-initiated polymer films in the modification and processing of materials, Adv. Mater. 16 (22) (2004) 1983–1994.
[14] B. de Boer, H.K. Simon, M.P.L. Werts, E.W. van der Vegte, G. Hadziioannou, "Living" free radical photopolymerization initiated from surface-grafted iniferter monolayers, Macromolecules 33 (2) (2000) 349–356.
[15] R. Ahmad, A. Mocaer, S. Gam-Derouich, A. Lamouri, H. Lecoq, P. Decorse, P. Brunet, C. Mangeney, Grafting of polymeric platforms on gold by combining the diazonium salt chemistry and the photoiniferter method, Polymer 57 (2015) 12–20.
[16] A. Olivier, F. Meyer, J.M. Raquez, P. Damman, P. Dubois, Surface-initiated controlled polymerization as a convenient method for designing functional polymer brushes: from self-assembled monolayers to patterned surfaces, Prog. Polym. Sci. 37 (1) (2012) 157–181.
[17] N. Tsubokawa, M. Satoh, Surface grafting of polymers onto glass plate: polymerization of vinyl monomers initiated by initiating groups introduced onto the surface, J. Appl. Polym. Sci. 65 (11) (1997) 2165–2172.
[18] R. Advincula, Polymer brushes by anionic and cationic surface-initiated polymerization (SIP), Adv. Polym. Sci. 197 (2006) 107–136.
[19] T. Farhan, W.T.S. Huck, Synthesis of patterned polymer brushes from flexible polymeric films, Eur. Polym. J. 40 (8) (2004) 1599–1604.
[20] C. Slugovc, The ring opening metathesis polymerisation toolbox, Macromol. Rapid Commun. 25 (14) (2004) 1283–1297.
[21] A. Zengin, G. Karakose, T. Caykara, Poly(2-(dimethylamino)ethyl methacrylate) brushes fabricated by surface-mediated RAFT polymerization and their response to pH, Eur. Polym. J. 49 (10) (2013) 3350–3358.
[22] A. Khlifi, S. Gam-Derouich, M. Jouini, R. Kalfat, M.M. Chehimi, Melamine-imprinted polymer grafts through surface photopolymerization initiated by aryl layers from diazonium salts, Food Control 31 (2) (2013) 379–386.
[23] V.D. Salian, C.J. White, M.E. Byrne, Molecularly imprinted polymers via living radical polymerization: relating increased structural homogeneity to improved template binding parameters, React. Funct. Polym. 78 (2014) 38–46.
[24] K. Matyjaszewski, D. T.P., Handbook of Radical Polymerization, John Wile & Sons Inc, 2002, p. 936.
[25] T. Otsu, M. Yoshida, Role of initiator-transfer agent-terminator (Iniferter) in radical polymerizations - polymer design by organic disulfides as Iniferters, Makromol Chem-Rapid 3 (2) (1982) 127–132.
[26] W. Wan, M. Biyikal, R. Wagner, B. Sellergren, K. Rurack, Fluorescent sensory microparticles that "light-up" consisting of a silica Core and a molecularly imprinted polymer (MIP) Shell, Angew. Chem. Int. Ed. 52 (27) (2013) 7023–7027.
[27] Y. Ma, G.Q. Pan, Y. Zhang, X.Z. Guo, H.Q. Zhang, Narrowly dispersed hydrophilic molecularly imprinted polymer nanoparticles for efficient molecular recognition in real aqueous samples Including River water, milk, and bovine serum, Angew. Chem. Int. Ed. 52 (5) (2013) 1511–1514.
[28] G.Q. Pan, Y. Zhang, Y. Ma, C.X. Li, H.Q. Zhang, Efficient one-pot synthesis of water-compatible molecularly imprinted polymer microspheres by facile RAFT precipitation polymerization, Angew. Chem. Int. Ed. 50 (49) (2011) 11731–11734.
[29] C. Gonzato, M. Courty, P. Pasetto, K. Haupt, Magnetic molecularly imprinted polymer nanocomposites via surface-initiated RAFT polymerization, Adv. Funct. Mater. 21 (20) (2011) 3947–3953.
[30] M.R. Halhalli, E. Schillinger, C.S.A. Aureliano, B. Sellergren, Thin walled imprinted polymer beads featuring both uniform and accessible binding sites, Chem. Mater. 24 (15) (2012) 2909–2919.
[31] X.G. Hu, Y.N. Fan, Y. Zhang, G.M. Dai, Q.L. Cai, Y.J. Cao, C.J. Guo, Molecularly imprinted polymer coated solid-phase microextraction fiber prepared by surface reversible addition-fragmentation chain transfer polymerization for monitoring of Sudan dyes in chilli tomato sauce and chilli pepper samples, Anal. Chim. Acta 731 (2012) 40–48.
[32] S.D. Azevedo, D. Lakshmi, I. Chianella, M.J. Whitcombe, K. Karim, P.K. Ivanova-Mitseva, S. Subrahmanyam, S.A. Piletsky, Molecularly imprinted polymer-hybrid electrochemical sensor for the detection of beta-estradiol, Ind. Eng. Chem. Res. 52 (39) (2013) 13917–13923.
[33] Y. Li, X. Li, C.K. Dong, Y.Q. Li, P.F. Jin, J.Y. Qi, Selective recognition and removal of chlorophenols from aqueous solution using molecularly imprinted polymer prepared by reversible addition-fragmentation chain transfer polymerization, Biosens. Bioelectron. 25 (2) (2009) 306–312.
[34] R.R. Chen, L. Qin, M. Jia, X.W. He, W.Y. Li, Novel surface-modified molecularly imprinted membrane prepared with iniferter for permselective separation of lysozyme, J. Membr. Sci. 363 (1–2) (2010) 212–220.
[35] A. Roy, J. Gao, J.A. Bilbrey, N.E. Huddleston, J. Locklin, Rapid electrochemical reduction of Ni(II) generates reactive monolayers for conjugated polymer brushes in one step, Langmuir 30 (34) (2014) 10465–10470.
[36] M. Schaeferling, S. Schiller, H. Paul, M. Kruschina, P. Pavlickova, M. Meerkamp, C. Giammasi, D. Kambhampati, Application of self-assembly techniques in the design of biocompatible protein microarray surfaces, Electrophoresis 23 (18) (2002) 3097–3105.
[37] X. Zhang, A. Tretjakov, M. Hovestaedt, G.G. Sun, V. Syritski, J. Reut, R. Volkmer, K. Hinrichs, J. Rappich, Electrochemical functionalization of gold and silicon surfaces by a maleimide group as a biosensor for immunological application, Acta Biomater. 9 (3) (2013) 5838–5844.
[38] X. Zhang, G.G. Sun, M. Hovestadt, V. Syritski, N. Esser, R. Volkmer, S. Janietz, J. Rappich, K. Hinrichs, A new strategy for the preparation of maleimide-functionalised gold surfaces, Electrochem. Commun. 12 (10) (2010) 1403–1406.
[39] X. Zhang, F. Rosicke, V. Syritski, G.G. Sun, J. Reut, K. Hinrichs, S. Janietz, J. Rappich, Influence of the para-substitutent of benzene diazonium salts and the solvent on the film growth during electrochemical reduction, Z. Phys. Chem. 228 (4–5) (2014) 557–573.

[40] A. Benedetto, M. Balog, P. Viel, F. Le Derf, M. Sallé, S. Palacin, Electro-reduction of diazonium salts on gold: why do we observe multi-peaks? Electrochim. Acta 53 (24) (2008) 7117–7122.
[41] S. Trasatti, Systematic trends in the crystal face specificity of interfacial parameters: the cases of ag and au, J. Electroanal. Chem. 329 (1–2) (1992) 237–246.
[42] J. Wang, M.A. Firestone, O. Auciello, J.A. Carlisle, Surface functionalization of Ultrananocrystalline diamond films by electrochemical reduction of Aryldiazonium salts, Langmuir 20 (26) (2004) 11450–11456.
[43] S. Barral, A. Guerreiro, M.A. Villa-Garcia, M. Rendueles, M. Diaz, S. Piletsky, Synthesis of 2-(diethylamino)ethyl methacrylate-based polymers, Effect of cross-linking degree, porogen and solvent on the textural properties and protein adsorption performance, React. Funct. Polym. 70 (11) (2010) 890–899.
[44] S.A. Agnihotri, T.M. Aminabhavi, Novel interpenetrating network chitosan-poly (ethylene oxide-g-acrylamide) hydrogel microspheres for the controlled release of capecitabine, Int. J. Pharm. 324 (2) (2006) 103–115.
[45] T. Kuila, S. Bose, P. Khanra, N.H. Kim, K.Y. Rhee, J.H. Lee, Characterization and properties of in situ emulsion polymerized poly(methyl methacrylate)/graphene nanocomposites, Compos Part a-Appl S 42 (11) (2011) 1856–1861.
[46] R.L. Rich, D.G. Myszka, Grading the commercial optical biosensor literature-class of 2008: the mighty binders, J. Mol. Recognit. 23 (1) (2010) 1–64.
[47] J.A. Garcia-Calzon, M.E. Diaz-Garcia, Characterization of binding sites in molecularly imprinted polymers, Sensor Actuat B-Chem 123 (2) (2007) 1180–1194.
[48] R.J. Umpleby 2nd, S.C. Baxter, A.M. Rampey, G.T. Rushton, Y. Chen, K.D. Shimizu, Characterization of the heterogeneous binding site affinity distributions in molecularly imprinted polymers, J. Chromatogr. B Anal. Technol. Biomed. Life Sci. 804 (1) (2004) 141–149.
[49] R.J. Umpleby 2nd, S.C. Baxter, Y. Chen, R.N. Shah, K.D. Shimizu, Characterization of molecularly imprinted polymers with the Langmuir-Freundlich isotherm, Anal. Chem. 73 (19) (2001) 4584–4591.
[50] X.L. Wei, A. Samadi, S.M. Husson, Synthesis and characterization of molecularly imprinted polymers for chromatographic separations, Sep. Sci. Technol. 40 (1–3) (2005) 109–129.
[51] V.L. Mendoza, R.W. Vachet, Probing protein structure by amino acid-specific covalent labeling and mass spectrometry, Mass Spectrom. Rev. 28 (5) (2009) 785–815.
[52] J.N. Miller, J.C. Miller, Statistics and Chemometrics for Analytical Chemistry, 6th ed., Pearson Education Limited, Harlow, 2010.
[53] Z. Stojanovic, J. Erdossy, K. Keltai, F.W. Scheller, R.E. Gyurcsanyi, Electrosynthesized molecularly imprinted polyscopoletin nanofilms for human serum albumin detection, Anal. Chim. Acta 977 (2017) 1–9.

Publication III

A. Kidakova, J. Reut, R. Boroznjak, A. Öpik, V. Syritski, Advanced sensing materials based on molecularly imprinted polymers towards developing point-of-care diagnostics devices, Proc. Est. Acad. Sci. 68 (2019) 158–167.

Proceedings of the Estonian Academy of Sciences,
2019, **68**, 2, 158–167
https://doi.org/10.3176/proc.2019.2.07
Available online at www.eap.ee/proceedings

MATERIALS
ENGINEERING

Advanced sensing materials based on molecularly imprinted polymers towards developing point-of-care diagnostics devices

Anna Kidakova, Jekaterina Reut, Roman Boroznjak, Andres Öpik, and Vitali Syritski*

Department of Materials and Environmental Technology, Tallinn University of Technology, Ehitajate tee 5, 19086 Tallinn, Estonia

Received 20 December 2018, accepted 2 March 2019, available online 16 April 2019

Abstract. Today there is growing interest in the replacement of biological receptors in biosensing systems including point-of-care (PoC) diagnostics devices due to their high price and short shelf life. Molecularly imprinted polymers (MIPs), which are wholly synthetic materials with antibody-like ability to bind and discriminate between molecules, demonstrate improved stability and reduced fabrication cost as compared with biological receptors. Here we report, for the first time, a MIP-based synthetic receptor capable of selective binding of a clinically relevant protein – the brain-derived neurotrophic factor (BDNF). The BDNF-MIP was generated by surface-initiated controlled/living radical photopolymerization directly on a screen-printed electrode (SPE). The resulting BDNF-MIP/SPE electrochemical sensor could detect BDNF down to 6 pg/mL in the presence of the interfering HSA protein and was capable of discriminating BDNF among its structural analogues, i.e. neurotropic factors CDNF and MANF. We believe that the presented approach for the preparation of a neurotrophic factor-selective sensor could be a promising route towards the development of innovative PoC diagnostics devices for the early-stage diagnostics and/or monitoring the therapy of neurological diseases.

Key words: molecularly imprinted polymers, controlled/living radical polymerization, protein imprinting, brain-derived neurotrophic factor, neurotrophic factor, screen-printed electrode, sensing materials.

List of main abbreviations

BDNF	Brain-derived neurotrophic factor
BDNF-MIP/SPE	SPE modified by MIP film with molecular imprints of BDNF
CDNF	Cerebral dopamine neurotrophic factor
C/LR	Controlled/living radical
CV	Cycling voltammetry
DPV	Differential pulse voltammetry
EIS	Electrochemical impedance spectroscopy
HSA	Human serum albumin
IF	Imprinting factor
LOD	Limit of detection
LOQ	Limit of quantitation
MANF	Mesencephalic astrocyte-derived neurotrophic factor
mCD48	Mouse recombinant cluster of differentiation 48
MIP	Molecularly imprinted polymer
NF	Neurotrophic factor
NIP	Non-imprinted polymer
PBS	Phosphate buffer saline
PoC	Point-of-care
SPE	Screen-printed electrode
WE	Working electrode

* Corresponding author, vitali.syritski@taltech.ee

1. INTRODUCTION

Nowadays, healthcare is facing an increasing demand for fast and reliable analytical methods suitable for achieving appropriate sensitivity and selectivity with low limit of detection (LOD) while being low-cost, portable, and capable of in situ real-time monitoring.

The occurrence and use of point-of-care (PoC) devices have steadily increased in Europe [1] as well as globally for facilitating rapid testing in medical diagnostics, and thus clinical decisions [2,3]. Most of the current biosensing systems including PoC devices utilize labile biological recognition elements that offer high selectivity towards a target analyte, but limit the shelf life of the device and increase cost and analysis time. Growing interest in the replacement of biological receptors with wholly synthetic analogues such as molecularly imprinted polymers (MIPs) has made a substantial contribution to the expansion of the field [4,5]. Molecular imprinting is one of the state-of-the-art techniques to generate MIPs – materials with antibody-like ability to bind and discriminate between molecules [6]. The technique can be defined as the process of template-induced formation of specific molecular recognition sites in a polymer matrix. The main benefits of MIPs are related to their synthetic nature, i.e. excellent chemical and thermal stability coupled with their reproducible and cost-effective fabrication. MIPs have been shown to be a promising alternative to natural receptors in biosensors [7–10].

The sensors based on electrochemical transduction mechanisms seem to be prospective for diagnostics purposes since they combine real-time monitoring of an analyte binding event, simplicity in handling, and sufficient sensitivity at reduced cost [11,12]. Furthermore, screen-printed electrode (SPE) sensors, being fully compatible with large-scale fabrication and multiplexing technologies and the ease in their integration with microfluidic systems, represent an ideal starting point to realize low cost and portable sensing platforms suitable for PoC devices [13]. Therefore, robust interfacing of a MIP film with a SPE provides a considerable option to build a cost-effective but reliable PoC device [14,15].

In clinical diagnostics, the research aimed at the discovery and detection of biomarkers of human diseases, especially neurological and mental disorders, has become of great demand due to the increase in the prevalence of these diseases over the last decades and the need for early stage diagnosis [16]. For example, neurotrophic factor (NF) proteins, which are a family of proteins secreted from neurons and neuron-supporting cells, were found to be associated with a number of neurological and mental diseases [17–20]. There is a large number of publications associating brain-derived neurotrophic factor (BDNF) levels with various conditions affecting brain functioning, including depression and neurodegeneration (Alzheimer's and Parkinson's diseases) [21–23]. Therefore, BDNF can be considered as a potential biomarker for the pre-symptomatic diagnostics of these diseases or for monitoring therapies.

The application of MIP-based sensors for diagnostics has been extensively studied. Thus, the detection of cancer biomarkers (such as prostate specific antigen [24], epithelial ovarian cancer antigen-125 [25], carcinoembryonic antigen [26]), and cardiovascular disease biomarkers (myoglobin [27,28] and cardiac troponin T [29]) by MIP-modified sensors has been reported. In addition, MIP receptors for selective extraction of an Alzheimer's disease biomarker, α-Amyloid peptides, has been studied by Sellergren's group [30]. Although the selective recognition of a growth factor family protein, vascular endothelial growth factor, by hybrid MIP nanoparticles as well as by MIP thin layer on surface plasmon resonance (SPR) and screen-printed electrodes (SPEs) has been reported [31–33], to the best of our knowledge, there are no reports on the MIP designed for the recognition of NF proteins.

When synthesizing a MIP for sensing macromolecules such as proteins, it is essential that the synthesis strategy prevent the entrapment of the protein in the polymer matrix during the polymerization process and lead to a robust interfacing of the MIP with the surface of a sensor, i.e. to an efficient transduction of the binding event of this macromolecular analyte by the MIP into useful analytical signals. To address the issues, the implementing of surface-initiated controlled/living radical (C/LR) polymerization was shown to be a prospective solution [34,35]. The method of surface-initiated polymerization allows the formation of covalent bonding between the polymer film and the surface, which ensures a perfect interfacing between the MIP recognition layer and a sensor transducer. Moreover, the C/LR polymerization offers the capability of the film thickness control, uniform coating of surface, control over composition, and high density of grafting [36]. To perform surface initiated C/LR photopolymerization, an initiator, also called iniferter (initiator–transfer agent–terminator), was attached to a sensor surface using different techniques by Ahmad et al. [37].

In the present work, for the first time the MIP-based sensor for the detection of BDNF was prepared on a SPE by C/LR photopolymerization initiated from the surface. The main analytical characteristics of the BDNF-MIP/SPE sensor, such as its limit of detection (LOD) and limit of quantification (LOQ), were determined. The BDNF-MIP/SPE sensor was studied in terms of its recognition capability and selectivity towards

the target protein through the analysis of the responses of the BDNF-MIP-modified SPE sensors to the interaction of the target (BDNF) and interfering (cerebral dopamine neurotrophic factor (CDNF), mesencephalic astrocyte-derived neurotrophic factor (MANF), mouse recombinant cluster of differentiation 48 (mCD48)) proteins.

2. EXPERIMENTAL

2.1. Chemicals and materials

3,5-Dichlorophenyl diazonium tetrafluoroborate (3,5-DClPDT), sodium diethyldithiocarbamate (Na-DEDTC), acetonitrile (ACN), (3-glycidyloxypropyl)trimethoxysilane (3-GPS), N,N′-methylenebis(acrylamide) (BAA), diethylaminoethyl methacrylate (DEAEM), and human serum albumin (HSA, 66.5 kDa) were obtained from Sigma-Aldrich. Tetrabutylammonium tetrafluoroborate (Bu_4NBF_4, 99.0%,) was obtained from Fluka. Human recombinant BDNF (13.5 kDa, pI 9.43), human recombinant CDNF (18.5 kDa, pI 7.68), human recombinant MANF, (18.1 kDa, pI 8.55), and mCD48 antigen (cluster of differentiation 48, 22.2 kDa, pI 9.36) were provided by Icosagen AS (Tartu, Estonia). Ultrapure water (resistivity 18.2 MΩ·cm, Millipore, USA) was used for the preparation of all aqueous solutions. Phosphate buffered saline (PBS) solution (0.01 M, pH 7.4) was used to prepare analyte solutions. The screen-printed electrodes (SPEs) were obtained from BVT Technologies a.s. (Praha, Czech Republic). The SPEs (catalogue #AC1.W1.R2) include a gold working electrode (WE) (1 mm diameter), an AgCl covered silver reference electrode, and a gold counter electrode.

2.2. Synthesis of BDNF-MIP films

The BDNF-MIP films were synthesized directly on the WE of the SPE using the following main stages (Fig. 1): (a) functionalization of SPE with 3,5-DClPD, (b) grafting of the iniferter to 3,5-DClPD, (c) coating of the SPE with the solution containing a mixture of the functional (DEAEM) and crosslinking (BAA) monomers and the target protein (BDNF), (d) photopolymerization of the monomers under UV-irradiation, and (e) removing BDNF from the polymer to form BDNF-MIP on the surface of the SPE.

The WE of the SPE was cleaned electrochemically by placing a drop of 0.1 M H_2SO_4 solution on it and cycling the potential from 0.1 to 1.15 V at a scan rate of 100 mV/s for 15 cycles. The modification of the WE with the 3,5-DClP layer was performed electrochemically applying an ACN solution containing 1 mM 3,5-DClPDT and 0.1 M Bu_4NBF_4 and cycling the potential of the WE between the –0.1 V and 0.5 V vs Ag/AgCl/KCl electrode at a rate of 50 mV/s. The modified surface was washed with tetrahydrofuran (THF) and ultrapure water to

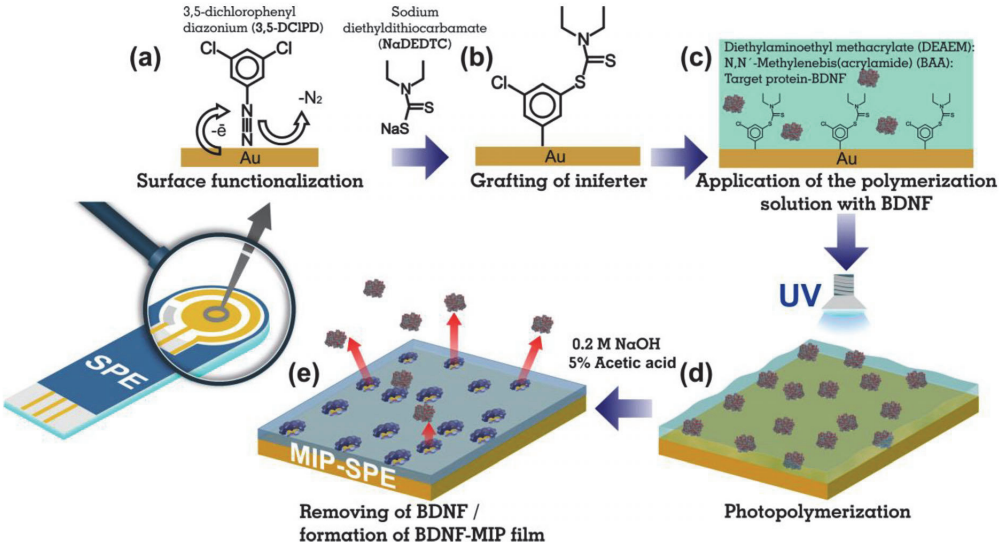

Fig. 1. Fabrication of the BDNF-MIP/SPE sensor.

remove the physisorbed loosely bound layers of a 3,5-DClP [38] and dried under a nitrogen flow. The resulting SPE sensor with a 3,5-DClP layer grafted on the WE was immersed in ethanolic solution of 2 mM Na-DEDTC and vortexed (600 rpm) overnight at room temperature in the dark. Finally, the SPE was thoroughly rinsed with ethanol and ultrapure water and dried with a nitrogen flow.

The charge transfer blocking behaviour of the 3,5-DClP layer was investigated by electrochemical impedance spectroscopy (EIS) and cyclic voltammetry (CV). The EIS and CV were conducted in 1 M KCl solution containing a 4 mM redox probe $K_3[Fe(CN)_6]/K_4[Fe(CN)_6]$ by an electrochemical workstation (Reference 600, Gamry Instruments, USA). The CV was performed scanning the potential between 0 and 0.5 V at a scan rate of 50 mV/s. The EIS was performed in the frequency range between 100 kHz and 0.1 Hz at open circuit potential with AC amplitude of 10 mV. Every CV and EIS was repeated 3 times. The EIS spectra were fitted to an equivalent electrical circuit using Echem Analyst software (Gamry Instruments, USA). The BDNF-MIP film on the DEDTC-modified WE of the SPE was generated by C/LR photopolymerization by using UV-irradiation.

The prepolymerization solution was prepared by mixing 12.5 µg/mL BDNF, 2.5 mM functional monomer, DEAEM, and 15 mM cross-linking monomer, BAA, in 0.05 M PBS. The prepolymerization solution (10 µL) was dropped onto the DEDTC-modified SPE sensor and left for 30 min. Then the SPE was covered by a mask with a hole 20% larger than the diameter of the WE and irradiated under UV light (500 W/m^2, 365 nm) during 30 min at room temperature. The optimum polymerization time was determined by comparing the normalized signals of the sensors after polymerization for 15, 30, and 45 min. The normalized signals were determined during incubation in 5 ng/mL BDNF solution in PBS. After photopolymerization the mask was removed and the SPE sensor was alternately immersed in aqueous solution of 0.2 M NaOH and 5% acetic acid and vortexed (600 rpm) for 30 min to remove the protein from the polymer matrix. The resulting BDNF-MIP/SPE sensor was washed with Milli-Q water and dried under nitrogen flow. The reference non-imprinted polymer (NIP) film was produced in the same way except that the prepolymerization solution was prepared without the addition of BDNF. The surface morphology of the BDNF-MIP and NIP films was characterized by high-resolution scanning electron microscope (HR-SEM Zeiss Merlin) equipped with an In-Lens SE detector for topographic imaging. Measurements were made at an operating voltage of 2.00 kV.

2.3. Rebinding, reusability, and selectivity studies of the BDNF-MIP/SPE sensor

The binding affinity and selectivity of the BDNF-MIP/SPE toward the target analyte BDNF were determined by means of differential pulse voltammetry (DPV). Measurements were performed in the 1 M KCl solution containing a 4 mM redox probe $K_3[Fe(CN)_6]/K_4[Fe(CN)_6]$. The DPV was conducted in the range 0–0.4 V with the pulse amplitude of 0.025 V, pulse time of 0.05 s, and step potential of 0.005 V. The DPV was performed after 30 min incubation of BDNF-MIP- and NIP-modified SPE sensors in solutions with increasing concentrations of the analyte (from 0.1 to 100 ng/mL of BDNF in PBS solution). After that, the unbound protein was removed by washing twice in PBS vortexed (600 rpm) for 5 min. The optimal incubation time was determined by incubating the BDNF-MIP/SPE sensor in the BDNF solution (2 ng/mL) for various times (5, 10, 15, 20, 30, 40, 60 min). The binding affinity of the BDNF-MIP films toward the target was measured by means of DPV. The DPV curves were recorded after the incubation of BDNF-MIP- and NIP-modified SPEs in solutions with increasing concentrations of the analyte (from 0.1 to 100 ng/mL of BDNF in PBS). The response signals of the BDNF-MIP/SPE were its normalized DPV current peaks, B_n, calculated according to Eq. (1):

$$B_n = \frac{I_0 - I_c}{I_0}, \tag{1}$$

where I_0 is DPV current peak measured after the incubation of the SPE in blank PBS solution, I_C is the DPV current peak measured after the incubation the SPE in PBS containing a particular concentration (C) of BDNF.

The binding isotherms were generated using B_n values. The values of the dissociation constant (K_d) and the maximum binding response at saturation (B_{max}) were derived from fitting the binding isotherm to Langmuir adsorption models (Eq. 2):

$$B = \frac{B_{max} C}{K_d + C}. \tag{2}$$

The reusability of the BDNF-MIP/SPE sensor was tested by measuring its responses after the regeneration procedure and repeated incubation in BDNF solution (2 ng/mL). The regeneration procedure was performed in the same way as the procedure for the removal of the protein from the polymer matrix employed after the synthesis of the BDNF-MIP film. The selectivity of the BDNF-MIP/SPE sensor was assessed by comparing the

responses of the BDNF-MIP/SPE sensor towards BDNF with those of the interfering proteins CDNF, MANF, and mCD48. The selectivity test was conducted at different concentrations of the proteins in the presence of 0.8 mg/mL HSA.

3. RESULTS AND DISCUSSION

3.1. Preparation of BDNF-MIP films

In this study the BDNF-MIP films were prepared by the surface-initiated C/LR polymerization technique directly on the WE of the SPE. First, the WE of the SPE was modified by a 3,5-dichlorophenyl (3,5-DClP) layer using the electrochemical reduction of the corresponding aryldiazonium salt, 3,5-DClPDT. This is a well-known method and widely used to modify metal surfaces by organic molecules providing the formation of a stable molecular layer as a result of covalent bonding of the aryl radical to the metal surface [39,40]. Figure 2 illustrates CV of the electrodeposition process of 3,5-DClP. The first cycle reveals well-defined reduction peaks, which can be attributed to the electrochemical reduction of 3.5-DClPDT to its corresponding radicals. The reduction peaks disappear during the second cycle, which corresponds to the formation of a blocking layer preventing further access of the diazonium species to the electrode surface [41].

The success of the modification of the WE by 3,5 DClP was confirmed by CV and EIS recorded in the presence of a $Fe(CN)_6^{3-/4-}$ redox pair. Figure 3a shows that the intensity of the pair of the current peaks associated with the redox activity of $Fe(CN)_6^{3-/4-}$ and defined well on the bare gold electrode, greatly diminished after the grafting of the diazonium salt on the gold electrode. This confirms the insulating nature of the deposited

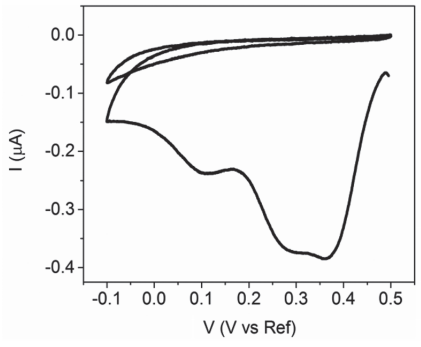

Fig. 2. Cyclic voltammograms recorded on the bare gold electrodes in the acetonitrile solution containing 0.1 M Bu_4NBF_4 and 1 mM 3,5-DClPDT; scan rate 50 mV/s.

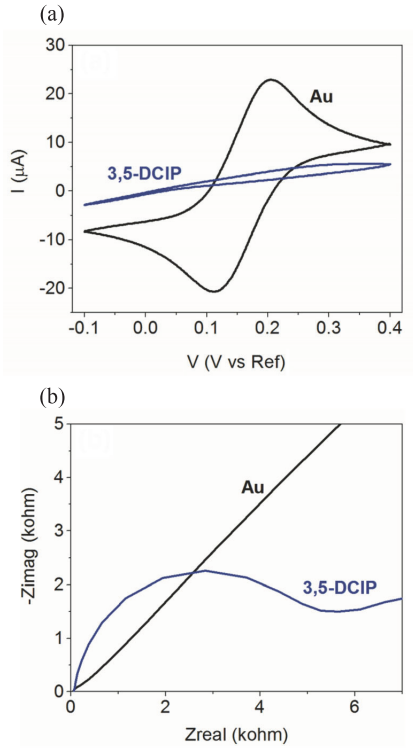

Fig. 3. Cyclic voltammogram at the scan rate of 50 mV/s (a) and the Nyquist plot for the bare gold (Au) and 3,5-DClP-modified gold (b).

organic monolayers. The charge transfer resistance, as estimated from the width of the semicircle in the Nyquist plot (Fig. 3b), increased from 68 Ω/cm^2 (the bare gold electrode) to 2.3 kΩ/cm^2 (after modification by the 3.5-DClP layer). The increase in the charge transfer resistance is a direct consequence of the partial passivation of the bare gold electrode, which reduces the ability of the redox probe to access its surface. The attachment of the iniferter DEDTC to the 3,5-DClP-modified surfaces by electrophilic substitution was discussed in detail in our previous work [35], where the successful functionalization of the gold electrode by a DEDTC layer was additionally confirmed by X-ray photoelectron spectroscopy data.

To synthesize a protein-selective MIP film, it is essential to prevent the entrapment of protein in the polymer matrix during the polymerization process. Therefore, in order to avoid the overgrowing of the polymer around the BDNF molecules, the thickness of the photopolymerized polymer film was controlled by the UV exposure time. The optimal exposure time was

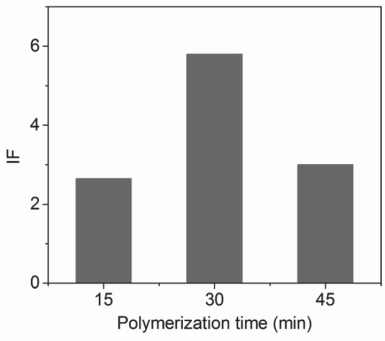

Fig. 4. Calculated *IF* values for the BDNF-MIP/SPE sensor prepared at different polymerization times.

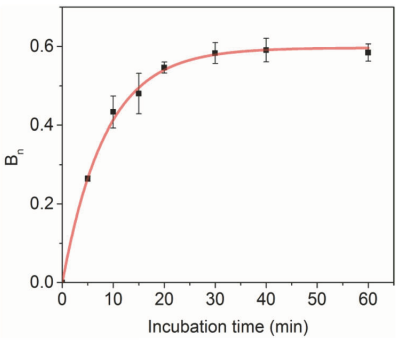

Fig. 5. Normalized response of a BDNF-MIP/SPE sensor as a function of the incubation time in 5 ng/mL BDNF solution.

determined by calculating the imprinting factor (*IF*) (Eq. 3), which characterizes the relative adsorption capacity of MIP.

$$IF = \frac{B_n MIP}{B_n NIP}, \quad (3)$$

where $B_n MIP$ and $B_n NIP$ are normalized signals after protein adsorption on MIP and NIP, respectively; *IF* reflects the quality of the imprinting effect, as a larger value of *IF* represents the availability of more binding sites with high affinity in the resulting polymer. As can be seen in Fig. 4, the BDNF-MIP shows a higher *IF* value after 30 min of photopolymerization. The UV irradiation of 500 W/m^2 was chosen as the optimal intensity that does not cause significant damage to the protein structure within 30 min of exposure [35].

3.2. Analytical performance of a BDNF-MIP/SPE sensor

The binding affinity of the BDNF-MIP/SPE toward the target analyte BDNF was determined by means of DPV recorded after the incubation of the sensor in the solution with an increased concentration of the analyte. Firstly, in order to select the optimal binding conditions, the relationship between the sensor signal B_n and the incubation time in the range of 5–60 min was studied. The current increased rapidly within the first 20 min of incubation and reached the saturation value after 30 min (Fig. 5), indicating that the adsorption equilibrium was reached. Thus, the optimal incubation time of 30 min was chosen for the rebinding study.

The B_n values calculated from Eq. (1) were used to plot the binding isotherms (Fig. 6). The BDNF-MIP/SPE sensor showed a hyperbolic response as a function of the BDNF concentrations. To describe the equilibrium

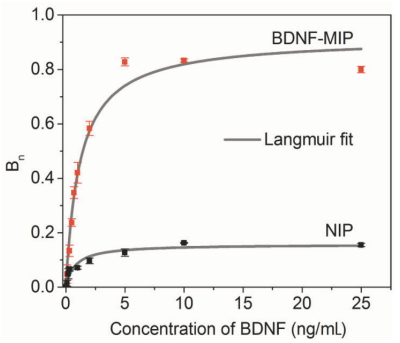

Fig. 6. Binding isotherms of BDNF to the BDNF-MIP- and NIP-modified SPE sensor.

binding events happening on the sensor surface, the Langmuir adsorption model was used in this study. The Langmuir binding model was previously successfully applied to fit the adsorption isotherm of MIPs by other authors [27,29,42]. According to the model, when all binding sites are occupied by molecules, no further adsorption will occur on the surface and the saturation response (B_{max}) will be obtained. The fitting results showed that BDNF-MIP bound the target protein, BDNF, with the dissociation constant K_d of 1.12 ng/mL and had an about 5.8 times higher binding capacity than NIP as judged by the respective B_{max} values (0.92 vs 0.16 a.u.).

The BDNF-MIP/SPE sensor showed a pseudo-linear response to the BDNF in the concentration range from 0.01 to 0.06 ng/mL and a fixed concentration of HSA (0.8 mg/mL), the main plasma protein (Fig. 7). The linear regression in this concentration range gives the coefficient of determination, *R*-squared, equal to 0.991 and LOD and LOQ values, determined as

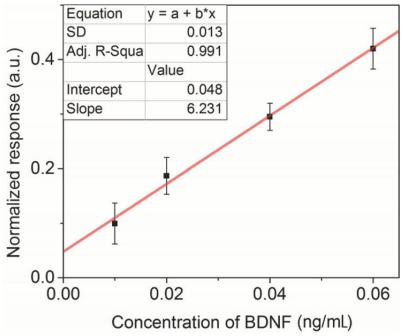

Fig. 7. Responses of the BDNF-MIP/SPE sensor at low concentrations of BDNF in the presence of 0.8 mg/mL HSA. The solid line represents the regression line.

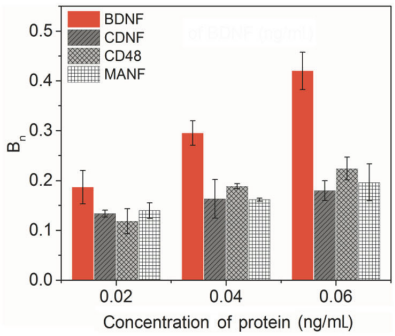

Fig. 8. Selectivity test of the BDNF-MIP towards BDNF, CDNF, CD48, and MANF conducted through incubated in 0.02–0.06 ng/mL solutions of the respective proteins in PBS in the presence of 0.8 mg/mL HSA.

3 and 10 times the standard deviation (SD) divided by the slope of the regression line, 6 pg/mL and 20 pg/mL, respectively.

3.3. Selectivity and reusability study

The BDNF-MIP/SPE sensor was characterized in terms of its capability to rebind selectively the target protein, BDNF, with respect to the interfering proteins of slightly different size and isoelectric point (pI) such as CDNF, MANF, and mCD48. Selection of CDNF and MANF as interfering analytes was stipulated by their permanent presence in a human serum and thus, they can interfere with the sensor response along with the target protein (BDNF). The third interfering analyte – mCD48 – has the molecular weight and pI value similar to those of BDNF. The selectivity of the sensor was studied in the presence of HSA at a concentration of 0.8 mg/mL, corresponding to a 50-fold dilution of its physiological norm in diluted human serum. For the selectivity study, the concentration of the interfering proteins was selected close to their LOQ value (0.02–0.06 ng/mL). The response of the BDNF-MIP/SPE sensor to the BDNF was higher than that to the interfering proteins (Fig. 8). The difference between the responses of the sensor upon the interaction with the BDNF and the interfering proteins increased with the increasing concentration, and at 0.06 ng/mL the BDNF caused about a two times higher response as compared to the interfering proteins. At the same time the responses to the interfering proteins remained at approximately the same level for all tested concentrations.

As to the possibility of regenerating and repeatedly using a sensor, protein-MIP based sensors have been considered to have a significant advantage over conventional antibody-based biosensors. Therefore, we examined the ability of the prepared BDNF-MIP/SPE sensor to withstand the regeneration procedure. The treatments in the acidic and alkaline solutions efficiently disrupting possible multiple hydrogen and electrostatic bonds between the protein and the MIP surface were assessed to regenerate the surface of the sensor. It was found that the response of the BDNF-MIP/SPE sensor was greatly reduced already after the first regeneration cycle (Fig. 9), indicating a poor reusability of the sensor. However, taking into account that a SPE-based sensor is expected to be used as a disposable sensor, its reusability is obviously not of great importance. On the other hand, comparison of the signals of three freshly prepared BDNF-MIP/SPEs showed that a good reproducibility of the sensor response (standard deviation 0.026) was achieved.

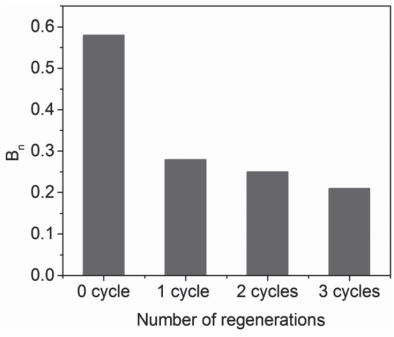

Fig. 9. Normalized responses of the BDNF-MIP/SPE sensor upon the injection of 2 ng/mL BDNF solution after 1, 2 and 3 regeneration cycles.

4. CONCLUSIONS

In the present study, we have developed for the first time a MIP synthetic receptor capable of selective binding of BDNF integrated with an inexpensive and disposable SPE. Surface-initiated C/LR photopolymerization was demonstrated to be a suitable method to prepare stable BDNF-MIP films directly on a SPE sensor. The prepared BDNF-MIPs were capable of binding BDNF with the dissociation constant, K_d, of 1.12 ng/mL and had about 5.8 times higher binding capacity than the reference film, NIP. The BDNF-MIP/SPE sensor could detect BDNF with the LOD value of 6 pg/mL and quantify BDNF with the LOQ value of 20 pg/mL in the presence of HSA as a highly abundant serum protein. Moreover, it was able to discriminate BDNF among analogous molecules, i.e. CDNF and MANF, and a molecule of a similar size, i.e. mCD48. Although further research is required, the presented approach to the preparation of a cost-effective MIP-SPE sensor capable of selective detection of a NF-family protein could be a promising route towards the development of innovative PoC diagnostics devices for the early-stage diagnostics of neurological diseases or for monitoring therapies.

ACKNOWLEDGEMENTS

This work was supported by the Estonian Research Council (grant PRG307) and Tallinn University of Technology (development project SS425). The authors thank Icosagen AS and Prof. M. Ustav personally for kindly providing us with the neurotrophic factor proteins. The publication costs of this article were covered by the Estonian Academy of Sciences.

REFERENCES

1. Larsson, A., Greig-Pylypczuk, R., and Huisman, A. The state of point-of-care testing: a European perspective. *Ups. J. Med. Sci.*, 2015, **120**, 1–10.
2. McMullan, J. T., Knight, W. A., Clark, J. F., Beyette, F. R., and Pancioli, A. Time-critical neurological emergencies: the unfulfilled role for point-of-care testing. *Int. J. Emer. Med.*, 2010, **3**, 127–131.
3. Wei, T-Y., Fu, Y., Chang, K-H., Lin, K-J., Lu, Y-J., and Cheng, C-M. Point-of-care devices using disease biomarkers to diagnose neurodegenerative disorders. *Trends Biotechnol.*, 2018, **36**, 290–303.
4. Piletsky, S. A. and Whitcombe, M. J. (eds). *Designing Receptors for the Next Generation of Biosensors*. Springer-Verlag, Berlin, 2013.
5. Mahon, C. S. and Fulton, D. A. Mimicking nature with synthetic macromolecules capable of recognition. *Nat. Chem.*, 2014, **6**, 665–672.
6. Mosbach, K. Molecular imprinting. *Trends Biochem. Sci.*, 1994, **19**, 9–14.
7. Tretjakov, A., Syritski, V., Reut, J., Boroznjak, R., and Öpik, A. Molecularly imprinted polymer film interfaced with Surface Acoustic Wave technology as a sensing platform for label-free protein detection. *Anal. Chim. Acta*, 2016, **902**, 182–188.
8. Cieplak, M. and Kutner, W. Artificial biosensors: How can molecular imprinting mimic biorecognition? *Trends Biotechnol.*, 2016, **34**, 922–941.
9. Haupt, K. and Mosbach, K. Molecularly imprinted polymers and their use in biomimetic sensors. *Chem. Rev.*, 2000, **100**, 2495–2504.
10. Ye, L. and Mosbach, K. Molecular imprinting: synthetic materials as substitutes for biological antibodies and receptors. *Chem. Mater.*, 2008, **20**, 859–868.
11. Espinoza-Castañeda, M., Escosura-Muñiz, A. d. l., Chamorro, A., Torres, C. d., and Merkoçi, A. Nanochannel array device operating through Prussian blue nanoparticles for sensitive label-free immunodetection of a cancer biomarker. *Biosens. Bioelectron.*, 2015, **67**, 107–114.
12. Tran, H. V., Piro, B., Reisberg, S., Huy Nguyen, L., Dung Nguyen, T., Duc, H. T., and Pham, M. C. An electrochemical ELISA-like immunosensor for miRNAs detection based on screen-printed gold electrodes modified with reduced graphene oxide and carbon nanotubes. *Biosens. Bioelectron.*, 2014, **62**, 25–30.
13. Tonello, S., Serpelloni, M., Lopomo, N. F., Sardini, E., Abate, G., and Uberti, D. L. (eds). *Preliminary Study of a Low-Cost Point-of-Care Testing System Using Screen-Printed Biosensors: For Early Biomarkers Detection Related to Alzheimer Disease*. IEEE International Symposium on Medical Measurements and Applications (MeMeA), 15–18 May 2016.
14. Lopes, F., Pacheco, J. G., Rebelo, P., and Delerue-Matos, C. Molecularly imprinted electrochemical sensor prepared on a screen printed carbon electrode for naloxone detection. *Sensor. Actuat. B-Chem.*, 2017, **243**, 745–752.
15. Ribeiro, J. A., Pereira, C. M., Silva, A. F., and Sales, M. G. F. Electrochemical detection of cardiac biomarker myoglobin using polyphenol as imprinted polymer receptor. *Anal. Chim. Acta*, 2017, **981**, 41–52.
16. WHO. *Neurological Disorders: Public Health Challenges*. World Health Organization, Geneva, Switzerland, 2006.
17. Cattaneo, A., Cattane, N., Begni, V., Pariante, C. M., and Riva, M. A. The human BDNF gene: peripheral gene expression and protein levels as biomarkers for psychiatric disorders. *Transl. Psych.*, 2016, **6**, e958.
18. Hashimoto, K. Brain-derived neurotrophic factor as a biomarker for mood disorders: an historical overview and future directions. *Psychiat. Clin. Neuros.*, 2010, **64**, 341–357.

19. Lindahl, M., Saarma, M., and Lindholm, P. Unconventional neurotrophic factors CDNF and MANF: structure, physiological functions and therapeutic potential. *Neurobiol. Dis.*, 2017, **97**, 90–102.
20. Lindholm, D., Mäkelä, J., Di Liberto, V., Mudò, G., Belluardo, N., Eriksson, O., and Saarma, M. Current disease modifying approaches to treat Parkinson's disease. *Cell. Mol. Life Sci.*, 2016, **73**, 1365–1379.
21. Laske, C., Stransky, E., Leyhe, T., Eschweiler, G. W., Wittorf, A., Richartz, E., et al. Stage-dependent BDNF serum concentrations in Alzheimer's disease. *J. Neural Transm.*, 2006, **113**, 1217–1224.
22. Sen, S., Duman, R., and Sanacora, G. Serum brain-derived neurotrophic factor, depression, and antidepressant medications: meta-analyses and implications. *Biol. Psychiat.*, 2008, **64**, 527–532.
23. Wang, Y., Liu, H., Zhang, B.-S., Soares, J. C., and Zhang, X. Y. Low BDNF is associated with cognitive impairments in patients with Parkinson's disease. *Parkinsonism Relat. D.*, 2016, **29**, 66–71.
24. Jolly, P., Tamboli, V., Harniman, R. L., Estrela, P., Allender, C. J., and Bowen, J. L. Aptamer–MIP hybrid receptor for highly sensitive electrochemical detection of prostate specific antigen. *Biosens. Bioelectron.*, 2016, **75**, 188–195.
25. Viswanathan, S., Rani, C., Ribeiro, S., and Delerue-Matos, C. Molecular imprinted nanoelectrodes for ultra sensitive detection of ovarian cancer marker. *Biosens. Bioelectron.*, 2012, **33**, 179–183.
26. Wang, Y. T., Zhang, Z. Q., Jain, V., Yi, J. J., Mueller, S., Sokolov, J., et al. Potentiometric sensors based on surface molecular imprinting: detection of cancer biomarkers and viruses. *Sensor. Actuat. B-Chem.*, 2010, **146**, 381–387.
27. Moreira, F. T. C., Sharma, S., Dutra, R. A. F., Noronha, J. P. C., Cass, A. E. G., and Sales, M. G. F. Protein-responsive polymers for point-of-care detection of cardiac biomarker. *Sensor. Actuat. B-Chem.*, 2014, **196**, 123–132.
28. Shumyantseva, V. V., Bulko, T. V., Sigolaeva, L. V., Kuzikov, A. V., and Archakov, A. I. Electrosynthesis and binding properties of molecularly imprinted poly-o-phenylenediamine for selective recognition and direct electrochemical detection of myoglobin. *Biosens. Bioelectron.*, 2016, **86**, 330–336.
29. Silva, B. V. M., Rodriguez, B. A. G., Sales, G. F., Sotomayor, M. D. T., and Dutra, R. F. An ultra-sensitive human cardiac troponin T graphene screen-printed electrode based on electropolymerized-molecularly imprinted conducting polymer. *Biosens. Bioelectron.*, 2016, **77**, 978–985.
30. Urraca, J. L., Aureliano, C. S. A., Schillinger, E., Esselmann, H., Wiltfang, J., and Sellergren, B. Polymeric complements to the Alzheimer's disease biomarker β-amyloid isoforms Aβ1–40 and Aβ1–42 for blood serum analysis under denaturing conditions. *J. Am. Chem. Soc.*, 2011, **133**, 9220–9223.
31. Cecchini, A., Raffa, V., Canfarotta, F., Signore, G., Piletsky, S., MacDonald, M. P., and Cuschieri, A. In vivo recognition of human vascular endothelial growth factor by molecularly imprinted polymers. *Nano Lett.*, 2017, **17**, 2307–2312.
32. Kamon, Y. and Takeuchi, T. Molecularly imprinted nanocavities capable of ligand-binding domain and size/shape recognition for selective discrimination of vascular endothelial growth factor isoforms. *ACS Sensors*, 2018, **3**, 580–586.
33. Johari-Ahar, M., Karami, P., Ghanei, M., Afkhami, A., and Bagheri, H. Development of a molecularly imprinted polymer tailored on disposable screen-printed electrodes for dual detection of EGFR and VEGF using nano-liposomal amplification strategy. *Biosens. Bioelectron.*, 2018, **107**, 26–33.
34. Salian, V. D., White, C. J., and Byrne, M. E. Molecularly imprinted polymers via living radical polymerization: relating increased structural homogeneity to improved template binding parameters. *React. Funct. Polym.*, 2014, **78**, 38–46.
35. Kidakova, A., Reut, J., Rappich, J., Öpik, A., and Syritski, V. Preparation of a surface-grafted protein-selective polymer film by combined use of controlled/living radical photopolymerization and micro-contact imprinting. *React. Funct. Polym.*, 2018, **125**, 47–56.
36. De Boer, B., Simon, H. K., Werts, M. P. L., Vegte, E. W. van der, and Hadziioannou, G. "Living" free radical photopolymerization initiated from surface-grafted iniferter monolayers. *Macromolecules*, 2000, **33**, 349–356.
37. Ahmad, R., Mocaer, A., Gam-Derouich, S., Lamouri, A., Lecoq, H., Decorse, P., et al. Grafting of polymeric platforms on gold by combining the diazonium salt chemistry and the photoiniferter method. *Polymer*, 2015, **57**, 12–20.
38. Roy, A., Gao, J., Bilbrey, J. A., Huddleston, N. E., and Locklin, J. Rapid electrochemical reduction of Ni(II) generates reactive monolayers for conjugated polymer brushes in one step. *Langmuir*, 2014, **30**, 10465–10470.
39. Pinson, J. and Podvorica, F. Attachment of organic layers to conductive or semiconductive surfaces by reduction of diazonium salts. *Chem. Soc. Rev.*, 2005, **34**, 429–439.
40. Anothumakkool, B., Guyomard, D., Gaubicher, J., and Madec, L. Interest of molecular functionalization for electrochemical storage. *Nano Res.*, 2017, **10**, 4175–4200.
41. Jian, W., Firestone, M. A., Auciello, O., and Carlisle, J. A. Surface functionalization of ultra-nanocrystalline diamond films by electrochemical reduction of aryldiazonium salts. *Langmuir*, 2004, **20**, 11450–11456.
42. Verheyen, E., Schillemans, J. P., van Wijk, M., Demeniex, M. A., Hennink, W. E., and van Nostrum, C. F. Challenges for the effective molecular imprinting of proteins. *Biomaterials*, 2011, **32**, 3008–3020.

Sensormaterjalid molekulaarselt jäljendatud polümeeridest patsiendimanusteks testideks

Anna Kidakova, Jekaterina Reut, Roman Boroznjak, Andres Öpik ja Vitali Syritski

Kliinilises diagnostikas on pidevalt kasvav vajadus kiirete, suure tundlikkuse ja selektiivsusega usaldusväärsete analüüsimeetodite järele, mis samal ajal on odavad, portatiivsed ning mugavad analüüside läbiviimiseks vahetult sündmuskohal (*point-of-care* (PoC)). PoC-testidele esitatavaid nõudeid võivad edukalt täita sensorid, mis põhinevad sünteetilistel retseptoritel molekulaarselt jäljendatud polümeeride (MIP) baasil ja mis erinevalt looduslikest retseptoritest on odavamad ning stabiilsemad. Antud töös on esmakordselt välja töötatud kliiniliselt olulise valgu neurotrofiini BDNF suhtes selektiivne MIP-retseptor ja ühendatud odava elektrokeemilise sensorplatvormiga SPE (*screen-printed electrode*). BDNF-MIP-kiled valmistati SPE pinnal "elava" radikaal-fotopolümerisatsiooni meetodil. Valmistatud BDNF-MIP/SPE elektrokeemiline sensor oli võimeline tuvastama BDNF-i konkureeriva HSA-valgu foonil avastamispiiriga 6 pg/mL ja eristama BDNF-molekuli selle struktuursetest analoogidest CDNF ning MANF. Väljapakutud meetod neurotrofiini BDNF suhtes selektiivse sensori valmistamiseks osutub perspektiivseks lahenduseks uute patsiendimanuste testide (PoC-testid) väljatöötamisel neuroloogiliste haiguste diagnostikaks ja/või ravi edukuse jälgimiseks.

Curriculum vitae

Personal data

Name: Anna Kidakova

Contact data

E-mail: anna.kidakova@taltech.ee

Education

2014–2020	Tallinn University of Technology—PhD
2013–2016	Tallinn University of Technology—MSc
2002–2007	Astrakhan State Technical University (Russia)—DI
1999–2001	Astrakhan general education school №5 (Russia)—Secondary education

Language competence

Russian	Native speaker
Estonia	Good
English	Good

Projects

PUT150 (PUT150) “Investigation and development of new generation biosensing selective recognition elements based on Molecularly Imprinted Polymers (1.01.2013−31.12.2016)”, Vitali Sõritski, Tallinn University of Technology, Faculty of Chemical and Materials Technology.

ETF9243 “p-type ZnO and ZnS (1.01.2012−31.12.2015)”, Andres Öpik, Tallinn University of Technology, Faculty of Chemical and Materials Technology.

PRG307 “Molecularly imprinted polymers as sensing materials for medical diagnostics and environmental monitoring (1.01.2019−31.12.2023)”, Vitali Sõritski, Tallinn University of Technology, School of Engineering, Department of Materials and Environmental Technology.

SS425 “Digital sensor platform for medical diagnostics and environmental monitoring (1.01.2018−31.12.2018)”, Vitali Sõritski, Tallinn University of Technology, School of Engineering, Department of Materials and Environmental Technology.

Industrial property

Invention: Molecularly Imprinted Polymer sensors for Neurotrophic Factors; Owners: Tallinn University of Technology; Authors: Vitali Sõritski, Jekaterina Reut, Anna Kidakova, Andres Öpik; Priority number: US16/377,414; Priority date: 8.04.2019.

Participation at international conferences

Baltic Polymer Symposium 2019, Vilnius, Lithuania, 18-20, 2019.

The 8th Graduate Student Symposium on Molecular Imprinting, Berlin, Germany, August 28-30, 2019.

Modern materials and manufacturing 2019, Tallinn, Estonia, 23-26 april, 2019.

The 10th International Conference on Molecular Imprinting, Jerusalem, Israel, June 24-28, 2018.

EUPOC 2018 – Biomimetic Polymers by Rational Design, Imprinting and Conjugation, Como, Italy, 20 - 24 May 2018.

The 9th International Conference on Molecular Imprinting, Lund, Sweden, June 26-30, 2016.

Honours

Best poster award. Conference: EUPOC 2018 – Biomimetic polymers by rational design, Imprinting and Conjugation. COMO (ITALY), 20-24 MAY 2018.

Elulookirjeldus

Isikuandmed

Nimi: Anna Kidakova

Kontaktandmed

E-post: anna.kidakova@taltech.ee

Hariduskäik

2014–2020 Tallinna Tehnikaülikool—PhD
2013–2016 Tallinna Tehnikaülikool—MSc
2002–2007 Astrahani Riiklik Tehnikaülikool (Venemaa)—DI
1999–2001 Astrahani üldkeskkool №5 (Venemaa)—Keskharidus

Keelteoskus

Vene keel Emakeel
Eesti keel Hea
Inglise keel Hea

Projektid

PUT150 (PUT150) "Uue põlvkonna biotundlike süsteemide uurimine ja väljatöötamine molekulaarselt jäljendatud polümeeride baasil (1.01.2013−31.12.2016)", Vitali Sõritski, Tallinna Tehnikaülikool, Keemia ja materjalitehnoloogia teaduskond.

ETF9243 "p-tüüpi ZnO ja ZnS (1.01.2012−31.12.2015)", Andres Öpik, Tallinna Tehnikaülikool, Keemia ja materjalitehnoloogia teaduskond.

PRG307 "Sensormaterjalid molekulaarselt jäljendatud polümeeridest meditsiiniliseks diagnostikaks ja keskkonnaseireks (1.01.2019−31.12.2023)", Vitali Sõritski, Tallinna Tehnikaülikool, Inseneriteaduskond, Materjali- ja keskkonnatehnoloogia instituut.

SS425 "Digitaalne sensorplatvorm meditsiiniliseks diagnostikaks ja keskkonnaseireks (1.01.2018−31.12.2018)", Vitali Sõritski, Tallinna Tehnikaülikool, Inseneriteaduskond, Materjali- ja keskkonnatehnoloogia instituut.

Tööstusomand

Patentne leiutis: Molekulaarselt jäljendatud polümeersensorid neurotroopsete faktorite määramiseks; Omanikud: Tallinna Tehnikaülikool; Autorid: Vitali Sõritski, Jekaterina Reut, Anna Kidakova, Andres Öpik; Prioriteedi number: US16/377,414; Prioriteedi kuupäev: 8.04.2019.

Osalemine rahvusvahelistel konverentsidel

Rahvusvaheline konverents "Baltic Polymer Symposium 2019", Vilnius, Leedu, 18-20. september, 2019.

Rahvusvaheline konverents "8th Graduate Student Symposium on Molecular Imprinting", Berliin, Saksamaa, 28-30. august 2019.

Rahvusvaheline konverents “Moodsad materjalid ja tootmine 2019”, Tallinn, Eesti, 23-26. aprill 2019-

Rahvusvaheline konverents “The 10th International Conference on Molecular Imprinting”, Jerusalem, Israel, 24-28 juuni, 2018-

Rahvusvaheline konverents “EUPOC 2018 – Biomimetic Polymers by Rational Design, Imprinting and Conjugation”, Como, Itaalia, 20-24. mai, 2018.

Rahvusvaheline konverents “The 9th International Conference on Molecular Imprinting”, Lund, Rootsi, 26-30. juuni, 2016.

Tunnustused

Parima stendiettekande preemia. Konverents: EUPOC 2018 – Biomimetic polymers by rational design, Imprinting and Conjugation. COMO (ITALY), 20-24 MAY 2018.